Evaluation of the role of Epsins and Notch1 in oral carcinogenesis

Halah Fawzi Ahmed

BDS, MSc

A thesis submitted in partial fulfilment of the requirements for the degree of Doctor of Philosophy

Northern Institute for Cancer Research and Centre for Oral Health Research,

School of Dental Sciences

Newcastle University, UK

January 2018

Declaration

I declare that this thesis titled “Evaluation of the role of Epsins and Notch1 in oral carcinogenesis” is my own work that has not been submitted for any degree or examination in any university, and that all materials have been acknowledged and referenced.

Abstract

There are around 300,000 new oral cancers diagnosed worldwide every year, the majority are oral squamous cell carcinomas (OSCCs). Most patients present with late stage disease and have a poor prognosis. However, some OSCCs develop within oral potentially malignant disorders and early stage OSCC is curable. Consequently, early detection of the disease is considered to be the most effective way of improving patient outcomes. Several biomarkers have been identified as indicators of oral cancer development and progression, however, none have been translated into clinical practice.

The aim was to investigate the role of the endocytic adaptor proteins called Epsins (Epsin1, 2, 3) and the transmembrane protein, Notch1, in oral carcinogenesis and explore their potential in diagnostic utility.

A panel of nine OSCC cell lines and an immortalized normal oral keratinocyte cell line were cultured. qRT-PCR, Western blot and immunocytochemistry were used to assess the expression levels of Epsins and Notch1. Epsin1 was detected at both the RNA and protein levels in all the cell lines tested, while Epsin2 was not detectable. Epsin3 and Notch1 showed differential expression across the cell lines. Reduced expression of Epsin3 through siRNA did not affect the expression of Notch1. In contrast, overexpression of Epsin3 resulted in a significant reduction of Notch1 expression. Immunohistochemical analysis of tissue samples from a well characterised cohort of patients revealed that Epsin3 expression was higher in oral epithelial dysplasia and OSCC by comparison with normal epithelium. In parallel, Notch1 was generally lower in the dysplasia and OSCC samples, supporting the in vitro data and the hypothesis that Notch1 has a tumour-suppressor function.

The results indicate that Epsin3 is dysregulated in OSCC and has potential to be used as a biomarker in oral epithelial dysplasia. Notch signaling is downregulated in OSCC, possibly through an Epsin3 induced de-activation pathway.

Acknowledgement

Firstly, I would like to express my sincere gratitude to my supervisors Dr. Max Robinson Dr. Ruth Valentine and Professor Marco Carrozzo for their constant support. Max and Ruth, the discussion we have had, the freedom you gave me, the enthusiasm and encouragement over the last four years have helped me reach this stage, without you this project would not have been possible – I could not have asked more and am so grateful for your help.

I am using this opportunity to express my gratitude to everyone who supported me throughout my work. I would like to acknowledge and thank Professor Ian Paterson, Department of Oral Biology and Biomedical Sciences, Faculty of Dentistry, University of Malaya/ Kuala Lumpur for carrying out qRT-PCR for Notch1, Hes1 and Hey1 genes. I acknowledge the kind gift of anti-epsin antibodies, from Professor Cremona, IFOM, Università Vita–Salute San Raffaele and Istituto Nazionale di Neuroscienze, Milano, Italy. I would like to thank Miss Anna Long, Department of Cellular Pathology, for her essential contribution to the processing, sectioning, and immunostaining of human tissue during this project. I am also grateful to Professor Dianne Ford for giving me the opportunity to work in the laboratory in the Institute for Cell and Molecular Bioscience. I am extremely grateful to Dr. Sadat Aziz, who trained me on Western blot technique and willingly answering and solving every query I had during my work, I am and will always be indebted for him.

I would sincerely like to thank my lovely friend Nadia Rostami for her kind help on performing plasmid transformation experiment. I wish to thank all my colleagues and friends in the Translational Oral Biosciences lab for their advice and support. Special thanks go to Ahmed Khudur, Waleed Mohammed, Mustafa Al-Musawi, and Nieka Wahono. I am also sincerely grateful to my faithful friend, Radhika for all the laughs and good times we have spent.

This acknowledgement wouldn't be complete without a deepest sense of gratitude to my beloved husband who supported and encouraged me from the first day to the last, to my lovely kids, thank you for your patience and love. Finally, thanks must go to my family. My parents for love and inspiration throughout my life, my brother and sisters for the ongoing moral support that has helped me believe in myself, your encouragement has been a source of inspiration during the hard times. Finally, I would like to thank Iraqi Ministry of Higher Education and Scientific reports for the sponsorship.

List of abbreviations

AP	Adaptor protein
ARF	ADP-ribosylation factor
bHLH	basic helix-loop-helix
BSA	Bovine Serum Albumin
CCV	Clathrin-coated vesicles
CDKN2A	Cyclin dependent kinase inhibitor 2A
CO2	Carbon dioxide
CSL	CBF-1/RBP-Jκ, Su(H), Lag-1
ct	threshold cycle
d.f.	Degrees of freedom
DMEM	Dulbecco's Modified Eagle's Medium
DNA	Deoxyribonucleic acid
dNTP	Deoxyribonucleoside trisphosphate
EGFR	Epidermal Growth Factor Receptor
EH	Eps15 Homology
ELRs	Epidermal Growth Factor like repeats
ENTH	Epsin N-terminal homology domain
FCS	Foetal calf serum
FDA	Food and drug administration
FFPE	Formalin-fixed paraffin-embedded
GAPDH	Glyceraldehyde 3-phosphate dehydrogenase
GAPs	GTPase-activating proteins
GEFs	Guanosine triphosphate exchange factor
GGAs	Golgi-localized, γ-ear-containing, ARF-binding proteins
GPCR	G Protein-coupled receptors

GSI	Gamma secretase inhibitor
Hes	Hairy and enhancer of split
HNSCC	Head and neck squamous cell carcinoma
hTERT	human Telomerase Reverse Transcriptase
ICC	Immunocytochemistry
IHC	Immunohistochemistry
LNR	Lin-12, Notch repeats
µg	Micrograms
µl	Microlitres
MAPK	Mitogen-activated protein kinase
Mib	Mind bomb
ml	Millilitres
µM	Micromolar
MML	Mastermind-like protein
MMLV	Moloney Murine Leukaemia Virus
mRNA	messenger ribonucleic acid
NBF	neutral buffered formalin
NECD	Notch extracellular domain
Neur	Neutralized
ng	Nanogram
NICD	Notch intracellular domain
NLS	Nuclear localization signals
NNK	4-methylnitrosamine 1 -3 pyridyl – 1 –buntanone
NPF	asparagine-proline-phenylalanine
NT	N-terminal domain
OED	Oral epithelial dysplasia

OFR	Oxygen free radicals
oligo dT	short sequence of deoxy-thymidine nucleotides
OSCC	Oral squamous cell carcinoma
PAHs	Polycyclic aromatic hydrocarbons
PBS	Phosphate buffered saline
PCR	Polymerase chain reaction
PEST	Proline, Glutamic acid, Serine and Threonine
PH	Pleckstrin Homology domain
PI3K	Phosphatidylinositol 3-kinase
PIP	phosphatidylinositol phospholipids
PPC	Percentage of positive cells
PPIB	peptidylprolyl isomerase B
PPN	Percentage of positive nuclei
PtdIns (4, 5) P2	phosphatidylinositol 4, 5 biphosphate
PtdIns(4) P-5-kinase	phosphatidylinositol 4-phosphate 5-kinase
PVL	Proliferative verrucous leukoplakia
qRT-PCR	Quantitative real time polymerase chain reaction
RalBP1	Ral-binding protein 1
RBP-Jκ	Recombination Binding Protein-Jκ
RIPA	Radio-immuno precipitation assay
RNA	Ribonucleic acid
rpm	Revolutions per minute
RTKs	Tyrosine kinase receptor
RT-PCR	Reverse-transcription polymerase chain reaction
SCC	Squamous cell carcinoma
Shh	Sonic hedgehog

siRNA	Small interfering RNA
TACE	Tumour necrosis factor alpha converting enzyme
TGF-βR	Transforming growth factor-β Receptor
TGN	Trans-Golgi network
TMN	Tumour, Node, Metastasis
UIM	Ubiquitin Interacting Motifs
VEGF	Vascular Endothelial Growth Factor
VEL	Visually Enhanced Lesion
WB	Western blot
xg	Times gravity

Table of contents

List of figures

List of tables

Chapter 1 **Introduction**

1.1 Oral Squamous Cell Carcinoma

Oral cancers are malignant neoplasms of epithelial tissue or other structures in the mouth. They can either originate from the oral cavity or represent metastasis from other sites. Oral cancer is the 8th and 13th most frequent malignancy in the world for males and females, respectively (McCullough et al. 2010). The most common type of oral cancer is squamous cell carcinoma (OSCC) which constitute more than 90% of all types (Johnson et al. 2011). Conway et al reported that between 1990 and 1999 there was an increase in the incidence rates for oral cancers in UK (Conway et al. 2006). Despite recent therapeutic advances, prognosis has not improved over the last decades and the 5-year survival rate remains within 35-45% (Lacy et al. 2000; Warnakulasuriya 2009) largely because of the advanced stage at diagnosis of most of the oral cancers.

1.1.1 Aetiology

There are different aetiological risk factors that are thought to be responsible for developing an OSCC. The main are: smoked and smokeless tobacco, excessive alcohol consumption, viral infection, mainly with Human Papilloma Virus (HPV), but also hepatitis C virus (Mahale et al. 2016). In addition, other risk factors, such as diet and nutrition, have been suggested to play an important role in oral and pharyngeal cancer (Lucenteforte et al. 2009). Previous studies reported that intake of diet rich in fruit and vegetable is inversely associated with the risk of cancer of the oral cavity and pharynx. The vegetable and fruit contain several micronutrients, as well as flavonoids, other polyphenols, and fibres. These components have antioxidant effects, and exhibit ability to bind and dilute carcinogens in the digestive tract (Lucenteforte et al. 2009). Other factors such as chewing betel quid habit, ionising radiation, and immune impairments can be sometimes relevant (Scully and Bagan 2009). Certainly, the principal cause for OSCC is tobacco (Johnson et al. 2011), as it contains about 60 different carcinogens, including tobacco-specific nitrosamines, polycyclic aromatic hydrocarbons (PAHs) and aromatic amines. Nitrosamines such as tyrosine kinase receptor 4-(methylnitrosamino)-1-(-3-pyridyl)-1-butanone (NNK) are the most significant carcinogens (Hecht 2003). Metabolization of NNK via hydroxylation lead to formation of methyldiazo-hydroxide, which bind to guanine residues of DNA (Kanojia and Vaidya 2006). These chemical changes activate trans-versions of nucleotide in important genes, such as tumour suppressor TP53 gene (Hunter et al. 2005).

Moreover, tobacco produces oxygen free radicals (OFR) that cause oxidative stress on the cells. Long-term oxidative stress can lead to DNA damage and mutagenesis (Dreher and Junod 1996).

Alcohol can enhance oncogenesis in several ways, for example ethanol which is the main constituent of alcohol increases the permeability of the cell membrane through impairment of its phospholipids and as a result the entrance of tobacco-specific carcinogens across the oral mucosa can be promoted (Howie et al. 2001). An emerging oropharyngeal squamous cell carcinoma risk factor is HPV. A meta-analysis reported that HPV mainly HPV16 may be an important risk factor for OSCC (Miller and Johnstone 2001). Multiple types of epithelial lesions usually associated with infection of HPV, most of which are benign hyperplasia. The high-risk HPVs subgroup, includes types 16, 18, 31, 33, 35, 39, 45 and 52 (Alani and Münger 1998; Miller and Johnstone 2001). Oncogenic types of HPV ,mainly HPV16 and HPV18, can promote carcinogenesis in head and neck epithelia especially in the base of tongue, tonsils and oropharynx (McCullough et al. 2010). After the integration of high-risk virus into host genome, the HPV genes are expressed and encode oncoproteins. Among them, E6 and E7 proteins promote cell-cycle progression and viral Deoxyribonucleic acid (DNA) replication in differentiated keratinocytes. The E6 protein of high risk HPV binds and induces the degradation of TP53 tumour suppressor protein, whilst HPV-E7protein inhibits retinoblastoma tumour suppressor genes (Alani and Münger 1998), promoting malignant transformation of oral epithelia (Chen et al. 2012).

1.1.2 Diagnosis of OSCC

Unfortunately most oral malignant epithelial lesions show few or no symptoms and the tumour is not diagnosed until it is at an advanced stage. Late-stage diagnosed OSCC (TNM stage IV) has a five-year survival rate as low as 9% (Dost et al. 2014) .

Therefore, early detection and treatment is considered the key to improve patient survival rates (Mehrotra and Gupta 2011). Gold standard for early detection is still a visual inspection followed by a surgical biopsy in suspicious cases. However, there are multiple methods and techniques that have been tried to improve the diagnosis of potentially malignant and malignant oral epithelial lesions. These clinical diagnostic tools can be used to investigate and monitor tissue alteration in suspicious oral lesions and help in the detection of oral cancer. They are not a substitute for, but are adjunctive to surgical biopsy and include vital staining, chemiluminescence and autofluorescence (Farah and McCullough 2008), cytological tests such as computer-assisted analysis

brush biopsy and oral exfoliative cytology either by smear or liquid-based oral cytology methods (Mendes et al. 2011).

The conventional brush biopsy technique is based mainly on the collection of samples from a suspicious oral lesions using a disposable circular brush. After fixation of the samples onto the glass slide and staining according to Papanicolaou method, they are scanned and analysed microscopically using a computer-based imaging system (Patton et al. 2008). It is an uncomplicated, affordable and non-hazardous method used to exclude dysplasia (Mehrotra and Gupta 2011). Furthermore, this technique has more than 90% sensitivity and specificity (Scheifele et al. 2004). In the liquid-based technique a disposable curette is used to scrape the surface of the suspicious lesion and transport it to the vial containing preservative fluid, (which helps in direct fixation of the cells in the sample) subsequently stained using Papanicolaou technique (Navone et al. 2007). All the scraped tissue can be involved in the diagnosis because the cells are immediately fixed, therefore, the cellularity of each slide is high, and this makes the detection of abnormal cells easier. These cells can be handled for additional diagnostic technique such as molecular analysis (Mendes et al. 2011). Specific molecular markers such as Ki67 (Mehrotra et al. 2006), can supply the examiner with additional information that will be helpful in the early detection of malignant oral lesions. This method has approximately 94.7% sensitivity and 98.9% specificity (Navone 2009). Vital staining such as toluidine blue can also assist to detect suspicious oral lesions and guide biopsy, in particular when high-grade dysplastic lesions are present, but it cannot be used as a screening test (Mehrotra and Gupta 2011). Previous studies reported that toluidine blue mouth rinse has about 20.5% false negative rate, and the sensitivity for invasive carcinoma was 100%, while for epithelial dysplasia it was 79.5% (Warnakulasuriya and Johnson 1996). Another procedure which is used to visualize white oral mucosal abnormalities is called ViziLite, and it uses chemiluminescent light. The oral tissue that has to be assessed is treated with acetic acid solution, and then visualized with ViziLite. Normal epithelia will absorb the light and appear dark with a blue shade; whereas an abnormal lesion will appear white, the so called aceto-white lesions (Farah and McCullough 2007). The nuclear to cytoplasmic ratio of dysplastic tissue is increased, and the enlarged nucleus reflects the light and appears white. However, ViziLite illumination is unable to discriminate between keratotic, inflammatory, malignant or potentially malignant white lesions (Farah and McCullough 2007). Despite the lack of rigorous scientific and clinical evidence, ViziLite has been approved by the FDA as an adjunctive screening tool for use in oral cavity, thus,

making it the only FDA-cleared medical device for such an application. Visually Enhanced Lesion Scope (VELScope) is another direct visualization method that has been employed to examine the oral tissue by fluorescence to detect the high-risk, potentially malignant and early malignant lesions. A blue excitation light is applied to evoke green-red fluorescence from fluorophores and is directed to the suspicious oral lesion. The examiner can watch the changes in the colour directly via an attached eye object. The normal tissue will emit pale green fluorescence while potentially malignant or dysplastic cells appear from dark green to black. Preliminary evidence suggests that VELScope unlike ViziLite can differentiate between inflammatory mucosal lesions and dysplastic lesions (Farah and McCullough 2008).

1.2 Oral epithelia dysplasia

The presence of dysplastic areas in the epithelium of the upper aero-digestive tract is believed to be associated with a high likelihood of progression to OSCC. However, non-dysplastic lesions may transform too. The term dysplasia identifies architectural disturbance of oral mucosa accompanied by cytological atypia (variation in the size and shape of the keratinocytes) (Warnakulasuriya et al. 2008). The percentage of malignant transformation of oral mucosal lesions that display dysplasia varies between 6 and 36% (McCullough et al. 2010). The histological examination of squamous epithelium showed different changes which can be divided into five stages : Squamous cell hyperplasia, Mild dysplasia, Moderate dysplasia, Severe dysplasia and Carcinoma in situ (Barnes 2005). Recently, the WHO classification of epithelial dysplasia has been modified, the grade of epithelial dysplasia is divided into three stages: mild, moderate and sever dysplasia which represent carcinoma in situ (Müller 2017). However, the binary grading system (high-grade and low-grade) is recommended but requires validation before being used (Gale et al. 2014).

Squamous cell hyperplasia characterized by formation of simple hyperplasia. The mild stage of dysplasia shows disruption in the structure of the lower third of the epithelium with slight cytological atypia. In moderate dysplasia, the disruption involves the middle third of epithelium and there is considerable increase in the degree of cytological atypia. In the severe form more than two thirds of the epithelium shows architectural disruption and the cytological atypia become more obvious. Carcinoma in situ is characterized by involvement of the full thickness of the epithelium with marked cytological atypia (van der Waal 2009). Clinically oral epithelial dysplasia (OED) has

two main different appearances: leukoplakia, and erythroplakia and a combination of the two (erythroleukoplakia) (Ho et al. 2012). However, the histological features are insufficient to identify accurately which dysplastic lesion can progress to Squamous cell carcinoma (SCC) (Zhang and Rosin 2001).

Leukoplakia has been defined as ‘‘White plaques of questionable risk having excluded (other) known diseases or disorders that carry no increased risk for cancer’’(van der Waal 2009). Clinically, leukoplakia can be subdivided in a homogeneous type and a non-homogeneous type. The clinically appearance of homogeneous leukoplakia is a white smooth flat lesion that sometimes shows fissures and wrinkles on its surface. Non-homogenous leukoplakia usually presents as a white or white and red lesion, which could be irregularly flat (speckled), nodular or verrucous (warty-like) (van der Waal and Axéll 2002). Verrucous leukoplakia can be difficult to be distinguished from a verrucous carcinoma. Proliferative verrucous leukoplakia (PVL) is a subtype of verrucous leukoplakia that is characterized by multifocal presentation, resistance to treatment and a high rate of malignant transformation (Arduino et al, 2013). Clinically, PVL can be seen as a multifocal disease that may involve any site of the oral mucosa. It has a white grainy or verrucous keratotic surface. The lesion at the beginning looks flat, but then with progression it becomes more exophytic and has a verrucous appearance. PVL is typically recalcitrant to treatment and shows high degree of malignant transformation (Cabay et al. 2007). Erythroplakia appears as an intense red patch that cannot be defined clinically or pathologically as any other lesion and can occur in any site of the oral cavity. The lesion is almost always unilateral which makes distinguishing it from other red lesions such as for example erosive lichen planus easier because the latter is usually bilateral (van der Waal 2009).

1.3 Molecular alteration in OSCC

Oral carcinogenesis develops through a multistep process, and there are several histological and molecular alterations that participate in the development of OSCC, involving the accumulation of multiple genetic alterations. The alterations such as mutation, loss of heterozygosity, deletions, or epigenetic modifications such as methylation. The targets of mutation include growth-promoting oncogenes, growth-inhibiting tumour suppressor genes and genes that regulate apoptosis (Perez-Sayans et al. 2009). Proto-oncogenes encode protein responsible for activation of cell division and inhibition of differentiation and death. Mutated proto-oncogenes, which are called oncogenes, causes normal cells to escape from normal growth control mechanisms

and become cancerous (Chial 2008). Amplification of different oncogenes such as c-myc, K-ras, ErbB-1 genes (Wong 1987; Eversole and Sapp 1993; Caulin et al. 2004) was reported to be associated with the progression of OSCC. Ki67 a human nuclear protein which is associated with cell proliferation and it is widely used as a proliferation marker. It was reported that dysplastic mucosa and mucosa which undergoes malignant transformation have higher Ki67 expression than normal mucosa (Humayun and Prasad 2011). Moreover, cases of high risk of oral epithelial dysplasia have higher Ki67 expression than low risk cases of oral epithelial dysplasia, suggesting that Ki67 is a proliferative marker which can be used for the diagnosis of oral epithelial dysplasia which have a tendency to undergo malignant transformation (Birajdar et al. 2014).

Tumour suppressor genes in oral cancer have been analysed in many studies. Mutations and subsequent inactivation of a tumour suppressor genes causes loss of function and loss of activity that leads to malignancy. The tumour suppressor genes TP53 and Rb are the most studied genes (Naik et al. 2015). TP53 encodes a critical tumour-suppressor protein and is mutated in over 50% of squamous cell carcinomas of head and neck (Nylander et al. 2000). In normal cell biology, TP53 acts as a gatekeeper of G1 phase of cell cycle. It is responsible for regulation of DNA synthesis and in case of DNA damage, TP53 protein level strongly increases permitting repair of damaged DNA prior to DNA synthesis. If the damage is too big, and the DNA repair fails, TP53 may trigger apoptosis (Liu and Gelmann 2002). Accordingly, mutation of TP53 therefore resulting in loss of this critical tumour-suppressor function. TP53 is upregulated in OSCC and oral premalignant lesions such as oral leukoplakia, and oral sub mucous fibrosis when compared to normal oral mucosa (Varun et al. 2014). Cyclin dependent kinase inhibitor 2A (CDKN2A) is a tumour suppressor gene that encodes p16INK4 and is localized on chromosome 9p21 and can be found mutated or methylated in SCC of head and neck (Reed et al. 1996).

OSCC has about 45% survival rate, this is mainly because most OSCC cases are diagnosed at late stage and OSCC has high recurrence rate (Lacy et al. 2000; Warnakulasuriya 2009). The suspicious oral lesions are usually diagnosed by clinical and histological examination, but malignant changes may be undetectable. Thus the need for sensitive and specific biomarkers that are objectively measurable in small biopsy samples, and altered in high-risk tissue in the earliest stages of carcinogenesis may be helpful for screening high-risk patients. This can help in diagnosis and

treatment of oral cancer without delay and could lead to better prognosis (Wu et al. 2010).

1.4 Endocytosis

Endocytosis is the mechanism used by mammalian cells in order to uptake and internalize extracellular materials (small molecules, macromolecules and particles) and target them to specific closed organelles within the cytoplasm. Endocytosis consists of different pathways including: phagocytosis (cell eating) which is found in several cells types particularly in specialized cells like macrophages and it is responsible for the uptake of large particles (Swanson 2008); macropinocytosis (cell drinking) or the uptake of fluids (Kerr and Teasdale 2009), and micropinocytosis, which is the uptake of smaller particles. Micropinocytosis comprises clathrin-dependent receptor-mediated endocytosis (clathrin-mediated endocytosis) and clathrin-independent endocytosis (non-clathrin-mediated endocytosis), which are found in all nucleated vertebrate cells and have an important role in several physiological processes (Mukherjee et al. 1997).

1.4.1 Clathrin dependent receptor-mediated endocytosis

The major and the best understood route for endocytosis in most cells, is mediated by the molecule clathrin (Mukherjee et al. 1997). The clathrin-mediated endocytosis pathway is responsible for uptake and internalization of nutrients, pathogens, growth factor receptors and different plasma membrane related molecules, and it has an essential role in signal transduction (McMahon and Boucrot 2011). The macromolecules to be internalized first bind to specific cell surface receptors that are concentrated in specialized regions of the plasma membrane, called clathrin-coated pits. These pits bud from the membrane to form small clathrin-coated vesicles containing the receptors and their bound macromolecules known as ligands (Goldstein et al. 1979). The clathrin-coated vesicles (CCV) then fuse with early endosomes, in which their contents are sorted for transport to lysosomes or recycling to the plasma membrane. These CCV are surrounded by a skeleton of clathrin protein and connected to the cell membrane through the clathrin adaptors. The clathrin adaptors are proteins which work to join the grate of clathrin with the protein or lipid constituent of a membrane during clathrin-mediated endocytosis events (Owen et al. 2004), and have the main function of choosing which cargo molecules should be incorporated into CCV.

1.4.2 Types of adaptors for coated vesicles

The coated vesicle adaptors were called adaptor proteins or assembly polypeptide (AP) (Robinson 2004). It had been thought that, in mammalian cells there are two types of clathrin-associated adaptors: AP-1, which is found on the trans-Golgi network (TGN) and endosomes, and AP-2 which is found close to the cell membrane (Ahle et al. 1988). Two additional adaptor complexes were discovered, AP-3 and AP-4, although these two types are not enriched in CCV, and are usually localized on the TGN and endosomal membrane (Robinson and Bonifacino 2001).

Golgi-localized, γ-ear-containing, ARF-binding proteins [(ADP-ribosylation factor) family of proteins belongs to the Ras superfamily of small GTPases] (GGAs), is another group of clathrin adaptors that have been recently discovered. They are monomeric and have a C-terminal domain which is connected to the ear domain of the γ subunit of AP-1 (Robinson 2004). More recently, new adaptors which are correlated to the appendage domain of α or β chain of AP-2 have been discovered. These proteins called Epsins act as a cargo-specific adaptor on the endocytic pathway (Traub 2003).

1.4.3 The structure of adaptor proteins (AP)

Each adaptor complex is a hetero-tetramer (Pearse and Robinson 1990), which is comprised of four subunits, two ≈100 kDa, one ≈ 50 kDa medium chains(μ) and one ≈ 20 kDa small chain (σ). AP-1 usually contains β1, γ, μ1 and σ1, while AP-2 contains β2, α, μ2, σ2 (Mellman 1996). The structure of these adaptor complexes is presumed to be similar, which appears like Mickey Mouse's head. The medium and small subunits with amino-terminal domains of large subunits form the head, which is connected to its carboxy-terminal appendage through a flexible hinge (Robinson and Bonifacino 2001).

1.4.4 Membrane recruitment of adaptors

Clathrin adaptors are peripheral membrane proteins and recruitment of these proteins to appropriate organelles can be achieved through one of two pathways: the first one is activated membrane-associated small G proteins which are from the Arf/Arl/Sar and Rab family. The second one is a short-lived phospholipid species, mainly phosphatidylinositol phospholipids (PIP) (Owen et al. 2004). The location of the GTP exchange factor (GEFs) and the GTPase-activating proteins (GAPs) is the determinant for distribution of the small G proteins to the considered location, while the distribution of the PIP factor is determined by the enzymes which add or remove the phosphate group from its head groups (Munro 2002). It seems that the two mechanisms are

interconnected, as some PIP enzymes are peripheral membrane proteins themselves and can be recruited concurrently with the activation of small G proteins, for example: phosphatidylinositol 4-phosphate 5-kinase (PtdIns(4)P-5-kinase) depends in its recruitment to the plasma membrane on Arf6 (Krauss et al. 2003). Moreover, some peripheral membrane proteins like AP1 attach to both PIPs and Arf1 (Wang et al. 2003). PIPs are considered as markers for different organelles of the membranes for example, phosphatidylinositol 4, 5 biphosphate [PtdIns (4, 5) P2 or PIP2] and PtdIns (3, 4, 5) P3 are responsible for marking the plasma membrane. PtdIns(4)P mark Golgi and PtdIns(3)P, PtdIns(3,5)P2 mark various endosomal tracts and yeast vacuole (Simonsen et al. 2001; Munro 2002) . Different clathrin adaptor domains connect in particular to these PIPs in order to assist the mechanism for targeting the adaptors with clathrin and other proteins to their exact position. PtdIns(4,5)P2 has been shown to be the main factor in the regulation of plasma membrane trafficking (Cremona and De Camilli 2001). It has a binding site on the α subunit of AP-2, and if there is mutation on this site, the normal localization of AP-2 complex will break down (Collins et al. 2002). It was reported that when the lysine residues of the α subunit, which is found at the core of the PtdIns(4,5)P2 binding site, are replaced by alanine, the affinity of AP-2 for plasma membrane is reduced (Gaidarov and Keen 1999). In agreement with these findings, further research showed that the blocking of PtdIns(4,5)P2 with either neomycin, or the pleckstrin homology domain (PH) of phospholipase C, suppresses the binding of AP-2 to the plasma membrane (West et al. 1997).

1.4.5 Endocytosis and signals

Endocytosis has long been thought as a relatively simple process for cells to transport and internalize nutrients and other plasma membrane molecules. However, advancement in knowledge has led to expand the general understanding of endocytosis, suggesting that the endocytosis play an important role in regulating cell signalling. Endocytosis regulates signals at the plasma membrane through modulating the presence of receptors and their ligands. Ligands-induced activation of signaling receptors at the plasma membrane, the active signalling receptors will be removed from the plasma membrane by entering the endocytic pathway and consequently lead to signal attenuation. The regulation of signalling by endocytosis takes place either before entry of the receptor at the plasma membrane or by entry of receptors into different endocytic routes that modify the signalling duration or it can occur after endosome formation (Sigismund et al. 2012).

At the plasma membrane, different mechanisms take place to control receptor signalling. The negative regulation of cell surface signals is one of these mechanisms (negative-feedback loop). In this mechanism, ligand-induced internalization of their relative receptors, such as tyrosine kinase receptors (RTKs) and G protein-coupled receptors (GPCRs). Continuous ligand stimulation induces receptor degradation and reduction of their numbers at the plasma membrane, which result in signals attenuation (Sorkin and Von Zastrow 2009). At the plasma membrane, endocytosis can also regulate ligand accessibility that results in activation of signals, for example Notch signalling. Binding of Notch receptors to active ligand results in several proteolytic cleavages and leads to release of the notch intracellular domain which is translocated to the nucleus to activate transcription of target genes (see section below).

The other signalling controlling mechanisms take place by entry of receptors into different endocytic routes that determined the final output of the signals. Epidermal Growth Factor Receptor (EGFR), Transforming Growth Factor-β Receptor (TGF-βR), Notch and Wnt receptors are some of these receptors that can be internalized by two routes, either clathrin-mediated endocytosis or non-clathrin-mediated endocytosis. For example EGFR and TGF-βR utilize the clathrin-mediated endocytosis route for recycling which results in sustainment of signalling, whereas non-clathrin-mediated endocytosis for degradation which results in attenuation of signals (Scita and Di Fiore 2010). The signal controlling can occur at the endosomes. At this stage the internalized receptors or cargo proteins are sorted into intracellular organelles called endosomes. From these endosomes, the internalized cargo is either transported to lysosomes for degradation or recycled back to the plasma membrane (Sorkin and Von Zastrow 2009).

1.5 Notch signalling pathway

The Notch signalling pathway is a highly conserved mechanism that is found in almost all multicellular organisms, and plays an important role in cell fate through regulation of the programs responsible for cell growth, apoptosis and differentiation (Artavanis-Tsakonas et al. 1999). Mammalians have four Notch genes (Bianchi et al. 2006).

Notch1 gene usually encode proteins which are expressed in presomitic mesoderm (Wong et al. 1997). Notch2 complements Notch1, and both are required to regulate the interaction of somite condensation cells. Notch3 and Notch4 have been only identified in mammals (Bianchi et al. 2006).

1.5.1 Notch structure

Notch signalling has a simple framework which consists of a notch receptor and its ligand and both are transmembrane proteins (Bray 2006). The notch gene, which was identified at first in Drosophila melanogaster, encodes a 300 kDa transmembrane receptor located on the plasma membrane surface. This receptor is composed of a large extracellular domain that is required for binding the ligand and of an intracellular domain needed for transporting the signal (Artavanis-Tsakonas et al. 1999). The Notch Extracellular Domain (NECD) contains varying numbers of repeated motifs (about 26-36 repeats) which belong to the epidermal growth factor, called EGF like repeats (ELRs), constantly three LNR repeats (Lin-12, Notch Repeats), and area that binds to the transmembrane protein and intracellular particle (Bray 2006). Notch Intracellular Domain (NICD) containing a RAM23 motif which is responsible for the activation of the CSL DNA binding protein interaction, six cdc10/ ankyrin (Ank) repeats that regulate the interaction with CSL [CBF1 in mammals, Su(H) Suppressor of Hairless from Drosophila and LAG1 from C-elegans] (Kimble and Simpson 1997; Greenwald 1998) and other proteins. There is also a C-terminal domain which is rich in more than one type of amino acids residues such as proline, glutamic acid, serine and threonine (PEST). In addition, NICD contains nuclear localization signals (NLS) (Weinmaster 1997) (Figure 1.1).

Notch ligand is also has an extracellular domain which is composed of Delta, Serrate and LAG-2 (DSL) family that contain N-terminal (NT) domain that is necessary for interaction with the extracellular domain of notch receptors. These ligands are usually classified into two types: Delta or Delta-like (Dll) and Serrate (Jagged in mammals)

(Bray 2006). The ligand family of mammals is typically composed of the following five groups: jagged1, jagged2 and Delta-like 1, 2, 3. Moreover, the extracellular domain of these ligands in all species contain different numbers of ELRs which are thought to play a role in receptor binding stabilization (Leong and Karsan 2006). The NT domain with adjoining DSL part constitute the EGF-motif binding domain (EBD), which mediates the binding of ligand and receptor (Fleming 1998).

1.5.2 The mechanism of Notch signalling pathway

The notch protein is a large single-chain that needs to be glycosylated and cleaved in order to be introduced into the cell surface. The glycosylation of Notch usually takes place in the endoplasmic reticulum (ER) and is accomplished in the Golgi. When still intracellular, Notch is cleaved by a furin-like protease at the S1 cleavage site, producing a mature heterodimeric receptor (Bianchi et al. 2006). Then, ligand binding initiates notch signalling. The binding of the Delta Serrate ligand to the ELR 11and 12 of extracellular domain of notch receptor will activate the subsequent two proteolytic cleavage processes in this receptor at S2 and S3 cleavage sites (Figure 1.1). After ligand binding, endocytosis is stimulated by the action of the neutralizing protein such as Mind bomb (Mib) and Neutralized (Neur) which add an ubiquitin protein to the delta intracellular domain (Bianchi et al. 2006). Delta signalling in Drosophila and C-elegans can also be activated by adaptors of clathrin-mediated endocytosis called Epsins (Overstreet et al. 2004). The S2 cleavage will immediately start, activated by an ADAM-family metalloprotease called Tumour Necrosis Factor Alpha Converting Enzyme (TACE) and it leads to the release of an extracellular portion of notch receptor just outside the membrane of the signal receiving cell (Brou et al. 2000). As a result, the ubiquitinated ligands with NECD are endocytosed by the signal sending cell. The Notch receptor then goes through another proteolysis at S3 cleavage site of the intracellular domain through the action of γ-secretase complex enzyme (presenilin, nicastrin, PEN2 and PAH-1) (Edbauer et al. 2003). Accordingly, the NICD is released in the cytoplasm of the signal receiving cell and transferred to the nucleus in order to interact with the DNA- bound CSL protein complex (CBF1/RBP-Jκ (Recombination Binding Protein-Jκ) in humans, Su(H) in *Drosophila*, and Lag-1 in *Caenorhabditis elegans*) (Borggrefe and Oswald 2009). NICD converts the complex from a repressor to an activator of Notch target gene transcription (Kopan 2002) with presence of Mastermind-like protein (MIML) as co-activator (Bray 2006). The co-activator MIML binds with the histone acetyltransferase p300 that activates assembly of co-activator

complex and as a result promotes transcription (Wallberg et al. 2002). The NICD is then phosphorylated by cyclin-dependent kinase-8 (CDK8) that makes NICD a substrate for SEL-10 (nuclear ubiquitin ligase) (Bray 2006) and exported to the cytoplasm in order to degrade. The absence of notch activity promotes CSL to bind with co-repressors such as SMRT (NcoR), SHARP (MINT/SPEN), SKIP and CIR (CBF) (Kao et al. 1998; Oswald et al. 2005) and causes inhibition of transcriptional activation (Mumm and Kopan 2000).

It has been shown that Notch signalling has a role in the self-renewal of stem cells and their fate, apoptosis, proliferation and migration (Politi et al. 2004). It is essential for the development of mammals, because the renewal of tissues during life is usually dependent on the storage of uncommitted stem cells (Artavanis-Tsakonas et al. 1995). Notch signalling is involved in the development of embryonic tissues derived from all 3 primary germ layers and regulates the development of postnatal tissues and maturation of adult tissues (Artavanis-Tsakonas et al. 1999). It is thought that Notch signalling can affect both apoptosis as well as proliferation. For instance, Notch activation in murine erythroleukemic cells inhibits apoptosis (Jehn et al. 1999; Shelly et al. 1999) . Conversely, expression of the active Notch receptor on the dorsal-ventral or anterior-posterior edge of *Drosophila* wing causes triggering of mitotic activity (Artavanis-Tsakonas et al. 1999). Accurately regulated Notch signalling is considered as a key factor in tissue development, and any disturbances to Notch signalling can result in tissue abnormalities that may manifest as neoplasia (Leong and Karsan 2006). For example: in Drosophila, when Notch signalling is manipulated in uncommitted cells, it can push these cells to follow abnormal fates. Similarly, Notch activation in the immature mammalian cells could lead to change the fate of these cells (Artavanis-Tsakonas et al. 1995).

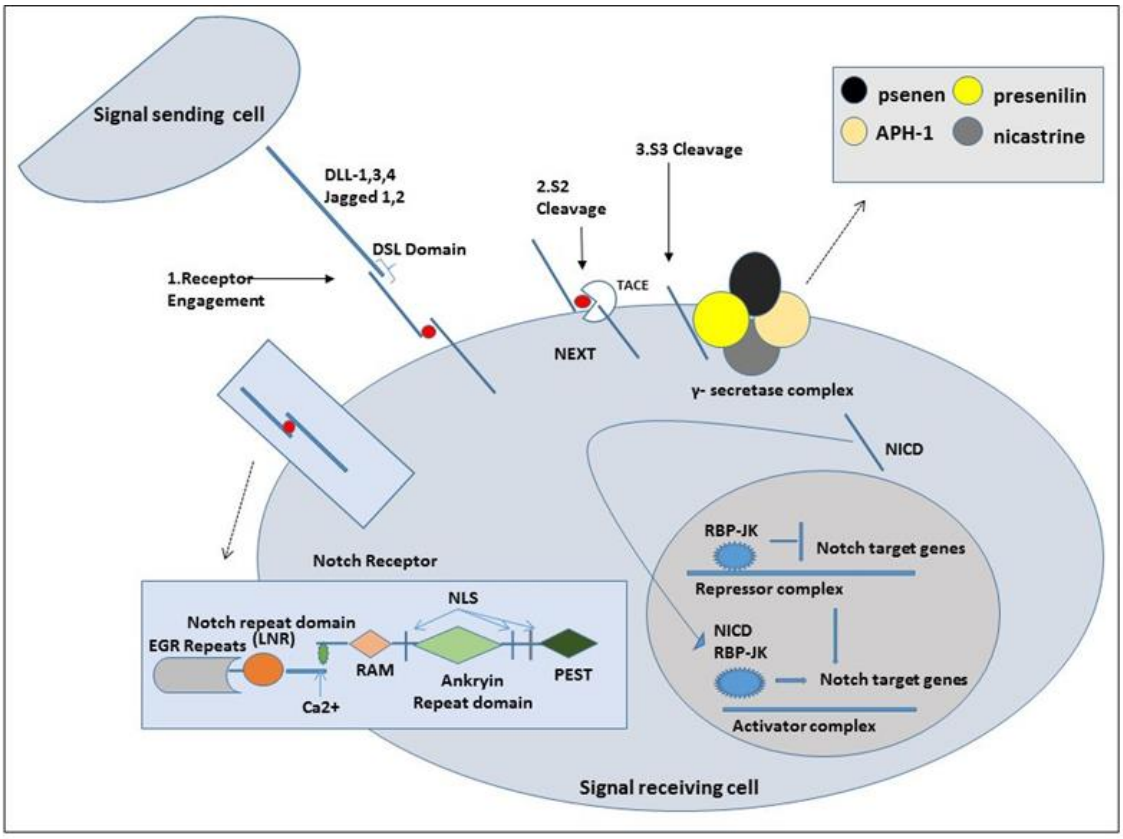

Figure 1.1: Notch Signalling

Binding of Notch receptor with its specific ligands leads to cleavage of the receptor at site S2 which is activated by TACE. The remaining Notch receptor is subjected to another cleavage at site S3, which is activated by gamma secretase complex enzyme. The released NICD is translocated to nucleus and binds with repressor complex RBP-JK converting it to the activator complex which promotes transcription of target genes. Inset, schematic representation of Notch receptor protein. The EGF repeats are contributing to attraction of the ligand; LNR is a negative regulator of Notch protein activity; the RAM motif activates interaction between NICD and RBP-Jκ; Ankyrin repeats regulate the interaction with the RPB-Jκ; C-terminal PEST domain is rich in different amino acids residues such as proline, glutamate, serine and threonine and plays role in degradation of the NICD. Adapted from (Capaccione and Pine 2013).

1.5.3 Notch target genes

The interaction of Notch receptors with their ligands (Delta or Jagged) results in activation of the signals and release of NICD that bind with RBP-Jk and convert it from corepressor to coactivator which subsequently activate transcription of target genes. The best studied examples are the Drosophila proteins hairy and enhancer of split, homologues to human hairy and enhancer of split (Hes) (Jarriault et al. 1998) and hairy/enhancer-of-split related with YRPW motif (Hey) families (Bailey and Posakony 1995). Both Hes and Hey have basic helix-loop-helix domain, and WRPW motif, that directly bind to DNA and act as direct repressors of transcription. Hes1, Hes5, Hes7, Hey1, Hey2 and HeyL are the main Notch target genes and they can be activated by Notch1 (Borggrefe and Oswald 2009). In mammals, these genes are expressed in various tissues and play an essential role in development (Fischer and Gessler 2007). There is some evidence suggesting that these genes are the direct Notch target genes. For example, endogenous expression of Hey1 and Hey2 is usually upregulated by NICD in some cell lines (Iso et al. 2003). Moreover, impaired Notch pathway in double knockout mice results in reduction of target genes expression mainly of Hes1, 5, 6, 7, Hey1 and 2 and HeyL (Chen et al. 2009). In human osteosarcoma, Notch signalling is upregulated and its target genes Hes1 and Hey2 show transcriptional upregulation (Engin et al. 2009). In another study, treatment of OSCC cell line CAL-27 with curcumin, which is known to inhibit cell growth and induce apoptosis, results in downregulation of Notch1 and its target genes Hes1 and 5 and Hey1 (Liao et al. 2011). Furthermore, treatment of hemangioma stem cells with the gamma secretase inhibitor (GSI) Compound E, which blocks the cleavage by γ-secretase and thus impairs the release of the NICD into the nucleus, caused down regulation of Notch signalling. Consequently, the transcript levels of several HES/HEY genes were reduced, indicating that active Notch signalling maintains the expression of these genes (Adepoju et al. 2011).

1.5.4 Notch and cancer

The highly conserved Notch signalling pathway has a fundamental role during development of embryo. It regulates the programs responsible for differentiation, proliferation, and apoptosis, and control cell fate through maintenance cell-to-cell interactions. The Notch signalling has diverse roles during development: the signal outcome is mainly determined by signal dose and condition and it could lead to survival

or death, increase proliferation or inhibition of growth and promote or inhibit differentiation. In cancer, Notch can be either oncogenic or suppress tumour formation (Roy et al. 2007). Dysregulation of Notch signalling components (receptors and ligands) results in disturbance of the signals and aberrant Notch activation and it has been linked to a variety of human neoplasms. Several studies showed that the activation of Notch could be oncogenic. The most typical example is T-acute lymphoblastic leukaemia/lymphoma (T-ALL). It was reported that two types of activating mutations in Notch-1 are present in most cases of human T-ALL (Weng et al. 2004). Recent studies reported that Notch1 suppresses TP53 in T-ALL which may result in promotion of oncogenesis by increases cell survival and genomic instability (Beverly et al. 2005). The expression of Notch receptors and their downstream target genes is upregulated in several other cancers. For example, ovarian adenocarcinoma and adenoma revealed elevation of Notch1 expression, and stable transfection of A2780 ovarian cancer cell line with NICD enhance cell proliferation suggesting a role for Notch1 signalling in ovarian tumour growth (Hopfer et al. 2005).

High level of expression of Jagged1 ligand is reported to be associated with metastasis in prostate cancer as compared with localized prostate cancer or benign prostatic tissues, and the level of expression is high in cases with recurrence, indicating that Jagged1 expression level is associated with prostate cancer progression and metastasis (Santagata et al. 2004).

Increased expression levels of Notch1 and Jagged1 are associated with poor prognosis in breast cancer, suggesting that Notch signalling is activated in aggressive breast cancer (Reedijk et al. 2005). Additional evidence suggests that most breast cancer cell lines display loss of Numb expression that is an inhibitor of Notch signalling. The loss of Numb gene in these cells was inversely correlated with NICD expression, cell proliferation and tumour grade (Pece et al. 2004).

Moreover, Notch receptors and their target genes have been thought to be up regulated in human melanoma (Hoek et al. 2004; Balint et al. 2005). Studies reported that pharmacological blocking of Notch signalling in the melanoma cell lines could suppress the growth of these cells (Nickoloff et al. 2005). Moreover, constitutive activation of Notch1 stimulates primary melanoma cells to proliferate and enhances tumour cell survival. Activation of Notch signalling in melanoma cells mediates activation of the mitogen-activated protein kinase (MAPK) and Akt pathways and

inhibition of either the MAPK or the phosphatidylinositol 3-kinase (PI3K)-Akt pathway reverses the effect of Notch1 signalling to induce tumour cell growth (Liu et al. 2006).

Other studies reported that inhibition of Notch signalling occured in medulloblastoma cell lines and primary tumour cultures resulted in reduction of viable cells number. Indeed, the use of γ-secretase inhibitor or soluble Delta ligands resulted in increased apoptosis and reduction of viable cells, confirming that Notch signalling has a role in proliferation and survival of cells in human medulloblastoma (Hallahan et al. 2004).

Notch receptors, ligands and target gene Hes1 were found to be also upregulated in pre-neoplastic lesions and invasive pancreatic cancers in human and mice (Miyamoto et al. 2003; Kimura et al. 2007).

Non-small-cell lung cancer is another form of malignant tumour where Notch signalling promotes oncogenic function, transgenic mice overexpressing active Notch1 in alveolar epithelium developed alveolar hyperplasia and cooperation of Notch1 with Myc led to change in the ratio of apoptosis and proliferation of cells, which promotes progression from adenomas to adenocarcinoma (Allen et al. 2011). It was also reported that high Notch1 expression was associated with poor outcomes in non-small-cell lung cancer (Donnem et al. 2010).

However, Notch signalling can also have a tumour-suppressor activity. The best studied example is the role of Notch in skin. Human and mouse in vitro studies suggest that Notch signalling induces differentiation of keratinocytes, which is associated with end of cell cycle (Lowell et al. 2000; Rangarajan et al. 2001; Nguyen et al. 2006). In the keratinocytes, Notch signalling induces two different pathways that result in inhibition of growth and differentiation of keratinocytes. The first one triggers the expression of Notch target gene $p21^{WAF/Cip1}$ which is a cell cycle regulator that leads to cell cycle withdrawal and terminal differentiation. The second pathway activates the expression of early differentiation markers, including Keratin1/10 and involucrin, and downregulates the expression of late markers including integrin (Rangarajan et al. 2001). Moreover, loss-of-function mutation in Notch receptors was reported in cutaneous squamous cell carcinoma reflecting the suppressor function of Notch signalling (South et al. 2014). Nicolas et al. (2003), reported that epidermal knockout Notch1 in mouse display epidermal hyperplasia which developed into cutaneous basal cell carcinoma-like lesions. Any chemical injury to the epidermis of these mice that

inactivated Notch-1 causes cutaneous lesions that appear like basal cell carcinoma and squamous cell carcinoma (SCC). Deficiency of Notch1in the mouse skin led to increase Gli2 expression, which is downstream component of Sonic hedgehog (Shh) pathway, and resulted in dysregulation of this pathway and formation of basal-cell carcinoma like lesions. Upregulation of Gli2 gene and overexpression of Shh signaling in mice epidermis usually induces basal cell carcinoma (Grachtchouk et al. 2000; Dahmane et al. 2001).

Furthermore, inactivation of Notch1 leads to increased β-catenin-mediated signals , which are downregulated during epithelial differentiation of keratinocytes, and sustained Wnt signalling, that is the pathway dysregulated in basal cell carcinoma (Nicolas et al. 2003). In another study, Proweller et al. (2006) showed that generation of mice expressing a dominant negative Mastermind-like protein (MML), which inhibits Notch signalling, leads to development of lesions resembling cutaneous squamous cell carcinoma (CSCC) . Development of CSCC in the transgenic mice is associated with accumulation of nuclear β-catenin and cyclin D1, which is upregulated by β-catenin signalling. β-catenin signalling, is repressed directly or indirectly by Notch signalling (Hayward et al. 2005). Taken together, these observations suggest that Notch signalling may have a crucial role in the development and progression of skin basal cell carcinoma and SCC.

In conclusion, the function of Notch signalling, as oncogenic in some cancers and tumour suppressor in other cancers, suggest its dual role in normal biology: it may promote stem cell maintenance in some tissues and terminal differentiation in others (Roy et al. 2007).

1.5.5 Role of Notch signalling in head and neck cancer

Head and neck cancer is to a certain extent a homogeneous disease as more than 95% are squamous cell carcinomas (HNSCCs). However, HNSCCs, like many solid tumours, are thought to initiate and to progress through a multi-step carcinogenesis process with alteration of signalling pathways, suggesting that HNSCC is de facto a heterogeneous disease. Several cellular signalling pathways are dysregulated in HNSCCs such as, for example, TP53 and CDKN2A and they play a critical role in its pathogenesis (Leemans et al. 2011). Also Notch signalling has been demonstrated to have a crucial role in progression and development of HNSCC. However, the role of Notch signalling in OSCC is poorly identified, it appears that Notch signalling can have

either a tumour suppressing or promoting (oncogenic) function in OSCC (Yoshida et al. 2017).

Tumour suppressor role of Notch signalling in HNSCC

Notch signalling was reported to be mutated in HNSCC. The mutation appeared to be loss-of-function mutation of Notch1, 2 and 3, suggesting that Notch acts as a tumour suppressor gene in HNSCC. The Notch1 mutation is mainly located at or near epidermal growth factor (EGF)-like repeat within extracellular domain (Agrawal et al. 2011; Stransky et al. 2011). Duan et al. (2006) demonstrated that Notch signalling exhibit tumour suppressor function in tongue cancer: transfection of human tongue cancer cell lines Tca8113 with active Notch1 domain (NICD) resulted in suppression of cells growth, increasing of TP53 and $p21^{WAF1/CIP1}$ and downregulation of β-catenin that lead to downregulation of Wnt/β-catenin signalling and decreased Bcl-2 (B-cell lymphocytic-leukaemia proto-oncogene 2) and Skp2 (S-phase kinase-associated protein 2) expression. Pickering et al. (2013), reported that mutation of Notch pathway elements, including Notch1 and 2 receptors, loss of MAML1 activator protein, copy number gains in Jagged1, Jagged2 ligands and NUMB protein was observed in oral squamous cell carcinoma (OSCC). Despite the fact that Jagged1 and Jagged2 ligands are known to activate Notch signalling, they can also block the pathway by the cis-inhibition mechanism (D'Souza et al. 2008). Pickering et al suggested that the overexpression of these two ligands may contribute to tumour suppressor role of Notch signalling in OSCC (Pickering et al. 2014). Song et al demonstrated an EGF-like repeats Notch1 mutation in OSCC. They reported that the patients with this mutation had poor prognosis and showed worst overall survival and disease free survival compared to patients without Notch1 mutation (Song et al. 2014a). A similar mutation was also found in another study in OSCC cell lines. Moreover immunohistochemical analysis of Notch1 expression levels in the primary OSCC tissues and non-malignant tissues revealed higher expression level of Notch1 in the normal tissues compared to the OSCC tissues, (Yap et al. 2015). Notch1 downregulation was also observed in precancerous and cancerous epithelial cells compared to the normal cells, and Notch1 knockdown led to formation of a dysplastic lesion indicating that reduction of Notch1 expression lead to cessation of terminal differentiation of keratinocytes and formation of immature epithelium (Sakamoto et al. 2012).

Oncogenic role of Notch signalling in HNSCC

Upregulation of Notch signalling in HNSCC was reported in several studies. Overexpression of Notch signalling and its elements, including Notch1, Notch2 receptors and Jagged1 ligand, was found in HNSCC, suggesting that the Notch pathway may have a role in squamous cell carcinogenesis (Leethanakul et al. 2000). Later on, Zeng et al. (2005), described the role of Notch signalling in HNSCC angiogenesis. Increased expression of Jagged1 ligands in the HNSCC activates Notch signalling which enhances endothelial cells and resulted in formation of new vasculature that promotes tumour growth, suggesting the oncogenic role of Notch signalling in HNSCC. Furthermore, activation of Notch1 signalling and Notch downstream target, Hes1, was found to enhance cancer stem-like cells in OSCC. Moreover Hes1 expression was upregulated in OSCC lesions compared to normal and precancerous dysplastic lesions, suggesting the possible involvement of Notch1 and Hes1 in OSCC progression (Lee et al. 2012). Upregulation of mRNA of Notch1, Notch2, Jagged1, Hes1 and Hey1 was demonstrated in the OSCC cell lines and biopsy specimens, and inhibition of Notch pathway using γ-secretase inhibitor (GSI) led to inhibition of tumour growth in vitro. Moreover, immunohistochemical analysis revealed the expression of NICD and Jagged1 was higher in OSCC specimens compared to normal oral tissues (Hijioka et al. 2010). Upregulation of RNA and protein of Notch1 and NICD was also found in OSCC cell lines, and loss of Notch1 expression led to inhibition of cell proliferation in vitro. In addition, clinico-pathological analysis showed that Notch1 expression was correlated with both T-stage and clinical stage of OSCC patients, indicating that Notch1 has a role in OSCC progression. Moreover, inhibition of Notch1 signaling using GSI or knockdown Notch1, effectively reduces expression of NICD and Hes1 and inhibits growth of OSCC cell lines (Yoshida et al. 2013; Sun et al. 2014). The expression of NICD and Hes1 was found to be higher in dysplasia and OSCC tissues compared to normal (Gokulan and Halagowder 2014). It was reported that Notch1 plays an important role in tongue cancer, the level of Notch1 expression was positively associated with lymph node metastasis and tumour invasion (Joo et al. 2009). Furthermore, the levels of mRNA of Notch1, Jagged2 were higher in the tongue carcinoma compared to non-neoplastic tongue tissues, and the expression of Notch1 and Jagged1 were higher in tongue cancer tissues that showed positive lymph node metastasis (Zhang et al. 2011).

1.6 Epsins

Epsins are endocytic AP which promote the internalization of ubiquitous receptors on the cell membrane during clathrin-mediated endocytosis events. They consist of yeast Epsins (1 and 2), Drosophila melanogaster Epsins (known as Liquid Facets) and mammalian Epsins. Mammalian Epsins include: Epsin1 and 2, which are highly expressed in neuronal cells (Chen et al. 1998; Rosenthal et al. 1999), and Epsin3 which is enriched in keratinocytes (Spradling et al. 2001). In recent years, another type has been identified which is called EpsinR (Owen et al. 2004). These proteins have multiple interaction motifs that work together to direct Epsins to the plasma membrane and thereby promote its connection with specific cell surface receptors and bind these receptors to the clathrin-coated pits for internalization (Wendland 2002). Epsins have an N-terminal homology domain (ENTH), which interacts with PtdIns(4,5)P2 and activates the binding of Epsins to the plasma membrane and promote membrane curvature required for clathrin-coated pit formation (Itoh et al. 2001). The ENTH domain is accompanied by a long extension, which consists of an unfolded peptide string containing clathrin-binding motifs (Owen et al. 2004), AP-2 binding motifs and NPF (asparagine-proline-phenylalanine) motifs that bind to EH-domain (Eps15 homology) (Chen et al. 1998). Through these proteins, Epsins with their ubiquitinated cargo can be recruited to the clathrin-coated pits (Wendland 2002). It was reported that Epsins have two ubiquitin interacting motifs (UIM).They are located between ENTH domain and carboxyl-terminal group and combine with ubiquitinated cargo (Polo et al. 2002). According to this structure, Epsins have three functional locations: ENTH domain, which functions to bind lipid [PtdIns (4, 5) P2], C-terminal region which contain: NPF motif of EH domain of Eps15, clathrin-binding motif and AP-2 binding motif (DPW). In between these two regions (ENTH and C-terminal region) there is UIM that is required for Epsins ubiquitination (Figure 1.2). It had been suggested that Epsins utilise this UIM in targeting proteins that have ubiquitinated membrane in order to mediate endocytosis (Shih et al. 2002). Example of these ubiquitinated membrane proteins are notch ligands called DSL, which bind with the notch receptors and are ubiquitinated by E3 ubiquitin ligase [Neutralized (Neur) and Mind bomb (Mib)] (Wang and Struhl 2005). After DSL ubiquitination, they could be internalised and endocytosed in the signal-sending cell through the action of Epsins and accordingly, activate Notch in the signal-receiving cell (Wang and Struhl 2004). It seems that the absence of Epsins in the signal-sending cell blocks endocytosis of NECD and consequently, inhibits notch signal activation.

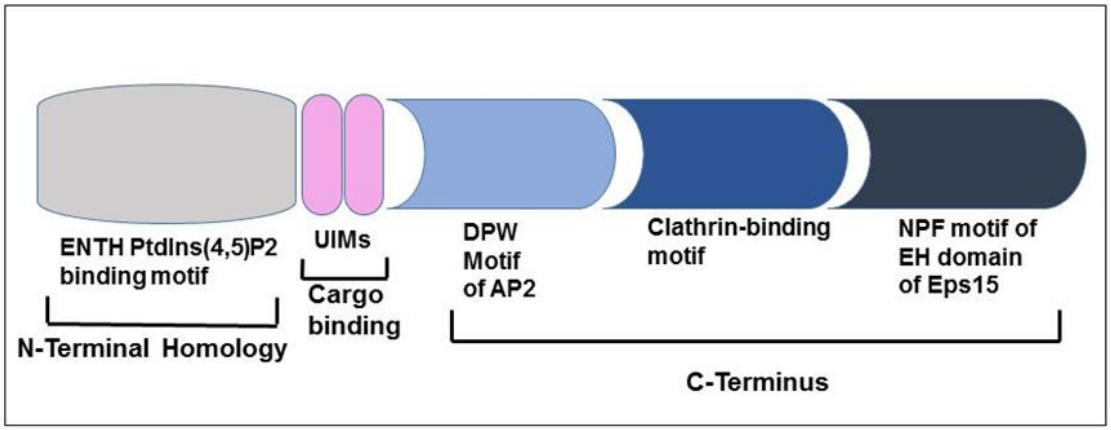

Figure 1.2: Schematic representation mammalian Epsin

Cartoon represents typical Epsin domain organization. Phosphatidylinositol-4, 5-bisphosphate; ENTH: Epsin N-terminus homology domain, UIM: ubiquitin-interacting motif. DPW: AP2-binding aspartate-proline-tryptophan (or aspartate-proline-phenylalanine) motifs. NPF, asparagine-proline-phenylalanine motif that binds to EH domain-containing proteins, such as Eps15. Adapted from (Wendland 2002).

1.6.1 Role of Epsins in cancer

It is widely accepted that endocytosis is one of the physiological process that is altered in cancer. The internalization, degradation or recycling of receptors by endocytosis through clathrin-coated vesicles (CCV) is usually dysregulated in cancer cells. CCV can select the receptors which intended for endocytosis by interacting with receptors that undergo posttranslational modification such as ubiquitination (Mellman and Yarden 2013). An irregularity in the endocytosis process could result in malignant changes of different tissues, as the endocytic proteins, such as Epsins, lack their normal function causing insufficient endocytosis (Coon et al. 2011). Epsins structure contain different domains: conserved NH2-terminal homology (ENTH) domain which is responsible for attachment of Epsins to the plasma membrane; ubiquitin-interacting motifs (UIM) which enable Epsins to interact with the ubiquitinated cargo, and an unstructured carboxyl-terminal motif which is responsible for bringing the cargo to coated vesicle for subsequent internalization. Epsins utilize these domains to select the specific cargos for endocytic internalization through clathrin-coated vesicles and regulation different pathways. As said above, the Notch signalling pathway, which determines the cell fate, requires endocytosis for its activation (Nichols et al. 2007). Chen et al. (2009), reported that double knockout of Epsin1 and 2 in mice resulted in developmental defects produced by inhibition of Notch signalling, suggesting a critical role of Epsins in the activation of Notch signalling. Epsins are the trigger for this pathway and it has been reported that any disturbance in the regulation of Notch signalling pathway would result in tumour formation. Epsins have been reported to be up regulated in multiple human cancers such as, for example, lung cancer (Coon et al. 2010). Moreover, Epsin3 shows high expression levels in gastric parietal cells of gastric tumours (Ko et al. 2010). Recently, Tessneer et al. (2013) reported that Epsin1 and 2 are upregulated in prostate epithelia and causes progression of prostate cancer. In addition to its role in endocytosis, Epsins were found to activate signalling through an additional mechanism that does not depend on the internalization of the receptors. It was reported that Epsins have the ability to interact with GTPase activating proteins (GAPs) of Rho GTPase family mainly Cdc42 and Rac1 (Mukherjee et al. 2009). The interaction of ENTH with N terminus of the Cdc42/Rac1GAP and ral-binding protein 1(RalBP1) causes inhibition of GAPs and as a result, the GTPase is accumulated. This accumulation leads to prolonged signalling transduction, which enhances cell invasion and migration (Coon et al. 2010). It was found that Epsin3 is highly upregulated in a mouse model of pancreatic cancer, invasive human pancreatic cell lines and breast

cancer cell lines, which suggests that overexpression of Epsin3 is mainly related to invasive cancer (Coon et al. 2011). In angiogenesis, it was proved that Epsin1 and 2 regulate the vascular endothelial growth factor (VEGF) signalling in mice model. Pasula et al. (2012), reported that removal of Epsin1 and 2 from endothelial tumour vasculature led to prolonged VEGF2 signalling and consequently results in formation of aberrant vessels which causes impairment of tumour genesis and could contribute to tumour growth retardation. In this regard, double knockout of endothelial Epsin1 and 2 in embryos resulted in formation of a disorganized vascular network, indicating the necessity of Epsins in angiogenesis regulation (Tessneer et al. 2014). To further support this observation, it was showed in a recent study that the binding of Epsin (1 and 2) and VEGFR2 is directed by a complex mechanism that includes ubiquitin-dependent and ubiquitin- independent interactions, suggesting that Epsins have a critical role in VEGF2 signaling adjustment (Rahman et al. 2016). Furthermore, Epsin1 was found to play a significant role in the internalization of Epidermal Growth Factor Receptor (EGFR) via recruitment of these receptors to the coated-pits in endocytosis and promotes EGFR downregulation. Epsin1 knockdown inhibits internalization of EGFR as the interaction between Epsin1 and EGFR is impaired (Kazazic et al. 2009). Deficient internalization of EGFR leads to activation of signalling and consequently resulted in malignant transformation, as EGF signalling was reported to be upregulated in many solid tumours (Grandal and Madshus 2008). Recently, Chang et al revealed that Epsins (1 and 2) were upregulated in both human and mouse colon cancer and Epsins expression levels tightly correlated with the aggressiveness of the tumour. It was reported that loss of intestinal epithelial Epsins inhibited Wnt signalling and colon cancer progression (Chang et al. 2015).

1.7 Oral keratinocyte cell lines

1.7.1 Normal oral keratinocytes cell lines

In vitro, normal human somatic cells display a limited replicative potential, even under sufficient nutritional and mitogenic requirements (Smith and Pereira-Smith 1996). In primary culture, the cells initially proliferate but ultimately enter in a permanent growth arrest state called senescence (Dickson et al. 2000). The onset of senescence is triggered by progressive shortening and erosion of telomeric DNA. Telomeres are located at the ends of chromosomes protecting them from degradation and end-to-end fusion. Telomere erosion occurs following ~50 to 100 successive replications (Allsopp et al. 1992). It has been found that introduction of human telomerase reverse transcriptase subunit (hTERT) into normal, non-neoplastic human fibroblasts leads to immortalization of these cells (Bodnar et al. 1998). The catalytic subunit, hTERT is usually expressed in cancer cells (Meyerson et al. 1997). This subunit enables the cells to synthesise telomeres (Feng et al. 1995), and maintain stable telomere length through a number of cell divisions (Counter et al. 1992). In vitro, ectopic expression of hTERT is not sufficient to immortalize normal human keratinocytes (Kiyono et al. 1998). It was reported that a complex pattern of $p16^{INK4A}$ protein expression is associated with senescence of cultured human keratinocytes in a pathway that is independent of telomere shortening. An oral keratinocyte cell line that has both ectopic expression of hTERT and increased $p16^{INK4A}$ level has been generated. This OKF6/hTERT cell line has the ability to overcome senescence without displaying abnormalities of either growth or differentiation (Dickson et al. 2000).

1.7.2 OSCC cell lines

Although two of the oldest cancer cell lines were originated from the oral cavity (Eagle 1955; Moore et al. 1955), human SCC cell lines are difficult to culture and characterise (Krause et al. 1981). In vitro, malignant and normal keratinocytes have different criteria and can be distinguished. However, OSCC derived keratinocytes exhibit a different phenotype and may show both malignant and normal characteristics (Prime et al. 1990). A range of OSCC-derived cell lines has now been established (Prime et al. 1990). Malignant oral keratinocyte cells can show different tumorigenicity, local spread and metastasis behaviour following orthotopic transplantation into athymic mice (Prime et al. 2004). There is an alteration of TGF-β receptor profile with a reduction in the cellular response to Transforming Growth Factor-β receptor (TGF-β1) in the metastatic oral cancer cells (Davies et al. 1999). The literature to date suggests that these cell lines can provide a model of oral carcinogenesis both in vitro and in vivo.

1.8 Conclusion

This review highlighted the role of the endocytic adaptor protein family called Epsins in the activation or downregulation of different pathways which are involved in human cancers. Notch signalling, which has an important role in cell growth, proliferation and differentiation, is one of the pathways that was found to be dysregulated in cancers. Evidence suggest that Epsins are responsible for Notch signalling activation through the endocytosis process. Binding of Notch receptors and their ligands is an ubiquitination dependent process which requires Epsins to start endocytosis and trigger Notch signalling in the signal-receiving cell. Dysregulation of Epsins expression was found in several human cancers. However, to date there is limited available evidence about the role of Epsins in oral carcinogenesis.

1.9 Hypothesis

This study will test the hypotheses that:

1. Epsins are deregulated in OSCC and can be used as a biomarker in oral dysplastic lesions and OSCC.
2. Notch signalling is downregulated in the OSCC and Epsins are required for its activation in the oral epithelial tissues.

1.10 Aims and objectives

1. To examine the expression of Epsins (1, 2, and 3) in oral squamous cell carcinoma cell lines (OSCC) and immortalized normal oral keratinocytes (OKF6) at the RNA (Ribonucleic acid) and protein levels. For these analyses, quantitative Real Time-PCR (qRT-PCR) and Western blot (WB) were used.
2. To investigate the expression of Notch signalling in the OSCC and OKF6 cell lines. Notch1 receptor was analysed at RNA and protein levels to identify the expression level of Notch signalling in the cell lines, and determined if there is a correlation between Epsin3 and Notch1 expression in the cell lines.
3. To determine the expression profiles of Notch signalling target genes Hes1, Hey1, and notch intracellular domain (NICD) in the OSCC cell lines.
4. To investigate the effect of Epsin3 expression level on the Notch signalling pathway. Epsin3 was knocked down using siRNA and knocked up using human Epsin3 overexpression vector in vitro. The expression of Notch1 receptor was measured at RNA and protein levels.
5. To assess the expression profiles of Epsins and Notch1 within the oral epithelium. These studies were undertaken by immunohistochemistry (IHC) in co-localization with known markers (including CK5/6, Ki67 and p63). Expression analyses involved normal oral tissues (n=21), oral dysplasia (n=79) and oral squamous cell carcinoma (n=31) to establish a possible correlation between expression profile of Epsins and Notch1 with patients' characteristics and clinical outcomes.

Chapter 2 **Materials and Methods**

2.1 Materials and reagents

Cell culture materials were purchased from Life Technologies (UK). All chemicals, unless otherwise stated, were of molecular biology grade and were purchased from either Sigma-Aldrich (UK) or Lonza (UK). Oligonucleotide primers were purchased from Integrated DNA Technology (IDT, UK).

2.2 Cell culture

Cell culture was performed in a level 2 tissue culture laboratory in the School of Dental Sciences using a category II safe flow 1.2 lamina flow hood (BIOAIR, UK).

2.2.1 Cell lines

The immortalized normal oral keratinocyte cell line, OKF6 (Dickson et al. 2000), was cultured in a defined media composed of keratinocyte serum-free media with 0.6µg/ml L-glutamine, supplemented with 0.2ng/ml human recombinant epidermal growth factor, 20µg/ml bovine pituitary extract, and 5mL penicillin streptomycin (200units/ml penicillin and 200µg/ml streptomycin). Nine established oral cancer cell lines were used in this study and are listed in Table 2.1(Prime et al. 1990; Edington et al. 1995). All cell lines were maintained in Dulbecco's Modified Eagle's Medium (DMEM/F12 1:1 mixture, with 15mM Hepes and 0.6µg/ml L-glutamine) supplemented with 10% (v/v) foetal calf serum (FCS), 0.5ug/ml hydrocortisone 21-hemisuccinate sodium salt and 10ml penicillin streptomycin (200units/ml penicillin and 200µg/ml streptomycin)..

The LnCap cell line was used as a comparator cell line. LnCap was derived from a lymph node containing metastatic prostate adenocarcinoma (Horoszewicz et al. 1980). The cells were maintained in RPMI 1640 medium containing L-glutamine and sodium bicarbonate, supplemented with 10% (v/v) FCS. Cells were cultured in 75cm2 flasks and incubated in a cell-line incubator (InCu Safe, Sanyo Electronics, Japan), which provided a humidified atmosphere of 95% air/5% CO2 and a temperature of 37˚ C. The culture medium was replaced every 3-4 days.

Cell line	Age (Years)	Sex	Site	Size (mm)	Differentiation	Lymph node metastasis	Distant metastasis	Tumour stage	Tumourigenicity in vivo [A]
H103	32	M	TO	<20	WD	-	-	I	T
H157	84	M	BM	20-40	WD	+	-	II	NT
H314	82	M	FOM	20-40	MD	+	-	II	T
H357	74	M	TO	<20	WD	-	-	I	NT
H376	40	F	FOM	20-40	WD	+	-	III	NT
H400	55	F	AP	20-40	MD	-	-	II	T
H413	53	F	BM	20-40	MD	-	-	II	T
BICR31	NK	NK	TO	>60	MD	-	-	IV	T
BICR56	NK	NK	TO	>60	MD	-	-	III	T

Table 2.1: Derivation of the oral cancer cell lines

TO: tongue, BM: buccal mucosa, FOM: floor of the mouth, AP: alveolar process, NK not known.

WD: well differentiated, MD: moderately differentiated.

A: Orthotopic transplantation in mice.

T: Tumourigenic, NT; Non-Tumourigenic. Tumour stage was calculated using the STNMP staging system (Langdon and Henk 1995)

2.2.2 Sub-culturing of cells

The cells were sub-cultured when they reached approximately 90% confluence. The culture media was discarded and the cells washed with phosphate-buffered saline (PBS: 137 mM NaCl, 2.7 mM KCl, 4.3 mM Na2HPO4.7H2O, 1.4 mM KH2PO4, pH 7.3). Cells were washed with 3ml trypsin/EDTA for 30 seconds. The cells were then detached from the floor of flask using trypsin enzyme 0.025 % (v/v) solution. Trypsin was applied to the cells and incubated for 5 minutes at 37˚C or until the cells detached. Trypsin was neutralised by adding an equal volume of growth medium. The suspension was then centrifuged at 750xg (LnCap cell line centrifuged at 250x g, OKF6 at 1000x g) for 8-10 minutes at 4˚C (Jouan CR3i Multifunction Centrifuge, Thermo Scientific, USA). The supernatant was discarded, the pellet re-suspended in 5ml of growth medium. The cells were counted using a haemocytometer (Bright-line Haemocytometer, USA). The number of cells present in 15µl of cell suspension were counted in each sixteen corner squares and 25 middle squares. The mean of five large squares was calculated and multiplied by dilution factor, and then multiplied by 10^4 to get the number of cells/ml of the cell suspension. The cells were then plated out at a density of 8 x10^5 cells per 75cm flask.

2.2.3 Cryopreservation of cell lines

Stocks of all cell lines were preserved in liquid nitrogen for long term storage. Cells were passaged, pelleted by centrifugation and then re-suspended in 5mL freezing medium [culture medium with 20% (v/v) FCS and 10 % (v/v) dimethyl sulfoxide (DMSO)], the number of cells was determined by haemocytometer counting to be between 5x10^5-1x10^6/ml. The cell suspension was transferred to cryotubes (CRYO-STM, Greiner Bio-one, UK) and these tubes were kept at-80˚C overnight (Ultra Low, Sanyo Electronics Ltd, Japan). The cryotubes were then transferred to a liquid nitrogen container (approximately -196˚C). Re-culture of cryopreserved cells was achieved by rapidly defrosting the cells at 37 °C and gently transferring them into 10 ml of pre-warmed growth medium. The cells were centrifuged and re-suspended in fresh medium to remove any residual DMSO. Cells were seeded into tissue culture flasks and incubated in a humidified atmosphere of 95% air/5% CO2 at a temperature of 37˚C.

2.2.4 Formalin-fixed paraffin-embedded cell pellets

The cells were seeded in 175cm flask at a density of approximately $16x10^5$ cells. After the cells reached approximately 90% confluence, they were harvested using one of two methods: trypsinisation (as described above) or by physical detachment (cell scraping). For the cell scraping method, the growth media was discarded and the cells detached from the flask using a cell scraper. The detached cells were resuspended in 6ml of growth medium then pelleted by centrifugation (as described for the trypsin method). The cell pellets from both methods were then re-suspended in 5ml PBS and centrifuged. Without disturbing the pellet, the PBS was removed and replaced by 4ml of 10% (v/v) neutral buffered formalin (NBF) and left overnight at room temperature to fix. Following fixation, the NBF was removed and discarded. The fixed cell pellet was placed on a filter paper, which was folded and placed in a standard plastic processing cassette. The cell pellets were processed and embedded in paraffin wax blocks in the Department of Cellular Pathology, Newcastle upon Tyne NHS Foundation Trust.

2.3 Molecular biology and protein techniques

2.3.1 RNA extraction from cultured cells

Cells for RNA extraction were seeded into a tissue culture dish at a density of 5×10^5 cells per dish. The cells were incubated under standard conditions, with media changed daily. When the cells were approximately 90% confluent, the culture medium was discarded and cells washed with PBS. RNA was extracted using one of two methods: TRIzol® extraction (Life Technologies, UK) or a proprietary RNA extraction kit (PureLink RNA Mini Kit (Ambion Life Technologies). For TRIzol® extraction 1ml of TRIzol® reagent (Life Technologies, UK) was added to each dish and pipetted vigorously to lyse the cells. The lysate was transferred to a 1.5 ml Eppendorf tube and stored at -80 °C until required.

2.3.2 RNA purification from the TRIzol® lysate

TRIzol® samples were defrosted at room temperature. Two hundred micro litres of chloroform was added and the tube was shaken vigorously (15 seconds) in a fume hood. The tubes were incubated at room temperature (3 minutes) and then centrifuged at 12,000x g, at 4˚C (15 minutes) (Centrifuge 5417B, Eppendorf, Germany). The aqueous phase was transferred to 1.5ml micro-centrifuge tube. To this, 500 µl isopropanol was added and incubated at room temperature (10 minutes). The samples were centrifuged at 12,000g at 4 °C (10 minutes). The supernatant was decanted and

the RNA pellet washed by adding 1 ml of 70% (v/v) ethanol. Samples were vortexed and centrifuged at 7500x g at 4 °C (5 minutes). The supernatant was decanted. The RNA pellet was air-dried for ~5 minutes and dissolved in 20µl sterile double distilled water. The RNA concentration (quantity) and quality was assessed using a Nanodrop 2000 UV-Vis Spectrophotometer (Thermo Scientific, UK).Samples were stored at -80^{0}C until required.

RNA purification

RNA samples were purified using ISOLATE II RNA Micro Clean-Up Kit (RMC, Bioline, UK). Briefly, 300µl lysate sample containing up to 90µg RNA was transferred into a sterile 1.5ml micro centrifuge tube, one volume of Clean-Up Buffer RMC was added and centrifuged gently (1s at 1,000xg) (Eppendorf Centrifuge, Germany). The lysate was transferred into ISOLATE II RNA Micro Clean-Up Column in 2ml Collection tube and centrifuged 30s at 11,000x g, then placed the column in a new 2ml Collection tube. The first wash was carried out by adding 400µl Buffer RW2 to the column and centrifuged 30s at 11,000x g. The flow-through was discarded and second wash was carried out, 200µl Buffer RW2 was added and centrifuged 2 minutes at 11,000x g to dry membrane. The column was placed into a nuclease-free 1.5ml Collection tube, 10µl RNase-free water was added directly onto centre of the silica membrane, centrifuged for 30s at 11,000x g. The RNA concentration and quality was assessed using a Nanodrop 2000 UV-Vis Spectrophotometer (Thermo Scientific, UK). Samples were stored at a concentration of 1µg/µl at-80^{0}C until required.

2.3.3 RNA extraction and purification using PureLink RNA miniKit

Firstly, 60ml ethanol (100%) was added to Wash Buffer II, and 1% 2-mercaptoethanol (v/v) was added to Lysis Buffer (10µl for every 1ml Lysis Buffer). The growth medium was discarded from cells and 600µl Lysis Buffer added. The cell lysis was transferred to an Eppendorf tube and vortexed and then homogenized using a rotor-stator homogenizer (Tissuelyser LT, QIAGEN, Germany) at maximum speed for 50 seconds. The homogenate was centrifuged at 20,000x g for 5 minutes, (Eppendorf Centrifuge, Germany). The supernatant was then transferred to a clean RNase-free tube. For RNA purification, one volume of 70% ethanol (v/v) was added to each volume of cell homogenate and vortexed thoroughly. Up to 700µl of the sample was transferred to a spin cartridge (with collection tube) and centrifuged at 12,000x g for 15 seconds at room temperature, the flow-through was discarded. This step was repeated until the

entire sample had been processed. Then 700µl of Wash Buffer I was added to the spin cartridge and centrifuged at 12,000x g for 15 seconds at room temperature, the flow-through discarded, 500µl of Wash Buffer II was added and centrifuged at 12,000x g for 15 seconds (this step was repeated twice). The flow-through discarded and the spin cartridge was centrifuged at 12,000x g for 2 minutes to dry the membrane which will have bound RNA. The spin cartridge was inserted into a clean tube. Fifty microliters RNase-free water was added to the centre of the spin cartridge and incubated at room temperature for 1 minute before being centrifuged for 2 minutes at 12,000x g. The RNA concentration and quality was assessed using a Nanodrop 2000 UV-Vis Spectrophotometer (Thermo Scientific, UK). Samples were stored at a concentration of 1µg/µl at-80^{0}C until required.

2.3.4 Reverse transcription of RNA to generate cDNA samples

The reverse transcription reaction contained 1µl oligo dT (0.62mM), 1µg RNA and sterile distilled water to a final volume of 12.5µl. This mixture was heated to 70˚C for 5 minutes (T100 Thermal Cycler, Bio-Rad, UK), and then incubated on ice for 1 minute. The product from this reaction was added to 12.5µl transcription mixture (Table 2.2) and heated at 37˚C for 60 minutes, then 70˚C for 15 minutes in the PCR machine. The samples were stored at -20˚C.

Reagent	**Quantity (µl)**
5x Moloney Murine Leukaemia Virus M-MLV reaction buffer (Promega)	5
10mM dNTP(New England Biolabs)	2
Sterile distilled water	4.5
M-MLVReverseTranscriptase enzyme (Promega)	1

Table 2.2: Pipetting protocol for RNA reverse transcription mixture

High-capacity cDNA reverse transcription

Reverse transcription was performed using the high-capacity cDNA reverse transcription kit (Applied Biosystems, Life Technologies, UK). Approximately 1µg RNA was mixed with reverse transcription master mix containing 0.8µL of dNTP (100mM), 2µl RT buffer, 2µl Random Primers, 1µl reverse transcriptase (50U/µl) and nuclease free water to final volume 20µl. Samples were incubated in the thermal cycler machine at 25 °C for 10 min to promote primer annealing followed by 37 °C for 120 min to promote reverse transcriptase-mediated extension, and finally at 85 °C for 5 min to inhibit enzyme activity. The samples were stored at -20˚C.

2.3.5 Semi quantitative reverse transcription polymerase chain reaction

The primers for human Epsin1 and its variants (v1, v2, and v3), human Epsin2 (v1, v2, and v3), and human Epsin3 were designed using software from NCBI (USA) and supplied by IDT (UK). Primers for GAPDH were from previously published work by our group (Jackson et al. 2007). Primer sequences are provided in Table 2.7. To 1µl of cDNA solution prepared previously (Section 2.3.4) was added the standard Taq 2x master mix: 12.5µl Taq Master Mix (New England Biolabs), 0.5µl Forward Primer (0.2µM), 0.5µl Reverse Primer (0.2µM), and sterile distilled water to a final volume 25µl. Negative samples containing water instead of cDNA were performed to control for contamination. The samples were heated sequentially at 95˚C for 5 minutes (Taq activation), 95˚C for 30 seconds, 58˚C for 30 seconds, 72˚C for 60 seconds over 30 cycles, the block was then held at 72˚C for 15 minutes. The product was stored in -20˚C. Verification of the PCR product size was carried out by running the product on a 2% (w/v) agarose gel. (Melford Biolaboratories, UK), containing 0.5x Gel Red (VWR, UK). Molecular weight marker (MWM)-Hyper ladder IV was used. (Bioline, UK)The image of the gel was taken using ultraviolet light (SYNE GENE, Gen Snap, UK). The photograph was saved and band intensities analysed using gene tools (SYNE GENE, UK). PCR products were all confirmed for identity by sequencing (MWG Eurofins, UK).

2.3.6 Quantitative real time polymerase chain reaction

Levels of RNA expression were analysed using Real Time PCR. cDNA amplification during the exponential phase was analysed and thus detected quantitative differences between mRNA expressions between samples.

A fluorescent reporter QuantiFast SyBR Green (QIAGEN, Germany) was used to detect the amount of DNA template in the samples. Upon binding with DNA, SYBR Green fluorescence is enhanced and can be detected by Real Time PCR thermocycling machine (DNA Engine Opticon 2 continuous fluorescence Detector, MJ Research, USA). cDNA of LnCap cells (1µg/µl), known to express the transcript of Epsin3 was used to quantify the relative amount of cDNA produced in the PCR reactions. cDNA was diluted to 1 in 10 in nuclease free water and 5 dilutions were prepared (0.001-100 ng/µl) (Figure 2.1). The cDNA samples, primers (1µM), and SYBR Green mix and nuclease free water were pipetted according to the manufacturer's instructions. Triplicate samples were then loaded onto 96-well plates. The plates were run on a Real Time PCR thermocycling machine. GAPDH was used as a reference gene to normalise expression levels.

Relative differences in the Epsin3 mRNA level of each sample were calculated using the comparative Ct method (Livak and Schmittgen 2001), as described in the equation below. The Ct value represents a threshold fluorescence value for each cycle. It detects the point at which fluorescence from accumulated PCR product exceeds the predetermined background value. Therefore, samples with high level of the gene of interest have low Ct value as the threshold is reached early.

1. $\Delta Ct = Ct_{(\text{gene of interest})} - Ct_{(\text{reference gene})}$
2. $\Delta\Delta Ct = \Delta Ct_{(\text{expression})} - \Delta Ct_{(\text{control})}$
3. $2^{-\Delta\Delta Ct}$

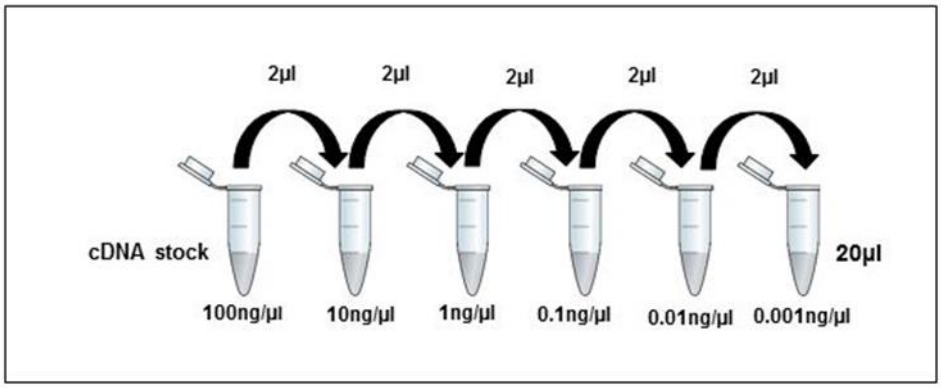

Figure 2.1: Serial Dilution of LnCap cDNA for standard curve

Serial dilution of the LnCap cDNA was prepared for standard curve of RT-PCR, 2µl of cDNA was serially diluted with 18µl nuclease free water to get cDNA diluants of appropriate concentrations

2.3.7 Protein extraction from cultured cells

Following subculture, the cell lines selected for protein isolation were seeded into 6-well plates (4 x 10^5 cells per well). The cells were incubated under standard conditions until approximately 90% confluent. A stock solution of 200µl 1 X PBS containing one protease inhibitor cocktail tablet (Roche Diagnostic Gmbh, Germany) was prepared and stored at -20˚C. Working stocks were made by addition of 15µl from this stock to 1ml of iced PBS and used for washing the cells in each well after the culture medium was discarded. The cells were scraped and the cell lysate was transferred to 1.5ml Eppendorf tube and centrifuged at 10,000rpm at 4˚C for 10 minutes. The supernatant was discarded. In 1.5 ml Eppendorf tubes, 50µl of lysis buffer (RIPA Buffer, Sigma, Aldrich UK) containing 0.75µl of stock solution (PBS containing protease inhibitor cocktail), was added to the pellet in each tube. The protein samples were stored at -80˚C until required.

.

2.3.8 Protein quantification

The protein was quantified using the Bradford Assay. The Bradford reagent was diluted in double distilled water (dH2O) (1 part Bradford reagent: 4 parts dH2O). Protein samples were thawed on ice and centrifuged at 13,000rpm at 4ºC for 15 minutes and

returned to ice. In 1.5 ml Eppendorf tubes, 2µl from each protein sample was added to 198µl dH2O, 800µl of diluted Bradford reagent was also added. A standard curve was prepared using a dilution series (0.02-0.1mg/ml) of standard protein BSA (Bovine Serum Albumin) of 100µg/ml concentration (Table 2.3). To each dilution, 800µL of diluted Bradford reagent was added. A 96 well plate was set up with 250µl of BSA protein in rows A to E in triplicate. 250µl of protein of unknown concentration was set up from column 4 in triplicate. The plate was measured using a plate reader (Synergy HT, Biotech USA), set at a wavelength of 595nm. Data were exported to an Excel spreadsheet and the mean protein quantity for each sample calculated.

Tube	**BSA µL**	**dH2O µl**	**Concentration mg/ml**
1	200	0	0.1
2	160	40	0.08
3	120	80	0.06
4	80	120	0.04
5	40	160	0.02
6	0	200	0

Table 2.3: Serial Dilution of BSA for standard curve

2.3.9 Protein expression analysis

Protein sample preparation

The protein samples were thawed on ice. A volume containing of 10µg/µl concentration was taken from each sample and sterile water added to a final volume of 10µl. Samples were prepared in duplicate. The protein loading buffer was prepared as shown in Table 2.4. To each protein sample, 5µl of loading buffer and 5% (v/v) (0.25µl) of β-Mercaptoethanol was added. The samples were heated to denature the protein, at 95˚C on a heat block for 10 minutes and centrifuged at 10,000x g for 30 seconds.

Reagent	**Quantity**
1M Tris base(pH6.8)	2.25ml
Glycerol	5ml
SDS (sodium dodecyl sulfate)	0.5g
Bromophenol blue	5mg
1M Dithiottreitol (DTT)	2.5ml

Table 2.4: Protein Loading Buffer. A total volume of 10ml was made up and aliquots of 1 ml were stored at – 20˚C.

SDS polyacrylamide gel electrophoresis (SDS PAGE)

Proteins were separated on 12.5% (w/v) separating gels, prepared using: 2.9 ml Acrylamide/ Bisacrylamide stock (30% (v/v) solution, 2.8ml separating gel buffer (1.857M Tris HCl and 0.25% SDS (pH 8.9)), 1.2 ml sterile distilled water, 6 µl TEMED (N, N, N', N-Tetramethylethylenediamine), and 65µl fresh 10% (w/v) APS (ammonium per sulphate). The separating gel was poured into the glass plates (Mini-protean®Tetra

cell, Bio-Rad, USA), with the addition of 1ml of sterile distilled water poured on the top to remove any air bubbles and to keep the surface smooth. The stacking gel was prepared using: 0.25ml Acrylamide/ Bisacrylamide stock (30% (v/v) solution), 0.4ml stacking buffer (0.3M Tris HCl and 0.5% SDS (pH 6.7)), 1.32ml sterile distilled water, 2.5µl TEMED and 18µl 10% (w/v) APS.

The upper surface layer of water on the separating gel was dried using filter paper and the stacking gel was pipetted on the top carefully to avoid any air bubbles. A plastic comb was inserted to form wells within the gel. Once set, 15µl of protein lysate was loaded per well and 6µl of 8-220 kDa electrophoresis marker (protein ladder) was run alongside as a molecular weight reference. The gel was placed in a tank (Mini-Protean® Tetra Bio-Rad, China) containing protein electrophoresis running buffer (0.5M Tris-HCl, 1.9M Glycine, 0.1 % (w/v) SDS). Samples were electrophoresed at 120V for 60-70 minutes. Then Semi-Dry blotting was carried out. The PVDF membrane (GE Healthcare, UK) was prepared by cutting into appropriate gel size, and soaking with 100% methanol for 30 seconds, rinsing with distilled water and incubating at room temperature for 2 minutes on the shaker. The water was replaced by transferring buffer (20ml of 100% methanol and 80ml of protein electrophoresis running buffer) and incubated for 15minutes. On the platinum base of the blotting apparatus (V10-SDB and V20-SDB, Harvard Apparatus, UK) three pieces of Whatman paper were placed (previously soaked in transferring buffer) and the air bubbles were removed using a blotting roller (Novex Blotting Roller, Life Technology, USA). The PVDF membrane was placed over them and then the gel, followed by a further three pieces of Whatman paper and the air bubbles were removed, some of transferring buffer was added at the surface of the Whatman paper to avoid drying of the membrane during the transfer. Transfer was carried out at 15V for 1 hour. The membrane was placed in a 5% (w/v) blocking solution (5% non-fat powdered milk (Marvel™, UK) in Phosphate Buffered Saline (PBS)-Tween-20 (0.05% v/v)) to block non-specific antibody binding. Membranes were then washed in PBS-Tween-20 (PBS-T). The membrane was then incubated in the appropriate primary antibody, diluted as required in 5% (w/v) non-fat milk PBS-T (Antibody concentrations used are outlined in Table 2.5) overnight at 4˚C on a shaker.

Product	Clone	Species	Manufacturer	Dilution
Epsin1	Polyclonal	Rabbit	Sigma-Aldrich (SAB 4200582)	1:500
Epsin2	Polyclonal	Rabbit	Fisher Scientific(PA5-12090)	1:1000
Epsin3	Polyclonal	Rabbit	Abcam (ab91225)	1:50
Epsin3	Polyclonal	Rabbit	Novus Biologicals	1:300
Notch1	Monoclonal	Rabbit	Cell Signaling (3608s)	1:1000
Alpha-Tubulin	Polyclonal	Rabbit	Abcam (ab1825)	1:2000
Anti-mouse Ig	Monoclonal	Sheep	GE Healthcare (NX931)	1:5000
Anti-rabbit Ig	Polyclonal	Goat	Sigma Aldrich	1:10,000

Table 2.5: Details of antibodies used in Western blot analysis

Following overnight incubation the membrane was washed with PBS-T 4X for 15 minutes on the shaker at room temperature. The membrane was then transferred to secondary antibody solution (secondary antibodies diluted as required in 5% (w/v) non-fat milk- PBS-T; Table 2.5) and incubated for 1 hour on the shaker at room temperature. The membrane was washed and placed on an acetate sheet and dried with Whatman paper. The PDVF membranes were covered with 400µl of ECL solution (Enhance Chemiluminescence) (Thermoscientific, U.S.A) and incubated for 1 minute. The PVDF membrane was dried with Whatman paper and placed between two acetate sheets in a transfer cassette. The cassette was taken into the dark room. An X-ray film (Kodak, USA) was removed and placed on top of the acetate sheet. The cassette was closed and incubated for between 2-15 minutes. The film was removed and placed in the developer 9SRX-101A, Konica Minolta, Medical and Graphic, Inc., China).

2.4 Production of Epsin3 Overexpression Vector

A commercially available mammalian expression vector containing the human Epsin3 sequence (Lenti ORF clone of Human Epsin3, Myc-DDK-tagged, 10µg OriGene) was transformed into a Top10 chemically competent DH5α Escherichia coli (E.coli) cells in order to generate a high concentration of vector to be used in the transfection experiments.

The transformation reaction was prepared in a 1.5 ml microcentrifuge tube, 0.5ml E.coli was thawed in ice, with approximately 0.5µg Epsin3 plasmid and mixed very gently by pipetting up and down. A negative control tube was prepared which contained only the competent cells without plasmid. The tubes were incubated in the ice for 30 minute, and then heat shocked in a water bath at 42˚C for 90 seconds. After that 1ml of Luria Bertani (LB) Broth medium (Melford Laboratories Ltd, UK) was added to each tube and incubated at 37˚C for one hour. The transfection reaction was cultured in 15 ml falcon tube. The tubes were centrifuged and pipetted up and down very well as the cells precipitated in the bottom. Subsequently 500µl from each tube (positive and negative) was added to 5ml LB medium containing 50µg/ml Kanamycin antibiotic (Sigma Aldrich) and incubated at 37˚C with shaking overnight. (Heidolph polymax 1040, SLS, UK). Cultures (100 µl) were then grown on nutrient agar plates with 50µg/ml kanamycin. The plates were incubated at 37˚C overnight in an oven (Genlab, UK). The negative transfection showed no growth overnight.

Plasmid purification using QIAprep Spin Miniprep kit. Culture media transformed with Epsin3 was centrifuged at 1000g for 5 minutes, the supernatant was discarded and pelleted bacterial cells were resuspended in 250µl Buffer P1 and transferred to a micro centrifuge tube. Then 250µl Buffer P2 was added and mixed thoroughly by inverting the tube 4-6 times. After adding 350µl Buffer N3 the preparations were mixed immediately and thoroughly and then centrifuged for 10 minutes at 13,000 rpm (PRismR, Labnet international, UK). The supernatant was applied to the QIAprep spin column by pipetting, centrifuged for 30-60 seconds and the flow-through was discarded. The spin column was washed by adding 0.5ml Buffer PB and centrifuged for 30-60 seconds, the flow-through discarded. Then 0.75ml Buffer PE added to the spin column and centrifuged for 30-60 seconds, the flow-through was discarded and the spin column centrifuged for additional 1 minute to remove residual buffer. The QIAprep column placed in a clean 1.5 ml micro centrifuge tube and 50µl Buffer EB was

added; to elute DNA, and centrifuged for 1 minute. The DNA concentration and quality was assessed using a Nanodrop 2000 UV-Vis Spectrophotometer (Thermo Scientific, UK) and the samples stored at -20˚C. In order to generate larger amount of high quality, purified plasmid DNA large batch bacterial culture was undertaken, DNA extracted and purified using EndoFree Plasmid Maxi (QIAGEN).

2.5 Transient transfection of mammalian cells

2.5.1 Overexpression of Epsin3 in H103, H357, BICR31 and BICR56 cell lines

Cells were grown in 6 well plates at $4x10^5$ cells/ well, until approximately 90% confluent. For one transfection 97µl of reduced serum medium (OPTi-MEM, Gibco Life Technologies, UK) was added to 3µl GeneJammer transfection reagent (Agilent Technologies, USA) mixed gently by pipetting up and down. This was incubated at room temperature for 5 minutes. Then 1µl (1µg) of Epsin3 plasmid (Myc-DDK-tagged)-Human Epsin3, OriGene, UK)) was added to the diluted transfection reagent and mixed gently. The transfection reaction was incubated at room temperature for 45 minutes, before adding to the cells along with fresh medium, and incubated at 37˚C CO2 incubator for 24 hours. The RNA and protein were then extracted. For negative control, cells transfected with empty vector (p3XFLAG-CMV-10, Sigma Aldrich) and untreated parental cells were used.

2.5.2 Knockdown of Epsin3 in BICR31 cell line

The cells were grown in 6 well plate at $4x10^5$/well, until approximately 90% confluent. Several methods with several different transfection reagents and siRNA constructs, were carried out to optimise knockdown experiments. The method and siRNA construct reported herein, were the most successful, in terms of knockdown, and reported in Chapter 5. For each transfection, 2µl Epsin3 siRNA (Santa Cruz Biotechnology, Germany) of 10пM/µl was diluted in 100µl siRNA Transfection Medium (OPTi-MEM). In another tube 2µl siRNA Transfection Reagent (Santa Cruz Biotechnology, Germany) was diluted in 100µl OPTi-MEM. For the control 2µl of control siRNA (Santa Cruz Biotechnology, Germany) was diluted in 100µl OPTi-MEM, and 2µl siRNA transfection reagent was diluted in 100µl OPTi-MEM. The diluted siRNA was mixed with diluted siRNA transfection medium by gently pipetting the solution up and down. The mixture was incubated for 45 minutes at room temperature, then 800µl siRNA transfection medium was added to the mixture, mixed gently and overlaid onto the cells after washing them with 2ml siRNA transfection medium. The cells were

incubated for 6 hours in a humidified atmosphere of 95% air/5% CO2 at a temperature of 37˚ C. At the end of incubation, 1ml of normal growth medium containing 20% FCS and antibiotic was added to the cells without removing the transfection mixture. The cells incubated for an additional 24 hours. After that the medium was aspirated and replaced with 2ml fresh normal growth medium containing 10% FCS and incubated for72 hours, after that the RNA and protein were collected.

2.6 Tissue samples

2.6.1 Formalin-fixed paraffin-embedded tissue blocks

Formalin-fixed paraffin-embedded (FFPE) blocks of normal oral mucosa, oral epithelial dysplasia and early stage (Stage I and II) oral squamous carcinoma were available for the study and were used according to a favourable ethics opinion (Evaluation of the prognostic potential and functional significance of biomarkers in oral cancer11/NE/0118 NRES Committee North East – Sunderland). All the samples were link-anonymised.

The following data were associated with the oral epithelial dysplasia samples:

1. Patient demographic data (sex, age at diagnosis).
2. Anatomical site.
3. Date of diagnosis.
4. Patient risk factors (i.e. alcohol/tobacco habits).
5. Clinical management (laser excision/surveillance).
6. Histological grade of epithelial dysplasia (WHO/binary classification).
7. Clinical outcomes were defined as: *no adverse outcome* (>24-month follow up): *local recurrence* of epithelial dysplasia at the same site: *new lesion* at a separate mucosal subsite: *malignant transformation* to oral squamous cell carcinoma (Diajil et al. 2013).
8. Date of the event was recorded (most recent clinical examination, local recurrence, new lesion, malignant transformation).
9. For the cases that underwent malignant transformation, the histological differentiation and Stage of the subsequent oral squamous cell carcinoma (OSCC) was also recorded.

The following data were associated with the early stage OSCC samples:

1. Patient demographic data (sex; age at diagnosis).
2. Anatomical site.
3. Date of diagnosis.
4. Histological grade of differentiation (Broder's classification).
5. Clinical outcomes were defined as: disease-free survival and overall survival.

Microtomy was carried out in the Department of Cellular Pathology by Biomedical Scientists. 4µm sections of FFPE cell blocks or tissue were mounted on adhesive slides (Superfrost Plus, Thermo Fisher Scientific, UK).

2.7 Immunohistochemistry

Immunohistochemistry was carried out by Anna Long (Biomedical Scientist, Department of Cellular Pathology) on a Ventana Benchmark Ultra autostainer (Ventana Medical Systems Inc, USA). The primary antibodies and optimised conditions are provided in Table 2.6. The antibodies were optimised using normal tonsil, breast cancer and prostate cancer specimens.

2.8 RNA in situ hybridisation

Detection of Epsin3 and Notch-1 mRNA in FFPE cells and tissue was performed using a proprietary RNA in situ hybridisation system (RNAscope® 2.5 VS Assay, Advanced Cell Diagnostics, Inc. USA) on a Ventana Discovery Ultra autostainer (Ventana Medical Systems Inc, USA). The RNAscope assays were carried out by Thomas Ness (Biomedical Scientist, Department of Cellular Pathology). Briefly, 4µm FFPE sections were deparaffinised and pre-treated with heat and protease before hybridisation with the target-specific probes (Epsin3 Cat. No. 458799; Notch-1 Cat. No. 311869, Advanced Cell Diagnostics, Inc. USA). PPIB, a constitutively expressed endogenous gene was used as a positive control. The bacterial gene, dapB was used as a negative control.

2.9 Scoring of immunohistochemistry and RNA in situ hybridisation

The sections were analysed by Dr Max Robinson (Oral Pathologist), the following parameters were recorded: cellular location (nuclear, cytoplasmic, membrane) and tissue location (epithelium, endothelium, connective tissue, lymphoid tissue), staining

intensity (0-3), percentage cells staining (0-100), H score (product of staining intensity and the percentage cells staining; 0-300). Data were recorded in an excel spreadsheet.

2.10 Image analysis

Slides were scanned using an Aperio Scanscope platform (x400 magnification). Files were analysed using the Aperio Spectrum image analysis system (Spectrum Version 11.1.0.751, Aperio Technologies, Inc.). Representative areas were annotated and analysed using the Aperio cellular algorithm. The algorithm generated data for a range of parameters including the number of cells analysed, the proportion of positive cells, and the proportion of strongly-positive cells. Data were collated in an Excel spreadsheet.

2.11 Statistical analysis

Statistical analysis was performed using SPSS 23.0 software (IBM, Portsmouth, UK). Descriptive analysis was used to explore the continuous data. The analysis included a Shapiro-Wilk test and Kolmogorov–Smirnov tests of normality. The Shapiro-Wilk test result was used due to the relatively small numbers of cases in each subgroup (<50 cases). The data were normally distributed when a Shapiro-Wilk test result >0.05. Normally distributed data were analysed using parametric tests. For comparison of multiple subgroups, a one-way analysis of variance (ANOVA) test with the Bonferroni correction was used. Binary comparisons were performed using the independent sample T-test and Paired samples T-test. Results were considered significant at $p \leq 0.05$. A Shapiro-Wilk test result of <0.05 indicated that the data significantly deviated from a normal distribution. These data were analysed using non-parametric tests Binary comparisons were performed using the Mann-Whitney U test. Results were considered as significant at $p \leq 0.05$. Kaplan-Meier survival curves were generated using Log Rank Mantel-Cox test. For oral epithelial dysplasia, adverse outcome or malignant transformation were designated as the defined event (=1). For early-stage OSCC, adverse outcome or death from disease was designated as the defined event (=1). Spearman's coefficient correlation analysis and Pearson's product-moment test was used to determine possible associations between pairs of parameters.

Product	Clone	Species	Manufacturer	Dilution	Retrieval	Detection
BMI-1	EPR3745(2)	Rabbit	Abcam	1:3000	MCC1	Optiview
CD44v6	VFF.7	Mouse	Leica	1:400	MCC1	Optiview
CK5/6[1]	D5/16B4	Mouse	Dako	1:50	SCC1	Ultraview
Epsin 1 & 2[2]	ZZ3	Mouse	San Raffaele Scientific Institute, University of Milan, Italy	1:600	MCC1	Optiview
Epsin1*	Polyclonal	Rabbit	Sigma-Aldrich	Failed optimisation		
Epsin2*	Polyclonal	Rabbit	Fisher Scientific	Failed optimisation		
Epsin3	Polyclonal	Rabbit	Sigma Aldrich	Failed optimisation		
Epsin3[2]	25G3-2	Mouse	San Raffaele Scientific Institute, University of Milan, Italy	1:25	SCC1	Optiview
Hes1	EPR4226	Rabbit	Abcam	1:200	SCC1	Ultraview
Hey1	Polyclonal	Rabbit	Millipore	Failed optimisation		
Ki67[1]	MIB-1	Mouse	Dako	1:100	SCC1	Ultraview
Notch1*	D1E11	Rabbit	Cell Signaling	1:200	SCC1	Optiview
Notch1	EP1238Y	Rabbit	Abcam	1:400	SCC1	Optiview
Notch 1 (Cleaved)	D3B8	Rabbit	Cell Signaling	1:100	MCC1	Optiview
p63[1]	NCL-L-p63	Mouse	Leica	1:50	SCC1	Ultraview

Table 2.6: Immunohistochemical reagents and conditions

[1]Verified diagnostic tests performed in a CPA(UK)Ltd accredited pathology laboratory. The remaining antibodies were optimised for the research study.
[2]Kind gift of Professor Cremona (IFOM, Fondazione Istituto FIRC di Oncologia Molecolare, Università Vita–Salute San Raffaele and Istituto Nazionale di Neuroscienze, Via Adamello 16, 20139 Milano, Italy).

SCC1 and MCC1 are Ventana Benchmark Ultra automated retrieval protocols. *These antibodies were used in the western blot analysis (Table 2.5).

Gene name	Transcript Variant	Accession number.	Primer sequence (5'---> 3')	Anneal temp (°C)
Epsin1	V1	NM_001130071.1	**Forward primer**: ^{415}TCTTCAGGTGCCTGGCTTTC^{434} **Reverse primer**: ^{603}ACTGGGCTCCTTACTCCTGG^{584}	60
	V2	NM_001130072.1	**Forward primer:** ^{235}GGCCGAGATGCGGTGAC^{251} **Reverse primer:** ^{403}TCCGCCTCTGAGTAGTTGTG^{384}	60
	V3	NM_013333.3	**Forward primer:** ^{1322}GAAGTTCCGATGGTGGGGTC^{1341} **Reverse primer:** ^{1479}AGAGAACTCGTCGGGCTCC^{1461}	60
Epsin2	V1	NM_148921.3	**Forward primer:** ^{97}CCTCTCGAGCGCTGCC^{112} **Reverse primer:** ^{289}GAAGCCATGACCAGGCTACA^{270}	59
	V2	NM_014964.4	**Forward primer:** ^{97}CCTCTCGAGCGCTGCC^{112} **Reverse primer:** ^{289}GAAGCCATGACCAGGCTACA^{270}	59
	V3	NM_001102664.1	**Forward primer:** ^{97}CCTCTCGAGCGCTGCC^{112} **Reverse primer:** ^{275}GTTCTTCCTGCTCAGCCACT^{256}	59
Epsin3		NM_017957.2	**Forward primer:** ^{1255}GTCCACCATCAGCGGGAC^{1272} **Reverse primer:** ^{1425}CGGCCTAAAACCTGGGATGT^{1406}	60

Table 2.7: Primers designed to anneal to the human Epsin variants. Annealing temperature is given. Numbers in superscript show where the primer anneal to individual variants.

Chapter 3 **Epsin expression in oral cancer cell lines**

3.1 Introduction

The work presented in this chapter is concerned with investigating the expression of Epsins (Epsin1, 2 and 3) in oral squamous cell carcinoma-derived cell lines. Immortalised normal oral keratinocytes were used as a comparator. The expression of Epsin RNA was measured using semi-quantitative RT-PCR, quantitative RT-PCR and RNA in situ hybridisation. Epsin protein was assessed using Western blotting and immunocytochemistry. The expression of Epsins in the oral squamous carcinoma has not been carried out previously, however, several studies have reported the role of Epsins in other human cancers.

3.1.1 Epsins and cancer

The Epsin family of endocytic adaptors are reported to be upregulated in different types of human cancers. For example, Epsin1, 2 and 3 expression are elevated in lung fibrosarcoma (Coon et al. 2010; Coon et al. 2011) and gastric cancers (Ko et al. 2010). Epsin2 is upregulated in breast adenocarcinoma (Pawlowski et al. 2009). The human prostate cancer cell line, LnCap, shows high levels of expression of Epsin1 and 2 (Tessneer et al. 2013) and the human lung non-small-cell carcinoma cell line, EKVX, shows elevated levels of Epsin3 (Wang et al. 2006).

3.1.2 Oral cancer cell lines and immortalized normal oral keratinocytes cell line

A panel of well characterised oral squamous cell carcinoma (OSCC) cell lines were used in this study. Their derivation have been described previously (Table 2.1; (Prime et al. 1990; Edington et al. 1995). The malignancy of the cell lines has been established in an orthotopic mouse model. Cells were injected into the floor of the mouth of athymic mice to establish tumorigenicity, local spread and metastasis (Prime et al. 2004). Consequently, the cells are valuable tools in the study of oral carcinogenesis. The immortalized oral keratinocytes cell line, OKF6, has the ability to overcome senescence without displaying abnormalities of either growth or differentiation (Dickson et al. 2000) and is considered to be a satisfactory model of normal oral keratinocytes. The prostate cancer cell line, LnCap, was used as a positive control as it is known that Epsins 1 and 2 are upregulated in this cell line (Tessneer et al. 2013).

3.2 Aims

To investigate Epsin expression in OSCC-derived cell lines and normal oral keratinocytes using a variety of different methods

3.3 Results

3.3.1 RT-PCR analysis of Epsin expression

RNA was extracted from each of the cell lines and cDNA was prepared. Semi-quantitative RT-PCR analysis was performed to assess the endogenous expression of Epsin1 (and its splice variants: v1, v2, v3), Epsin2 and Epsin3. The housekeeping gene GAPDH was used to normalize the expression of Epsin.

Epsin1v1 expression was very low, almost undetectable, in all cell lines, including the positive control cell line, LnCap (Figure 3.1a). By contrast, Epsin1v2 and Epsin1v3 transcripts were detectable and showed variable expression across the samples. There was no Epsin1v2 RNA in normal oral keratinocytes, but all the OSCC cell lines and LnCap had detectable Epsin1v2 RNA. H314 had the highest levels of Epsin1v2 RNA (Figure 3.1b). Epsin1v3 expression was heterogeneous, some of the cancer cell lines had higher levels of transcripts and some were lower than normal oral keratinocytes. LnCap had relatively low Epsin1v3 levels, whereas H314 had the highest. (Figure 3.1c). Epsin2 RNA could not be detected in any cell lines, including LnCap, which was predicted to have high levels of Epsin2 expression (Figure 3.2a). Epsin3 RNA was detected in all the samples and there were different levels of expression in the OSCC cell lines. H357, H400, H413, and BICR31 had the highest expression, the remaining cell lines had similar levels to normal oral keratinocytes (Figure 3.2b). These results suggest that the Epsin2 gene is not expressed in normal oral keratinocytes or OSCC, although there was no positive control to quality assure the method. Epsin1 gene expression was variable across the cell lines, H314 expressed the highest levels. Epsin3 gene expression was variable across the cell lines, H357, H400, H413, and BICR31 had the highest levels. Interestingly, the prostate cancer-derived cell line, LnCap, chosen as a likely positive control, had only modest levels of Epsin3 RNA.

.

3.3.2 Epsin protein expression by Western blot

The level of Epsin1 protein expression was relatively high in all the samples, including normal oral keratinocytes. H314 and H413 had the lowest levels of Epsin1 protein (Figure 3.3a). Interestingly, H314 had the highest level of Epsin1 gene expression, but one of the lowest levels of Epsin1 protein. Epsin2 protein could not be detected in any cell lines, including LnCap, which was predicted to have high levels of Epsin2 expression (Figure 3.3b). These data correlate with the absence of Epsin2 gene transcription in all the cell lines (Figure 3.2a). Epsin3 protein expression was relatively low in the normal oral keratinocytes and generally higher in the OSCC-derived cell lines (Figure 3.3d). Quantitative analysis of the band intensities, normalised to the reference protein α-tubulin, demonstrated that H400 had the highest level of Epsin3 expression, there was a 20 fold difference between Epsin3 levels of expression in H400 and OKF6 ($p<0.001$). There was around a 15 fold difference between H400 and H103, H314 H413, BICR56 ($p<0.001$), H357 and H376 ($p<0.01$) (Figure 3.4). Interestingly, H400 had relatively high levels of Epsin3 gene expression, which correlated with protein expression.

3.3.3 Immunocytochemical analysis of Epsin protein expression

The cell lines were cultured and cell pellets were fixed in formalin and processed to paraffin wax prior to immunocytochemical (ICC) staining. The cell pellets prepared by trypsinisation showed better preservation of the cellular details and the ICC was more reproducible between samples than the scraping method. Initial experiments, focused on confirming the squamous differentiation of the cell lines. Two well established markers of squamous differentiation, namely cytokeratin 5/6 and p63, were used for this purpose (Table 2.6). The normal oral keratinocytes and OSCC-derived cells showed strong cytoplasmic expression of cytokeratin 5/6 and strong nuclear expression of p63, by contrast, the prostate adenocarcinoma, LnCap, was negative for both markers (Figure 3.5). The ICC staining was quality assured by using control sections of tonsil, which showed the expected staining of squamous epithelium for cytokeratin 5/6 and p63 (Figure 3.5). The cell pellets were then stained with Ki67 to determine the proliferation index. All cell lines showed distinctive nuclear Ki67 expression. The ICC staining was quality assured by using control sections of tonsil, which showed the expected staining of squamous epithelium and lymphoid follicles for Ki67 (Figure 3.6A). Image analysis of the percentage of positive nuclei (PPN) demonstrated that H357 and BICR56 cells had lowest number of cells in cell cycle

compared to other OSCC, normal oral keratinocyte and LnCap cell lines ($p<0.001$) (Figure 3.6B).

Immunocytochemical analysis of Epsin1 and 2

The antibody ZZ3 (anti-Epsin1 and 2) was optimised for ICC by staining sections of normal tonsil (Table 2.6). The tonsil showed strong membrane and cytoplasmic staining of squamous epithelium, endothelium and lymphoid follicles (Figure 3.7A). All the cell lines showed strong membrane and cytoplasmic staining with the ZZ3 antibody (Figure 3.7A). Stained slides were scanned using the Aperio eSlide Manager, Leica Biosystems and the percentage of positive cells (PPC) was calculated. The mean number of cells analysed per cell line was 28355 (range: 4411-60816). The percentage of positive cells revealed that H314, H400 and H413 cell lines had significantly higher ZZ3 expression compared to other OSCC, normal oral keratinocyte and LnCap cell lines ($p<0.001$). The expression level of ZZ3 in the other OSCC, OKF6 and LnCap cell lines were similar and there was no significant difference between them (Figure 3.7B). The results of the Western blot analysis, showing high Epsin1 expression, but no Epsin2 expression, suggests that ZZ3 was likely to be detecting high levels of Epsin1 rather than Epsin2.

Immunocytochemical analysis of Epsin3

The anti-Epsin3 antibody was optimised for ICC by staining sections of normal tonsil (Table 2.6). The tonsil showed strong membrane and cytoplasmic staining of squamous epithelium (Figure 3.8A). Epsin3 protein was detected in all the samples and there were different levels of expression in the OSCC cell lines. H357, H400, H413 and prostate cancer cell line LnCap had the highest expression compared to the other OSCC cell lines and normal oral keratinocytes. H103, H314 and BICR56 had the lowest Epsin3 protein expression compared to the OSCC, normal oral keratinocytes and LnCap cells (Figure 3.8A). Stained slides were scanned using the Aperio eSlide Manager, Leica Biosystems. The staining for each cell line was subject to image analysis and the percentage of Epsin3 positive cells was calculated for each cell line. The mean number of cells analysed per cell line was 6276 (range: 1367- 16133). Between the OSCC-derived cell lines there was a significant difference: H357, H400, and H413 cell lines had the highest Epsin3 protein expression compared to H103, H157 and H314 ($p<0.001$). H357 and H400 was higher than BICR31 ($p<0.05$). However, H357 was the only OSCC cell line that had higher significant expression

compared to the OKF6 ($p \leq 0.05$). H103 and H314 showed lower expression compared to OKF6 ($p<0.001$). BICR56 cell line had the lowest expression (Figure 3.8B).

3.3.4 Quantitative RT-PCR analysis of Epsin3 expression

The cDNA samples were prepared using reverse transcriptase (Applied Biosystems, USA). The final concentration of the cDNA template was 100ng/µl. The mean fold was calculated using Δct values as previously described (Section 2.3.6). Epsin3 showed variable expression between the cell lines (Figure 3.9). The mean values showed similar patterns of expression to those identified by semi-quantitative RNA and Western blot analysis. H400 cells had the highest Epsin3 mRNA expression by qRT-PCR. It was significantly higher than all the other cell lines and normal oral keratinocytes ($p< 0.001$). H357 had the second highest Epsin3 gene expression and was significantly higher by comparison with, H103, H314, H376, BICR56, LnCap and normal oral keratinocytes ($p<0.001$). By contrast, H314 had virtually no Epsin3 RNA by qRT-PCR and was lower than normal oral keratinocytes and all the other cell lines ($p<0.05$). H314 also had the low Epsin3 protein levels by comparison with the other OSCC cell lines.

3.3.5 RNA in situ hybridization

Epsin3 RNA in situ hybridisation was performed using RNAscope® 2.5 VS Assay (Advanced Cell Diagnostics, Inc. USA) on a Ventana Discovery Ultra autostainer (Ventana Medical Systems Inc., USA). Epsin3 RNA could not be detected using this method, although the positive control gene PPIB was detectable, suggesting that the method was not sufficiently sensitive to detect Epsin3 RNA in formalin-fixed paraffin-embedded cell preparations (data not shown).

3.3.6 Correlation of Epsin3 RNA expression with protein levels

H400, H357 had consistently high levels of Epsin3 RNA and protein. By contrast H314 and H103 had consistently low levels of Epsin3 RNA and protein (Table 3.1).

Rank	Cell line	Epsin3 mRNA values	Cell line	Epsin3 protein values (WB)	Cell line	Epsin3 protein values (ICC)
1	H400	6.26	H400	19.68	H357	61.32
2	H357	3.07	LnCap	11.83	H400	60.87
3	BICR31	2.25	H157	11.14	LnCap	59.15
4	H413	2	BICR31	10.44	H413	55.42
5	H157	1.81	H357	5.29	OKF6	47.72
6	H376	1.22	H376	5.26	BICR31	46.01
7	LnCap	1.08	BICR56	4.9	H157	39.86
8	OKF6	1	H413	4.61	H376	35.64
9	BICR56	0.92	H103	4.24	H103	22.61
10	H103	0.82	H314	3.02	H314	22.60
11	H314	0.07	OKF6	1	BICR56	6.44

Table 3.1: Summary of Epsin3 RNA expression analysed by qRT-PCR and Epsin3 protein level analysed by Western blot (WB) and immunocytochemistry. Ranked high to low (1 = highest; 11= lowest).

To identify if Epsin3 RNA expression levels correlated with the protein levels, statistical analysis was carried out by bi-variate correlation analysis followed by Spearman's Rho test.There was a significant correlation between Epsin3 RNA expression and protein levels analysed by Western blot ($p< 0.001$) (Figure 3.10), and by immunocytochemistry ($p<0.001$) (Figure 3.11). A statistical analysis carried out by bi-variate correlation analysis followed by Pearson's Product-Moment test revealed a significant correlation between Epsin3 protein expression measured by Western blot and Epsin3 protein expression measured by immunocytochemistry ($p<0.001$) (Figure 3.12).

3.3.7 Investigation of the correlation between Epsin3 protein expression and the Ki67 proliferation index.

The relationship between Epsin3 protein levels and the Ki67 proliferating index was analysed by bi-variate correlation analysis followed by Spearman's Rho test. There was no significant correlation between Epsin3 and the proliferation index ($p>0.05$) (Figure 3.13).

3.3.8 Relationship between Epsin3 expression and characteristics of the OSCC cell lines.

The OSSC cell lines have different derivations and exhibited different behaviours in an orthotopic mouse model of tumourigenicity. There was no correlation between Epsin3 expression and the characteristics of the cell lines, namely site, differentiation and

tumour stage. There was no correlation between Epsin3 expression and tumourigenicity of the cell lines in mice.

3.4 Discussion

Work presented in this chapter was concerned with screening the expression of Epsins (1, 2, and 3) in the oral squamous cell carcinoma in vitro. A panel of OSCC-derived cell lines were used in addition to an immortalized normal oral keratinocyte cell line.

Epsins are a family of endocytic adaptor proteins that play an important role in clathrin-mediated endocytosis of ubiquitinated cell surface receptors. In mammals, three different types of Epsins are expressed; Epsin1 and 2 are expressed in all tissues with the highest concentration in the brain (Chen et al. 1998; Rosenthal et al. 1999; Chen et al. 2009). While Epsin3 is reported to be expressed in the parietal cells of stomach (Ko et al. 2010) and immature keratinocytes (Spradling et al. 2001). Clathrin-mediated receptor internalization is required for several signalling pathways that are involved in the proliferation of tumour cells, accordingly, Epsins may play role in mediating these pathways (Bache et al. 2004). The Epsins may have a potential role in carcinogenesis through its involvement in cell proliferation, differentiation and migration. Accordingly, Epsins expression was investigated and measured at both RNA and protein level in this study.

RT-PCR results revealed that the Epsin1 variant1 had very low expression through the panel of cell lines, while variant2 and 3 had high expression. Epsin1 variant1 represents the canonical sequence and all other splices refer to it. Its length is 576 and mass 60.293kDa. Variant 2 length is 662 and mass 69.040kDa, differs from canonical splice sequence that at positions 1-1 there is adding of amino acids and position 202-226 are missing. Variant3 length is 550 and mass 57.504kDa, its sequence differs from canonical splice as follow: 202-226 and 393-393 positions are missing (Morinaka et al. 1999; Gerhard et al. 2004). By contrast there was no expression of Epsin2. At the protein level, Western blot analysis revealed similar results, in which Epsin1 had high expression through all cell lines and Epsin2 didn't show any expression. So it can be concluded that Epsin1 has similar expression in the normal and cancer cells, whilst Epsin2 was not expressed in any of the cells. The ZZ3 antibody which represent Epsin1 and 2 expression analysed by immunocytochemistry was overexpressed in the cell pellets of all cell lines and there was no significant difference between them. However, these results are likely to represent Epsin1 protein expression, because the expression

of Epsin2 protein was not detected by Western blot analysis. In contrast, upregulation of Epsin2 expression has been reported in adenocarcinoma cell line and prostate adenocarcinoma (Pawlowski et al. 2009; Tessneer et al. 2013).

However, Epsin3 expression was significantly different between the OSCC-derived cell lines. Moreover, some OSCC-derived cell lines had significantly higher expression compared to the immortalized normal oral keratinocyte cell line at both RNA and protein level. It is possible that up-regulated Epsin3 has a role in oral carcinogenesis. Other studies have reported similar observations. For example, overexpression of Epsin3 was found in cutaneous wound healing and also elevated in migrating keratinocytes, but not in differentiating cells in vitro, suggesting Epsin3 has a key role in epithelial biology (Spradling et al. 2001). Moreover, human lung non-small-cell carcinoma cell line, EKVX, shows upregulation of Epsin3 expression (Wang et al. 2006). Comparably, other studies revealed upregulation of Epsins in cancer and their association with invasion and migration of cancer cells through activation of RhoGTPase pathway. Coon et al. (2010), reported that Epsin N-terminal homology (ENTH) domain interacts with the N terminus of the RalBP1 (Ral-Binding Protein), this non-classical mechanism does not require internalization and may have role in cell migration and invasion. It has been shown previously that Epsin-RalBP1 interaction is essential for cell invasion through the basement membrane in human fibrosarcoma cell lines. RalBP1 protein has been reported to be overexpressed in several invasive cancers such as bladder, lung, skin and prostate cancer (Smith et al. 2007; Awasthi et al. 2008). RalBP1 works as GAP (GTP activating protein) which inactivates GTPase, Epsin-GAP interaction inhibits GAP activity (Aguilar et al. 2006) and activate RhoGTPase signalling. Moreover, RalBP1 is known to affect Rac1 through an Arf6-dependent pathway and activates Arf6-dependent cell migration. It was reported that overexpression of Epsin, mainly Epsin2 and 3, or RalBP1 promotes cell invasiveness, and depletion of Epsin-RalBP1 complex leads to deficiency in Arf6 activation and abnormalities of cell migration and invasion (Coon et al. 2010).

The other role of Epsins was found in Notch signalling activation, which is an endocytosis dependent pathway (Nichols et al. 2007). Epsins are required for internalization of the ligand-receptor complex, the required process for Notch activation (Wang and Struhl 2004; Chen et al. 2009). The role of Notch signalling in cancer will be discussed in the next chapter in detail.

Moreover, Epsin was reported to play a role in angiogenesis; it was proved that Epsin1 and 2 regulate the vascular endothelial growth factor (VEGF) signalling in a mouse model and removal of Epsin1 and 2 from endothelial tumour vasculature leads to prolonged VEGF2 signalling and consequently results in formation of aberrant vessels which causes impairment of tumour genesis and could contribute to tumour growth retardation (Pasula et al. 2012). In this regard, double knockout of endothelial Epsin1 and 2 in embryos resulted in formation of a disorganized vascular network, indicating the necessity of Epsins in angiogenesis regulation (Tessneer et al. 2014). To further support this observation, it was showed in a recent study that the binding of Epsin (1 and 2) and VEGFR2 is directed by a complex mechanism that includes ubiquitin-dependent and ubiquitin- independent interactions, suggesting that Epsins have a critical role in VEGF2 signalling adjustment (Rahman et al. 2016). Furthermore, Epsin1 was found to play a significant role in the internalization of Epidermal Growth Factor Receptor (EGFR) and promotes EGFR downregulation. Epsin1 knockdown inhibits internalization of EGFR as the interaction between Epsin1 and EGFR is impaired (Kazazic et al. 2009). Deficient internalization of EGFR leads to activation of signalling and consequently results in malignant transformation, as EGF signalling was reported to be upregulated in many solid tumours (Grandal and Madshus 2008).

Our present results revealed that Epsin3 was up-regulated in some of OSCC-derived cell lines, while other cell lines showed low Epsin3 expression. The expression of Epsin3 was ranked in the panel of cell lines at RNA and protein level. H400, H357 and BICR31 had the highest expression, H103 and H314 had the lowest expression. Interestingly, immunocytochemistry results showed the same pattern. The difference in the expression of Epsin3 between cell lines is possibly due to the differences in the origin of these cells. Moreover, the tumourigenesis, local spread, capacity to form primary tumour at the site of inoculation and metastatic dissemination are variable (Prime et al. 2004).

Consequently, our results may simply reflect in vitro cell culture conditions. Further analysis was carried out to investigate Epsin3 RNA expression in the cell pellet of cell lines using RNA in situ hybridization. The Epsin3, however, did not give any signals. Interestingly the finding in this chapter revealed that Epsin3 is up-regulated in some of OSCC-derived cell lines compared to the immortalized normal oral keratinocytes at RNA and protein level. These results are consistent with previous studies that reported Epsin3 up-regulation in some invasive cancers such fibrosarcoma (Coon et al. 2011).

This indicates that Epsin3 may have a role in cancer progression by activation (Notch, RohGTPase) or downregulation (VEGFR, EGFR) pathways which are involved in carcinogenesis process via its endocytic activity. However, Epsin2 did not show expression in all cell lines. Expression of Epsin1 was high in OSCC-derived and OKF6 cell lines.

In summary, work presented in this chapter has established that Epsin1 expression was the same in OSCC-derived and immortalised normal oral keratinocyte cell lines. Epsin2 was not expressed in the OSCC-derived and immortalised normal oral keratinocytes. Epsin3 showed different expression within OSCC-derived cell lines with higher expression in H357, H400 and BICR31 cell lines compared to the immortalised normal oral keratinocytes.

.

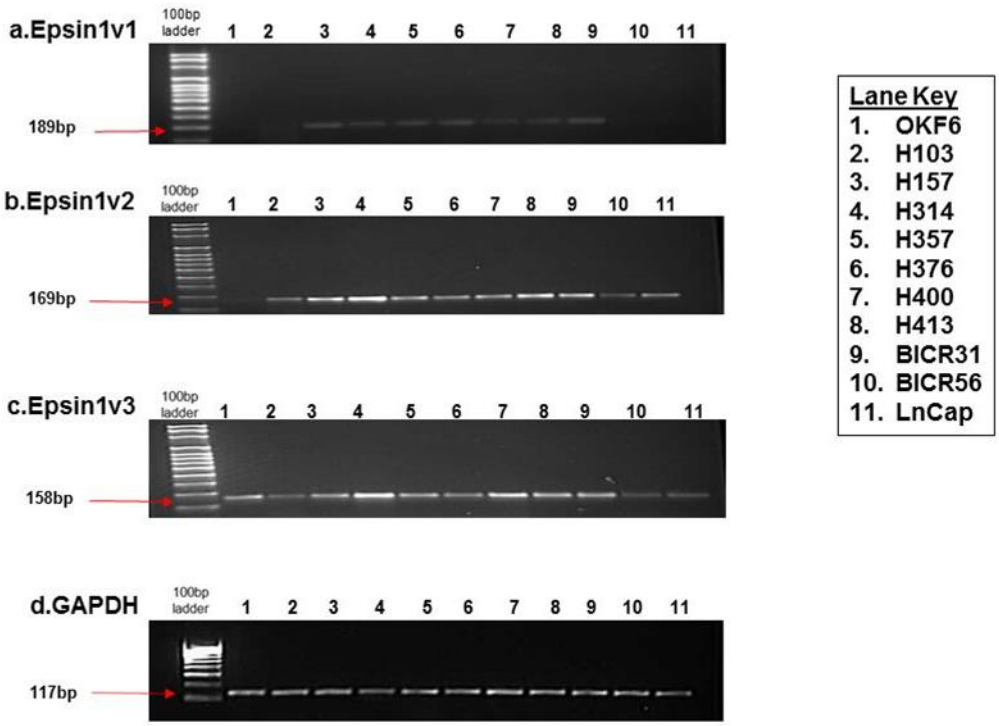

Figure 3.1: Levels of Epsin1 mRNA splice variants in the cell lines

Bands were generated by semi-quantitative RT-PCR from RNA samples extracted from cells grown under standard conditions. Cells were lysed and cDNA was prepared by reverse transcription for each cell line. Negative control RT-PCR identical to those yielding products shown except for the omission of MMLV-RTase resulted in no PCR products. **a)** Epsin1v1 (expected band at 189bp) expression was very low in all cell lines. **b)** Epsin1v2 (expected band at 169bp) expression in the OKF6 was low relative to most of the OSCC-derived cell lines. **c**) Epn1v3 (expected band at 158bp) expression was lowest in H103 and BICR56 cell line, and highest in H314, H400 cell lines. **d)** GAPDH (expected band at 117bp), all cell lines had similar band intensities for the reference gene, GAPDH indicating that the quantities of RNA in the samples were similar.

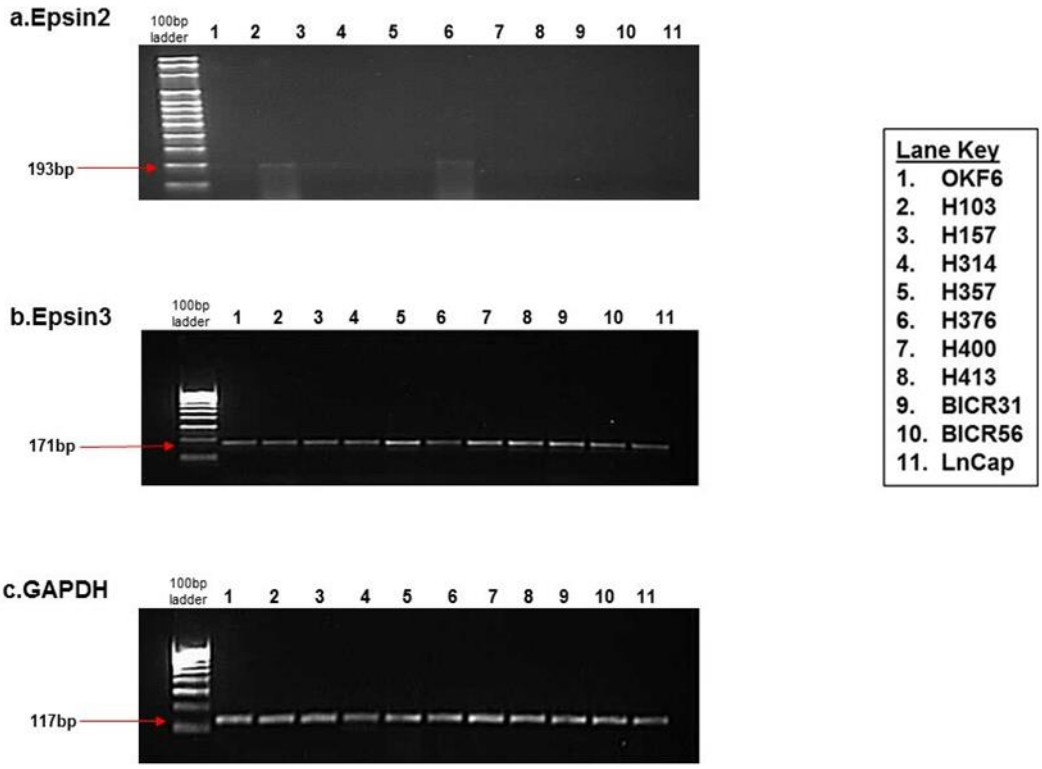

Figure 3.2: Levels of Epsin2 and Epsin3 mRNA expression in the cell lines.

Bands were generated by semi-quantitative RT-PCR from RNA samples extracted from cells grown under standard conditions. Cells were lysed and cDNA was prepared by reverse transcription for each cell line. Negative control RT-PCR identical to those yielding products shown except for the omission of MMLV-RTase resulted in no products. **a)** Epsin2 (expected band at 193bp) was undetectable. **b)** Epsin3 (expected band at 171bp) showed differential expression in the cell lines. H357, H400, H413 and BICR31 had higher levels of Epsin3 expression than OKF6, H103, and BICR56. **c)** GAPDH (expected band at 117bp), all cell lines had similar band intensities for the reference gene, GAPDH, indicating that the quantities of RNA in the samples were similar.

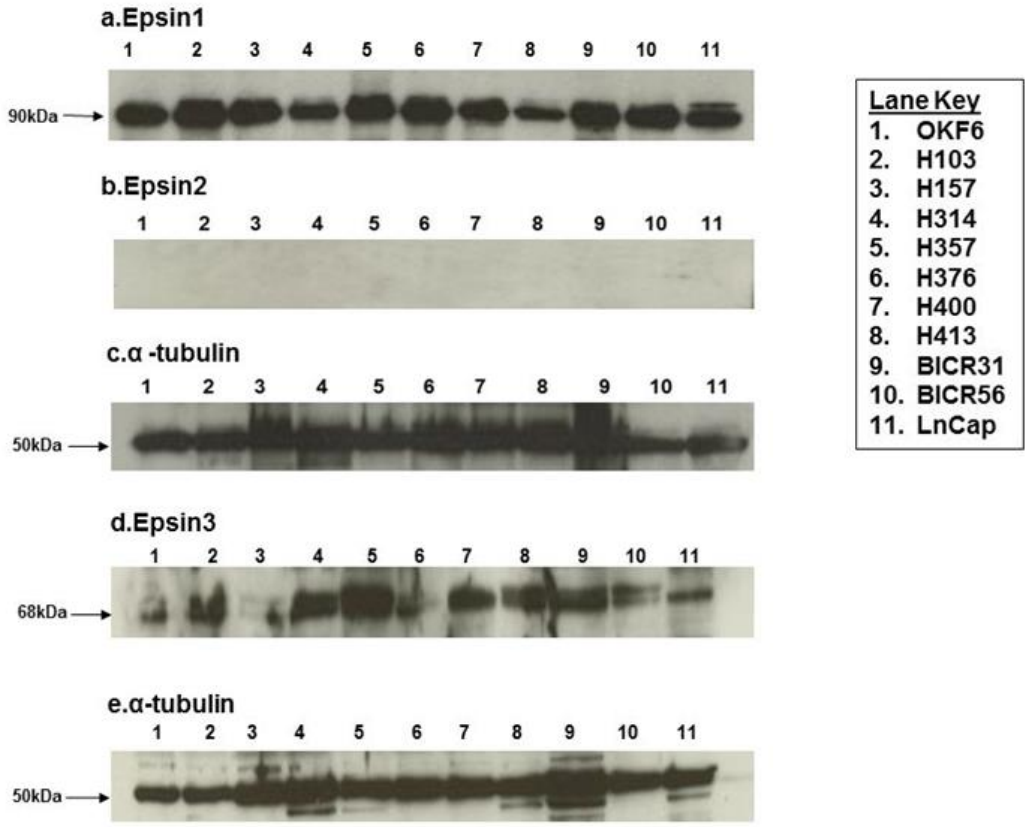

Figure 3.3: Representative Western blots showing expression of Epsins 1, 2 and 3 in the cell lines

The cells were cultured in 6 well plates in a maintenance medium to ~90% confluence. Protein was extracted using RIPA buffer plus inhibitor. 20µg of protein were electrophoresed on 12.5% SDS-PAGE gel and transferred to PVDF membrane. The membrane incubated with antibodies against the Epsin1 (1:500), Epsin2 (1:1000), Epsin3 (1:50) and α-tubulin (1:2000). **a)** Epsin1 protein detected at 90kDa, **b)** Epsin2 protein could not be detected, **c)** alpha-tubulin detected at 50kDa **d)** Epsin3 protein detected at 68kDa **e)** alpha-tubulin at 50kDa. Bands were visualized by chemiluminiscence (ECL) detection reagents (GE Healthcare).

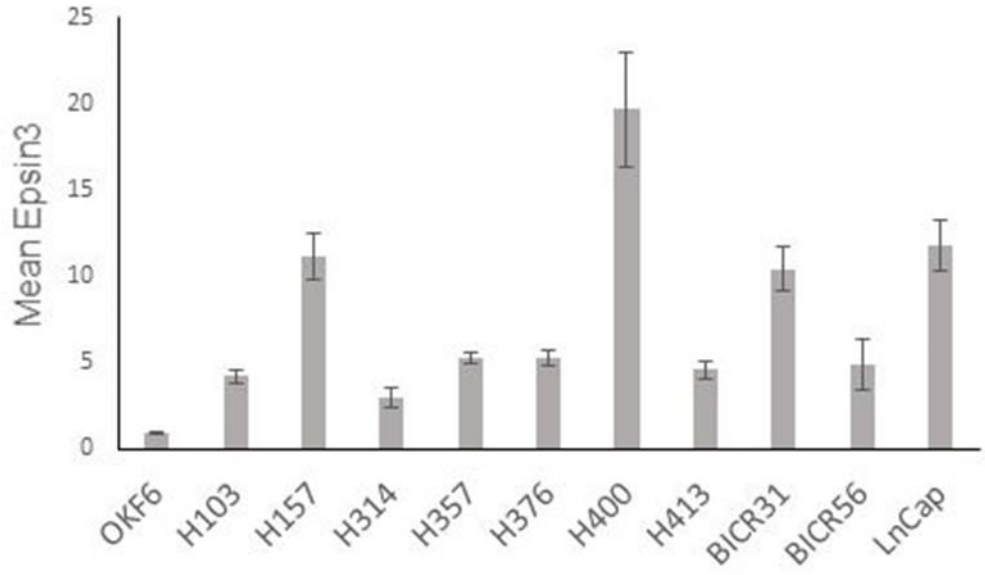

Figure 3.4: Quantitation of Epsin3 protein expression by densitometric analysis of Western blots.

Densitometry (Genetool from synGene, UK.) was adjusted for the background optical density of the X-ray film and normalised to α-tubulin. The results are expressed as the intensity of Epsin3 band (samples from triplicate biological independent experiments, technical replicates n=9) stated as mean ±SD n=9. Epsin3 expression was significantly lower in OKF6 compared to LnCap cell line ($p<0.05$). There was approximately a 10 fold difference between Epsin3 levels of expression in OKF6 and LnCap. H400 cell line had a significantly higher expression, there was about 20 fold difference between Epsin3 levels of expression in H400 and OKF6, and about 15 fold difference in H400 and H103, H314, H413, BICR56 ($p<0.001$), and H357, H376 ($p<0.01$). Significance measured by one-way ANOVA followed by Bonferroni post hoc correction.

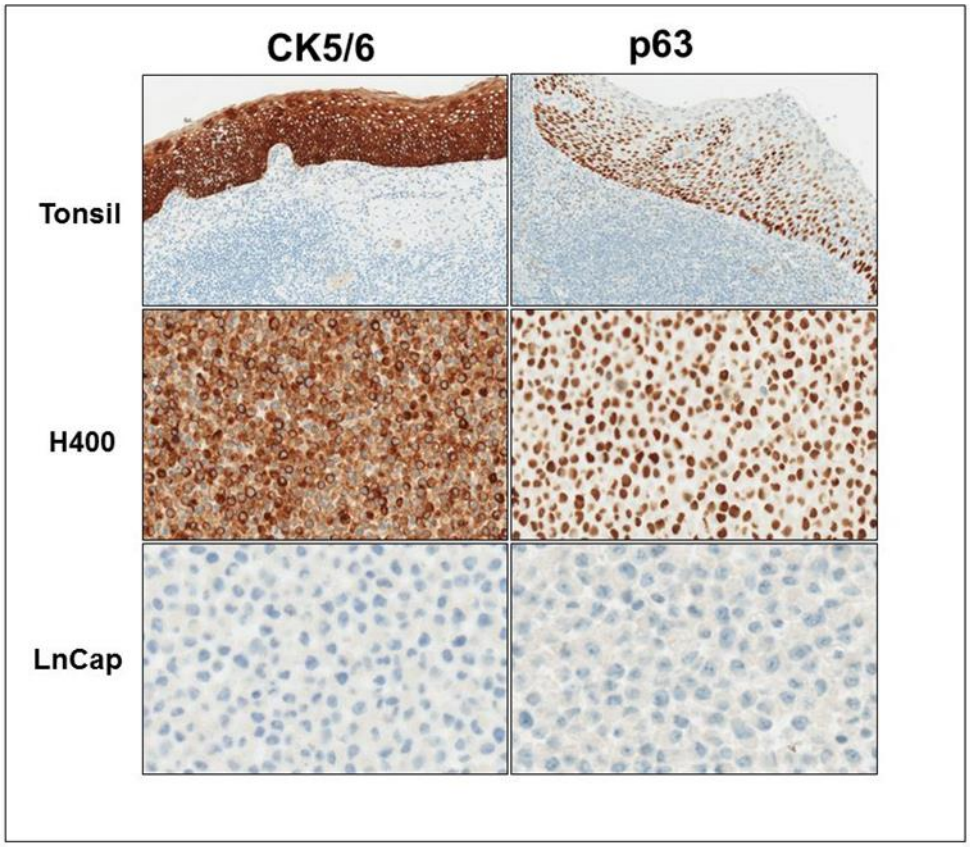

Figure 3.5: Squamous differentiation assessed by immunocytochemistry using cytokeratin 5/6 and p63

The tonsil sections shows high cytoplasmic cytokeratin 5/6 and nuclear p63 staining of squamous epithelium. H400 cell line showed strong cytoplasmic expression of cytokeratin 5/6 and strong nuclear expression of p63. The intensity of staining was similar in the other OSCC-derived lines and the OKF6 cell line indicating the squamous differentiation of these cell lines. By contrast, the prostate cancer cell line, LnCap, was negative for both markers. Images taken at 20x magnification.

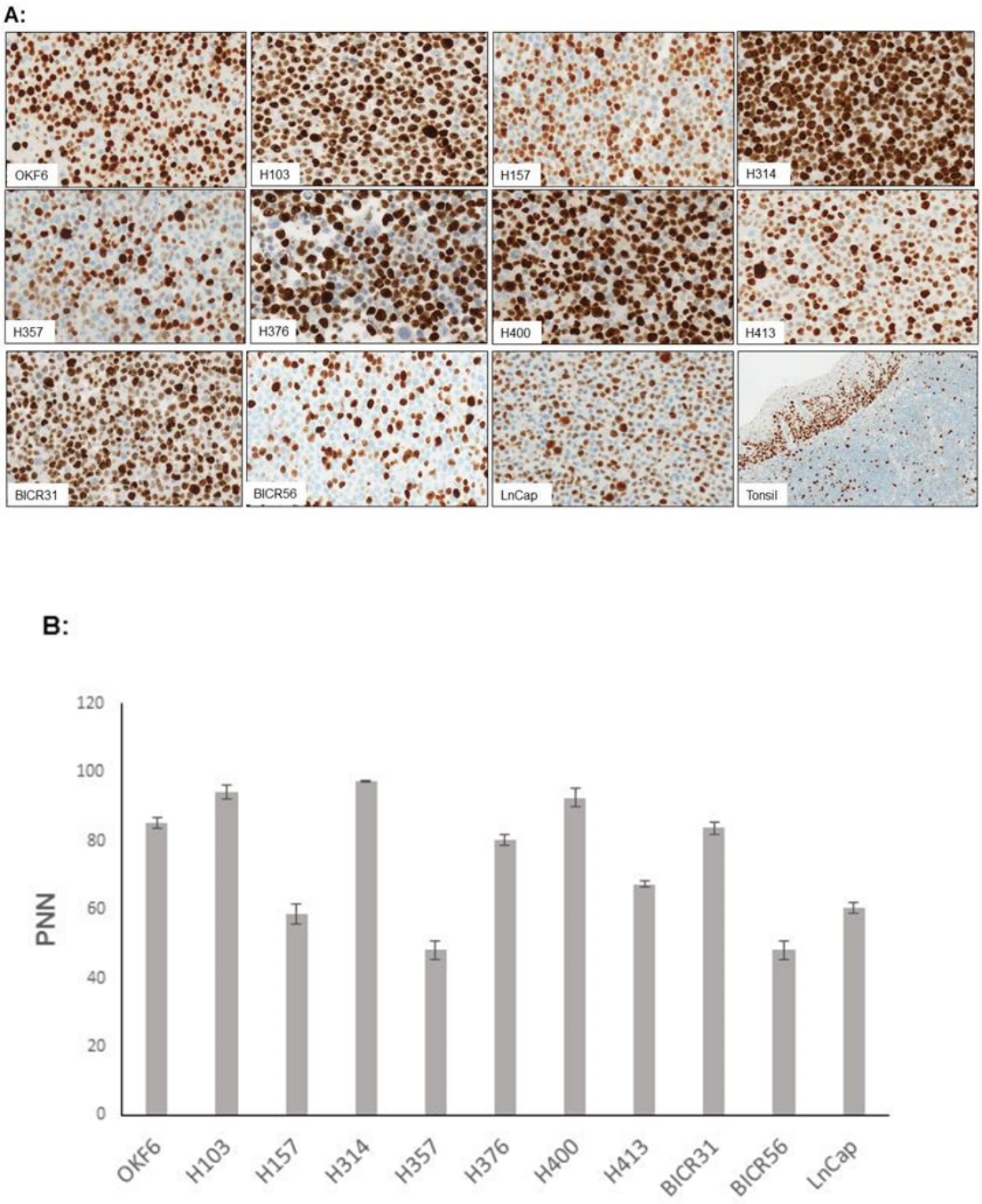

Figure 3.6: The proliferation index assessed by Ki67 immunocytochemistry.

A) The panel of cell lines showed strong nuclear staining of Ki67 protein. Images taken at 20x. The normal tonsil tissue showed positive nuclear staining of the squamous epithelium. Image taken at 10x.

B) The mean of percentage positive nuclei was calculated for each cell line. The expression of Ki67 was significantly lower in H357 and BICR56 cell lines than the other OSCC cell lines ($p<0.001$), OKF6 and LnCap ($p<0.01$). The percentage of positive nuclei stated as mean ±SD n =3. Significance measured by one-way ANOVA followed by Bonferroni post hoc correction.

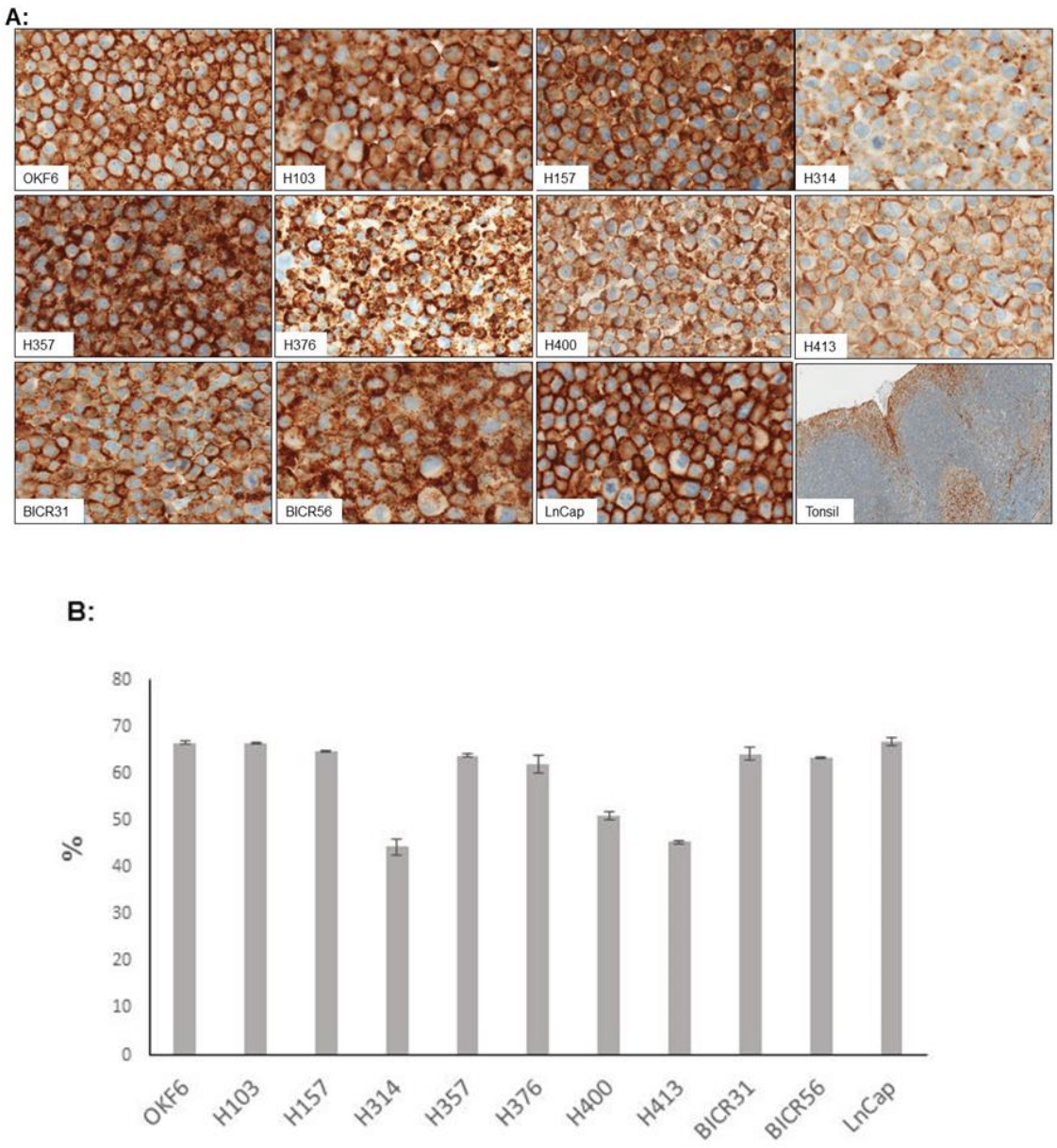

Figure 3.7: Epsin1 and 2 (ZZ3) expression by immunocytochemistry in cell lines and normal tonsil tissue.

A) All the cell lines showed strong membrane and cytoplasmic staining with the ZZ3 antibody. Images taken at 20x. In the normal tonsil tissue ZZ3 stained the squamous epithelium, endothelium and lymphoid follicles. Image taken at 10x.

B) Image analysis of ZZ3 immunocytochemistry showing the percentage positive cells. ZZ3 staining was significantly lower in the H314, H400 and H413 cells than other OSCC, OKF6 and LnCap cell lines ($p<0.001$). The percentage of positive staining stated as mean ±SD n =3. Significance measured by one-way ANOVA followed by Bonferroni post hoc correction.

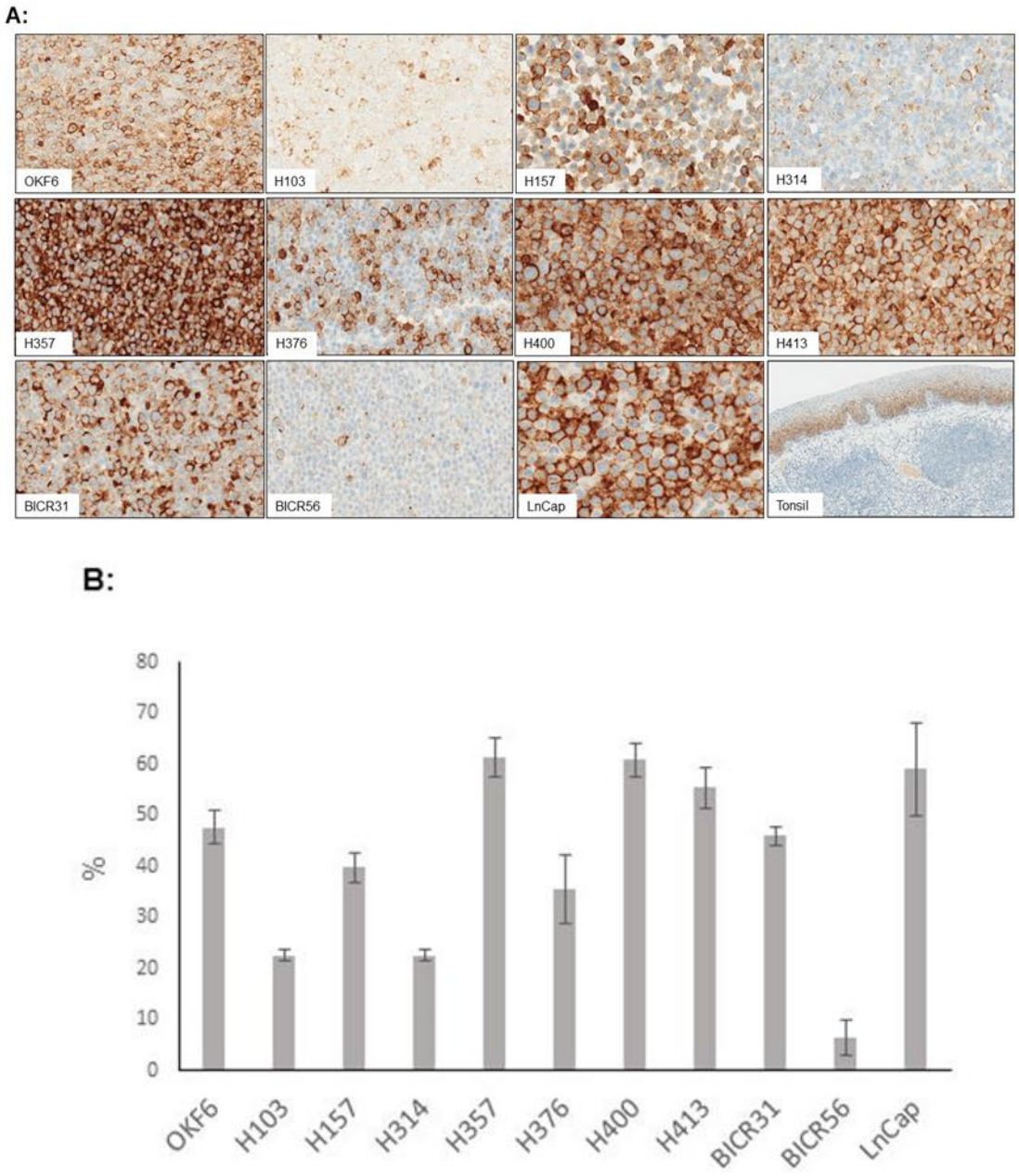

Figure 3.8: Epsin3 expression by immunocytochemistry in cell lines and normal tonsil tissue.

A) The cells showed membrane and cytoplasmic staining with Epsin3. Epsin3 expression was variable across the panel of cell lines. Image taken at 20x magnification. Normal tonsil tissue showed strong staining of squamous epithelium. Image taken at 10x magnification. **B)** Image analysis showing the mean percentage positive cells for each cell line. The expression of Epsin3 was significantly higher in OKF6, H357, H400, H413 and BICR31 cell lines than H103, H314 ($p<0.001$). H357 and H400 had higher significant expression than H157, H376 ($p<0.001$) and BICR31 ($p<0.05$). The BICR56 cell line showed significant low expression compared to OKF6, H157,H357, H376, H400, H413 BICR31, LnCap cell lines ($p<0.001$) and H103, H314 ($p<0.01$). The percentage of positive staining stated as mean ±SD n =3. Significance measured by one-way ANOVA followed by Bonferroni post hoc correction.

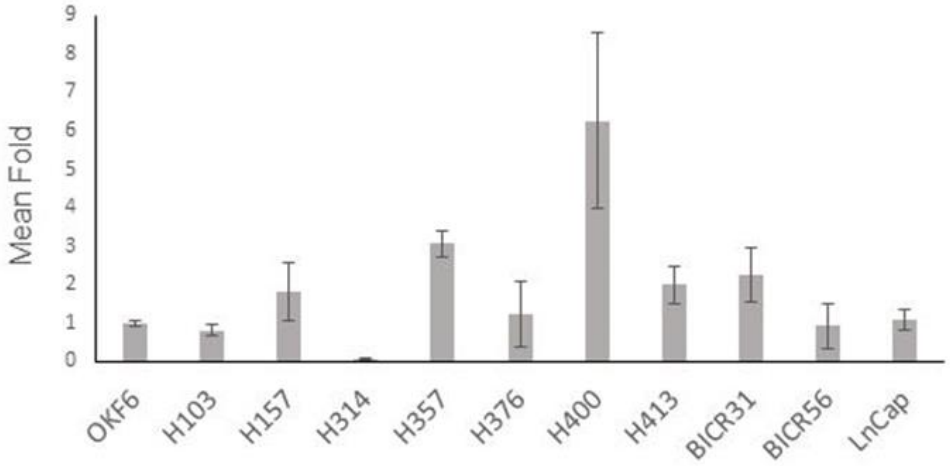

Figure 3.9: Epsin3 gene expression in cell lines by quantitative RT-PCR.

The cells were cultured at $5x10^5$ in 6 well plates. RNA was extracted (three independent experiments) using QIAGEN protocol and cDNA was prepared by reverse transcription. qRT-PCR was used to assess Epsin3 and GAPDH gene expression. Relative Epsin3 mRNA expression was determined using the $2^{-\Delta\Delta ct}$ method by using GAPDH as the reference gene. The data are expressed relative to GAPDH mRNA levels measured in the all cell lines and normalised to the OKF6 cell line. Data are shown as mean ±SD (n=3). H400 cell line showed highest significant Epsin3 expression compared to all OSCC-derived and OKF6 cell lines ($p<0.001$). Epsin3 expression was significantly lowest in H314 compared to H413, BICR31 ($p<0.001$) and H157 ($p<0.01$). H103 showed lower significant Epsin3 expression than BICR31 ($p<0.05$). Significance measured by one-way ANOVA followed by Bonferroni post hoc correction.

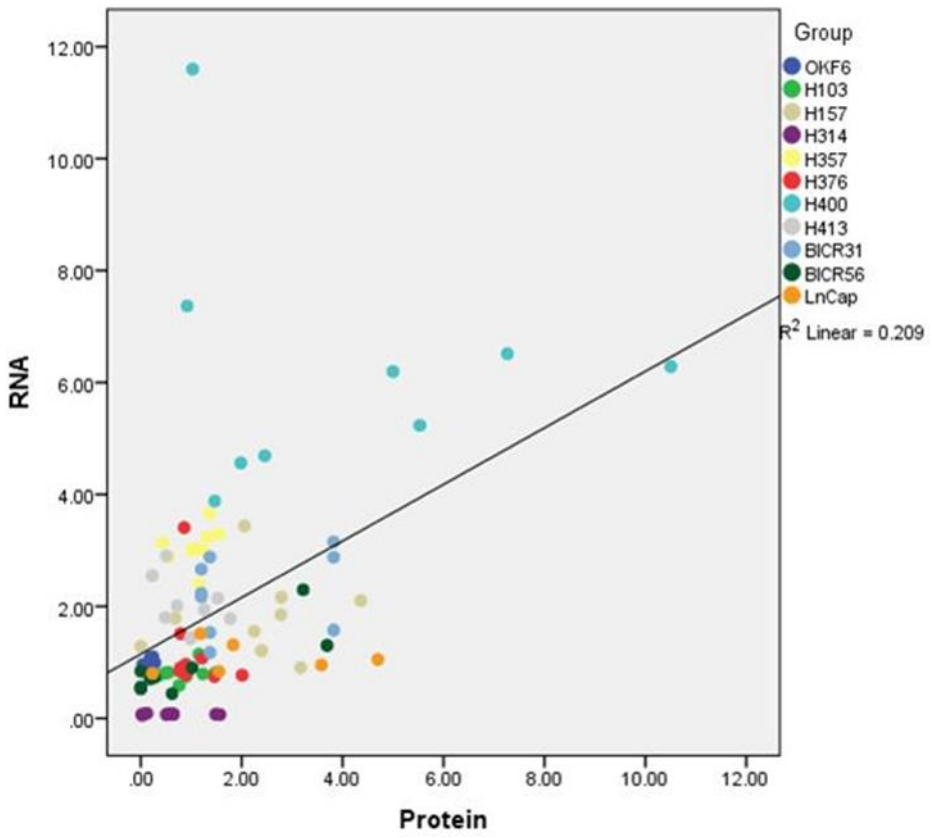

Figure 3.10: Relationship between Epsin3 RNA expression measured by quantitative RT-PCR and Epsin3 protein expression analysed by Western blot.

The correlation between the expression of Epsin3 at the RNA and protein level analysed by bi-variate analysis followed by Spearman's Rho test. The addition of the trend-line indicates a significant correlation ($p<0.001$).

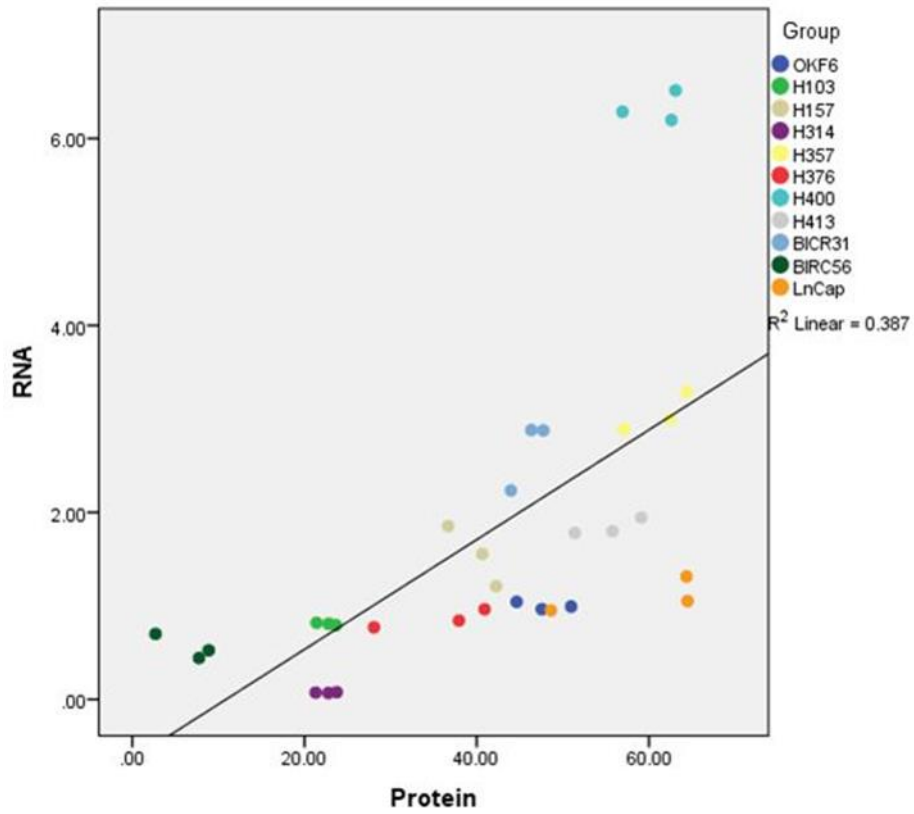

Figure 3.11: Relationship between Epsin3 RNA expression measured by quantitative RT-PCR and Epsin3 protein expression analysed by immunocytochemistry.

The correlation between the expression of Epsin3 at the RNA and protein level analysed by bi-variate analysis followed by Spearman's Rho test. The addition of the trend-line indicate a significant correlation ($p<0.001$).

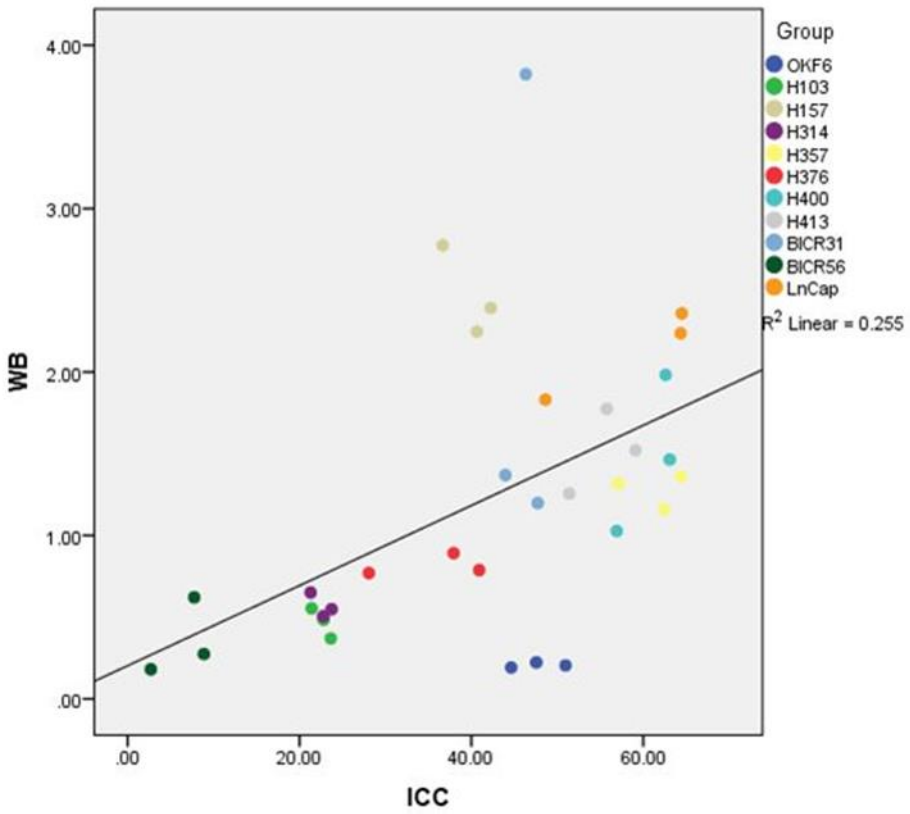

Figure 3.12: Relationship between Epsin3 protein expression measured by Western blot and Epsin3 protein expression analysed by immunocytochemistry

The correlation between the expression of Epsin3 protein levels measured by western blot and immunocytochemistry analysed by bi-variate analysis followed by Pearson's Product-Moment test. The addition of the trend-line indicate a significant correlation ($p<0.001$).

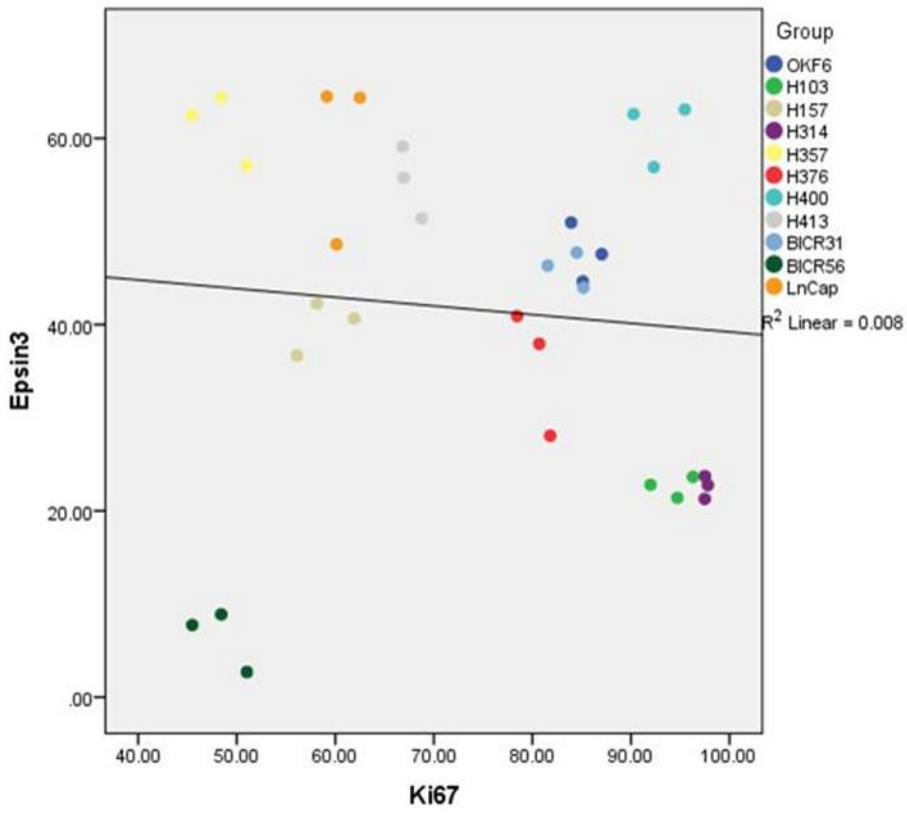

Figure 3.13: The relationship between of Epsin3 protein levels and the Ki67 proliferation index.

Figure show the correlation between Epsin3 and the Ki67 proliferation index, the data analysed by bi-variate correlation analysis followed by Person's Product-Moment test. The addition of trend-line indicate no significant correlation ($p>0.05$).

Chapter 4 **Notch1 expression in oral cancer cell lines**

4.1 Introduction

The work presented in this chapter is concerned with determining the expression of Notch1 in OSCC-derived cell lines. The level of Notch 1 expression was measured at both the RNA and protein levels. In addition, the expression of Notch target genes; Hes1 and Hey1, were analysed. Several studies have reported that Notch1 and its receptors are dysregulated in OSCC. Work presented in Chapter 3 revealed Epsin3 to be dysregulated in OSCC-derived cell lines. Epsins are known to trigger Notch signalling events (Section 1.5.2). Accordingly, we investigated the expression of Notch1 in five OSCC-derived cell lines and used the immortalised normal oral keratinocytes, OKF6, and the prostate cell line, LnCap as comparators. Notch1 expression was then correlated with Epsin3 expression.

Mammals have four Notch proteins which encode different transmembrane receptors these proteins are components of the Notch signalling pathway (Bianchi et al. 2006). When the Notch receptor binds with its ligand, Notch signalling is activated and results in the release of the Notch intracellular domain, which enters the nucleus and activates the transcription of target genes (Section 1.5.2). This pathway is conserved through evolution from Drosophila to vertebrates and plays an important role in cell fate by regulating cell-to-cell communication during development. Signals transmitted through Notch receptors control the development process by influencing proliferation, differentiation and apoptosis (Artavanis-Tsakonas et al. 1999). In Drosophila, active Notch signalling inhibits the expression of pro-neural genes and result in obstruction of neural differentiation (Parks et al. 1997). Notch signalling was also found to inhibit different progenitor cells during Drosophila development, involving cells of the visceral and somatic musculature, midgut and intestine, heart and other internal organs (Hartenstein et al. 1992), and in vertebrates it causes repression of neurogenesis and myogenesis (Chitnis et al. 1995). Active Notch signaling restricts cell differentiation in the above tissues via stimulation of the transcription of basic helix-loop-helix (bHLH) repressor genes, this is called the inhibitory role of Notch signalling that regulates the fate of progenitor cells (Lai 2004). Notch signalling can promote cell development through cell-cell interaction at the boundaries in specific cell population, for example in the development of Drosophila wings; Notch signaling stimulates development and specification of margins that organize the outgrowth of the wing (Kim et al. 1996). Given these observations, Notch signals have diverse roles, it can induce cell proliferation or

cell cycle arrest, lead to increased cell survival or cell death and activate or block cellular differentiation. Consequently, Notch can promote (oncogenic) or limit (suppressor) tumour growth and Notch mutations have been reported in different human cancers. For example, an activating mutation of Notch1 was found in human-acute lymphoblastic leukaemia/lymphoma (T-ALL) (Weng et al. 2004). Increased Notch1 expression has been reported in human breast cancer (Stylianou et al. 2006), lung adenocarcinoma (Donnem et al. 2010) and melanoma (Hoek et al. 2004; Balint et al. 2005). Conversely, transgenic mice with Notch1 knockout develop cutaneous basal cell carcinoma-like lesions, suggesting a suppressor role for Notch signalling (Nicolas et al. 2003). Notch signalling in head and neck squamous cell carcinoma (HNSCC) also has a dual role. Jagged1, Notch ligand, was found to be upregulated in HNSCC (Zeng et al. 2005). Other Notch pathway genes such as Notch1, NICD and Hes1 are reported to be overexpressed in OSCC (Yoshida et al. 2013; Gokulan and Halagowder 2014), suggesting that Notch has a tumour promoting function. Conversely, inactivating mutations of Notch1 were discovered in HNSCC-derived cell lines and OSCC tissues (Agrawal et al. 2011; Stransky et al. 2011; Kandoth et al. 2013; Pickering et al. 2013) and reduced Notch1 protein expression has been reported in precancerous lesions of the oral cavity (Sakamoto et al. 2012), suggesting Notch has a tumour suppressor effect.

4.2 Aims

1. To investigate the expression levels of Notch1 in OSCC-derived cell lines.
2. To examine the expression of Notch1 target genes; Hes1 and Hey1, in the OSCC-derived cell lines and relate these to Notch1 expression.
3. To investigate potential Notch1 and Epsin3 associations in these cell lines.

4.3 Results

The OSCC-derived cell lines; H103, H357, H376, BICR31 and BICR56, in addition to immortalized oral keratinocyte (OKF6) and LnCap cell lines were investigated

4.3.1 Quantitative RT-PCR Analysis of Notch1 expression

The cDNA samples were prepared using reverse transcriptase (Applied Biosystems, USA). The final concentration of the cDNA template was 100ng/µl. The samples were sent to University of Malaya, Kuala Lumpur, Malaysia and the qRT-PCR was performed.The mean fold was calculated using ∆ct values as previously described (Section 2.3.6). Notch1 showed different levels of expression in the cell lines, the BICR31 cell line had the highest level of expression compared to all other cell lines ($p<0.001$). LnCap, had the second highest Notch 1 levels and was significantly higher than H103, H357, H376 and BICR56 cell lines ($p<0.001$) (Figure 4.1). The OKF6 cell line showed the lowest level of expression in all cell lines analysed ($p<0.001$).

4.3.2 RNA in situ hybridization

To validate the qRT-PCR results, detection and quantification of Notch1 RNA was performed using RNAscope® 2.5 VS Assay (Advanced Cell Diagnostics, Inc. USA) on a Ventana Discovery Ultra autostainer (Ventana Medical Systems Inc., USA). The RNAscope assays were carried out by Anna Long (Biomedical Scientist, Department of Cellular Pathology). Sections of formalin-fixed paraffin-embedded cell pellets were prepared for RNAscope assay according to the company instructions. The signals of Notch1 were different between the cell lines (Figure 4.2A). The percentage of positive nuclei (PPN) was highest for BICR31 and was significantly higher than OKF6, H103, H376 and BICR56 cell lines ($p<0.001$). H357 showed significantly higher PPN values than OKF6, H103 and BICR56 ($P<0.01$) and H367 ($P<0.001$) (Figure 4.2B). The RNAscope findings correlated with the qRT-PCR results ($p<0.001$) (Figure 4.3). In summary, BICR31 had the highest levels of Notch1 RNA, by comparison OKF6 had consistently low levels of Notch1 RNA. The results were consistent between repeat samples and different methods.

4.3.3 Notch1 protein quantification by Western blot

The level of Notch1 protein expression was different between the cell lines. BICR31 and LnCap had the highest levels of Notch1 expression. In contrast, Notch1 protein could not be detected in H357 and BICR56 cell lines (Figure 4.4A). The band intensity were analysed by densitometry, normalized to α-tubulin in same samples. BICR31 and

LnCap cell line had the highest expression compared with other cell lines ($p<0.001$) confirming the higher levels of expression seen with qRT-PCR results. However, Notch1 protein was undetectable in H357 and BICR56 cells (Figure 4.4B).

4.3.4 Immunocytochemical analysis of Notch1 protein in the cell lines

Sections of formalin-fixed paraffin-embedded cell pellets were prepared for Notch1 (Cell Signalling, abcam; Table 2.6) immunocytochemistry. Stained slides were scanned using the Aperio eSlide Manager, Leica Biosystems. Tonsil tissue was used as positive external control, Notch1 showed moderate to strong cytoplasmic expression in the basal keratinocytes of the squamous epithelium. The expression levels were different between the cell lines as shown in Figure 4.5A. The mean number of cells analysed per cell line was 11,938 (range: 2934- 23962). The percentage of positive cells were calculated and analysed. The results revealed that BICR31 had significantly more Notch1 positive cells than OKF6, H103, H357, H376 and BICR56 cell lines ($p<0.001$) and LnCap ($p<0.01$). The LnCap cell line showed significantly higher expression compared with the OKF6, H103, H357, H376 and BICR56 ($p<0.001$). The H103 cell line was significantly higher than OKF6, H357, H37 and BICR56 ($p<0.001$) (Figure 4.5B). The ICC results showed a similar pattern of results as identified by western blot analysis, in which the BICR31 and LnCap cell lines have the highest expression, H357 and BICR56 have very low expression.

4.3.5 Immunocytochemical analysis of cleaved-Notch1 protein in the cell lines

Sections of formalin-fixed paraffin-embedded cell pellets were prepared for cleaved-Notch1 (c-Notch, Cell Signalling; Table 2.6) immunocytochemistry. The expression of c-Notch was nuclear. Stained slides were scanned using the Aperio eSlide Manager, Leica Biosystems. The expression levels were different between the cell lines as shown in (Figure 4.6A). The mean number of cells analysed per cell line was 4089 (range: 2764- 5347). The percentage of positive nuclei were calculated and analysed. The results showed that BICR31 had higher expression level than OKF6, H103, H357, H376 and BICR56 ($p<0.001$). The OKF6 cell line showed significantly higher expression level compared to H357 and H376 ($p<0.001$). The H103 cell line was significantly higher than OKF6, H357, H37 and BICR56 ($p<0.001$). The H357 and BICR56 cell lines had low significant expression than OKF6, H103, H376 and BICR31 ($p<0.001$) (Figure 4.6B). The Person product-moment analysis reveals a significant correlation between Notch1 and c-Notch1 protein expression analysed by ICC ($p<0.001$) (Figure 4.7).

4.3.6 *Investigation of the correlation between Notch1 RNA and protein expression levels*

To identify if Notch1 RNA expression levels correlated with protein levels analysed by different methods, statistical analysis was carried out by bi-variate correlation analysis followed by Pearson's Product-Moment test (Table 4.1). There was a significant correlation between Notch1 RNA levels analysed by qRT-PCR and Notch1 RNA in situ hybridization (Figure 4.3). There was a significant correlation between Notch1 RNA analysed by qRT-PCR and protein levels analysed by WB (Figure 4.8) and protein levels analysed by ICC ($p<0.001$). Similarly, levels of Notch1 RNA in situ hybridization was significantly correlated with Notch1 protein expression levels analysed by ICC (Figure 4.9) and protein analysed by Western blotting ($p<0.001$). The levels of Notch1 protein analysed by Western blotting was correlated with levels of protein analysed by ICC ($p<0.001$). The results were consistent between repeat samples and different methods.

Pearson Correlation				
	Notch1 RNA (qRT-PCR)	**Notch1 RNA (in situ hybridization)**	**Notch1 protein analysed by WB**	**Notch1 protein analysed by ICC**
Notch1 RNA (qRT-PCR)		**p<0.001**	**p<0.001**	**p<0.001**
Notch1 RNA (in situ hybridization)			**p<0.001**	**p<0.001**
Notch1 protein analysed by WB				**p<0.001**

Table 4.1: Correlation of Notch1 expression at RNA and protein levels in the cell lines

The table shows Pearson's Product-Moment test analysis of correlation of Notch1 RNA analysed by qRT-PCR and in situ hybridization and protein expression levels analysed by Western blot and ICC.

4.3.7 Quantitative RT-PCR analysis of Hes1 and Hey1 expression

The cDNA samples of seven cell lines were prepared using reverse transcriptase (Applied Biosystems, USA). The final concentration of the cDNA template was 100ng/µl. The samples were sent to University of Malaya, Kuala Lumpur, Malaysia and the qRT-PCR was performed. The mean fold was calculated using ∆ct values (Section 2.3.6).

The expression level of Hes1 was different between the cell lines (Figure 4.10). The BICR56 cell lines showed significantly higher expression than other cell lines ($p<0.001$). The H357 cell line had significantly higher expression compared to the H103, H367, BICR31 and LnCap ($p<0.001$). The expression in the BICR31 cell lines was significantly higher than OKF6, H103 and LnCap ($p<0.001$) and H376 ($p<0.01$). The OKF6 cell line had significantly lower expression compared to the H103 and H376 ($p<0.001$) and LnCap ($p<0.5$). A Pearson's Product-Moment correlation analysis revealed there was no correlation between Notch1 and Hes1 expression at RNA level ($p>0.5$, data not shown).

The Hey1 qRT-PCR analysis displayed the difference expression between the cell lines (Figure 4.11). The H376 cell line showed the higher significant difference than OKF6, H103, H357, BICR31 and BICR56 ($p<0.001$) and LnCap ($p<05$). The LnCap had higher significant expression compared to the OKF6, H103, BICR31 and BICR56 ($p< 0.001$) and H357 ($p\leq 0.01$). The H357 was significantly higher than OKF6 and BICR31 ($p< 0.05$). A Pearson's Product-Moment correlation analysis revealed there was no correlation between Notch1 and Hey1 expression at RNA level ($p>0.5$, data not shown).

4.3.8 Investigation of the correlation between Notch1 protein expression and Ki67 analysed by ICC in the panel of cell lines

The relationship between Notch1 protein and the Ki67 proliferation index was analysed by bi-variate correlation analyses followed by Pearson's product-moment test. There was a significant correlation between Notch1 protein levels and the proliferation index ($p<0.05$) (Figure 4.12). The cell lines with the highest Notch 1 levels had the highest proliferation index.

4.3.9 The correlation between Notch1 RNA and protein expression levels and Epsin3 RNA and protein expression levels in the panel of cell lines

To establish whether a correlation between Notch1 levels and Epsin3 levels in cells could be seen, a statistical analysis was carried out by bi-variate correlation analysis followed by Pearson's product-moment correlation was carried out (Table 4.2). The analysis revealed no correlation between Notch1 RNA and Epsin3 RNA expression levels, and Notch1 RNA and Epsin3 protein analysed by ICC ($p>0.05$, data not shown). However, there was statistically significant correlation between Notch1 RNA expression level and Epsin3 protein expression level analysed by western blot (WB) (Figure 4.13). Notch1 protein expression level analysed by WB has a significant correlation with Epsin3 protein expression level analysed by WB (Figure 4.14), nonetheless, Notch1 protein analysed by WB has no correlation with Epsin3 RNA and Epsin3 protein analysed by ICC ($p>0.05$, data not shown). The Person product-moment analysis revealed that Notch1 protein analysed by ICC was significantly correlated with level of Epsin3 protein analysed by WB ($p<.001$). Yet, Notch1 protein analysed by ICC has no correlation with Epsin3 RNA and Epsin3 protein analysed by ICC ($p>0.05$, data not shown).

Pearson Correlation			
	Notch1 RNA (qRT-PCR)	**Notch1 protein analysed by WB**	**Notch1 protein analysed by ICC**
Epsin3 RNA (qRT-PCR)	**p>0.05(ns)**	**p>0.05(ns)**	**p>0.05(ns)**
Epsin3 protein analysed by WB	**p<0.01**	**p<0.001**	**p<0.01**
Epsin3 protein analysed by ICC	**p>0.05(ns)**	**p>0.05(ns)**	**p>0.05(ns)**

Table 4.2: Correlation of Notch1 expression levels with Epsin3 expression levels in the cell lines.

The table shows Person product-moment analysis of Notch1 RNA and protein correlation with Epsin3 RNA and protein expression levels. (ns: not significant).

4.4 Discussion

Several studies have reported that Notch signalling is involved in different types of malignant tumour. Whilst Notch1 gene mutations have been reported in OSCC (Yoshida et al. 2013), little is known about the role of Notch signalling in oral squamous cell carcinoma. In this chapter we investigated the expression of Notch1 in vitro in the OSCC-derived cell lines. At RNA level, our data shows that Notch1gene has significantly different expression between the cell lines, it was significantly higher in H103 and BICR31 compared to the other OSCC cell lies and OKF6. It has been reported that Notch1 has a dual role in tumours, Notch can be either oncogenic or have a tumour-suppressor effect (Yap et al. 2015). Our results show that Notch1 mRNA was highly expressed in two of the OSCC cell lines, H103 and BICR31. Our result is consistent with Hijioka et al. (2010) study, the authors have reported that Notch 1 mRNA was upregulated in human OSCC cell lines (Ca99-2, HSC-2 and HSC-4). Furthermore, Zhang et al. (2011) reported elevated Notch1 mRNA in a human tongue carcinoma cell line.

At the protein level, Western blot analysis revealed that Notch1 protein was upregulated in BICR31, however it was not detected in H357 and BICR56 cell lines. This suggested that Notch1 may be mutated or epigenetically silenced in these cells.

Our results are in agreement with the observation that Notch1 protein was elevated in human OSCC cell lines, and loss of Notch1 expression is significantly correlated with inhibition of cell proliferation (Yoshida et al. 2013). To strengthen our results, immunocytochemical (ICC) analysis was performed. The same results were detected in ICC analysis of cell lines pellet, in which H103 and BICR31 cell lines had significantly higher expression of Notch1 protein and H357 and BICR56 cell lines showed very low expression. Therefore, considering the previous studies, we conclude that Notch1 may have oncogenic effect in the OSCC cells and these cells may require Notch1 expression for tumour progression.

On the other hand, we found that Notch1 was absent in H357 and BICR56 cell lines at protein level. However, in qRT-PCR analysis they showed evidence of Notch1 transcription. To confirm our results at RNA level, RNA in situ hybridisation was carried out. Interestingly, our data show that H357 and BICR56 have Notch1 transcripts, which was abundant in the H357 cell line. This difference in the Notch1 expression at RNA and protein level in these two cell lines may reflect the defect in the process of translation to protein. We can conclude that Notch1 has been mutated in these cell lines. The mutated Notch1 may contribute to loss of function phenotypes. Loss- of-function mutations in Notch members are the most common mutations in different squamous cell carcinoma, including head and neck squamous cell carcinoma (HNSCC) (Agrawal et al. 2011; Stransky et al. 2011). To date, most of identified mutations are found in the Notch receptors, predominantly in Notch1 (Nowell and Radtke 2017).

Downregulation of Notch1 protein in the H357 and BICR56 cell lines has been demonstrated previously (Mutvei et al. 2015; Yap et al. 2015). Both studies reported that Notch1 is mutated in these two OSCC cell lines and the mutation is in the EGF-like repeats. This mutation causes a truncated protein. The extracellular domain of human Notch1 receptor contain EGF-like repeats, which are involved in ligand binding. The ligands also have extracellular domain containing variable numbers of EGF repeats that involved in receptor binding. Upon binding, the ligand-receptor complex is ubiquitinated by Mib and Nuer at the cell membrane and endocytosed through the action of Epsin (Wang and Struhl 2005). This internalization event induces two proteolytic cleavage: S2 cleavage stimulated by ADAM/TACE family, and S3 cleavage activated by γ-secretase complex (Le Borgne et al. 2005) These events are initiating steps of Notch activation. Collectively these findings suggested that binding of EGF

repeat of Notch receptor with the ligand activates the next proteolytic events that lead to Notch signal activation. Absence of Notch1 protein in the OSCC cells that have Notch1 mutation was reported in other studies. Notch1 mutation, which is nonsense mutation that resulted in truncated protein, have been identified in OSCC tissue samples and EGF domain is the common region with the mutation (Song et al. 2014a) . Pickering et al. (2013), reported that Notch1 protein is absent in HNSCC cell lines that have truncating mutation (HN4, UM-SCC-47 and PCI-15B)

Loss-of-function mutations of Notch signalling suggests its tumour suppressive role. The tumour suppressor role of Notch1 in the OSCC was verified by Sakamoto et al. (2012) who reported that Notch1 downregulation in the OSCC cell lines lead to decrease terminal differentiation and formation of immature epithelium. In transgenic mice, Notch1 play a tumour suppressor role in epidermal carcinogenesis (Nicolas et al. 2003). Downregulation of Notch1 in the H357 and BICR56 cell lines in our study suggests that Notch1 has a tumour suppressor function in the OSCC.

Our results of Notch1 expression analysis in OSCC revealed its diverse role and suggests that Notch1 has both oncogenic and tumour suppressor roles in OSCC. Head and Neck Squamous Cell Carcinoma (HNSCC) is a heterogeneous disease, and the role of pathways is based on the genetic background of the tumour. The most of OSCCs are genetically unstable, and have high copy number alterations and loss of heterozygosity, while genetically stable OSCCs have less copy number alteration and loss of heterozygosity. Accordingly, it was reported that the Notch pathway has a tumour suppressor role in genetically stable OSCCs, but acts as oncogenic in genetically unstable OSCCs (Yap et al. 2015). Cleaved Notch1 is the active form of Notch signalling. Interestingly, our results show that there is a positive correlation between expression levels of Notch1 protein and cleaved Notch1 in the OSCC cell lines. The cell lines that had high Notch1 expression, also show high cleaved-Notch1 expression. While cell lines with mutated Notch1 did not show cleaved-Notch1 expression This result is comparable with previous studies that demonstrated that OSCC with high Notch1 expression showed high expression level of cleaved-Notch1 (Yoshida et al. 2013; Gokulan and Halagowder 2014).This suggests the positive correlation between Notch1 and cleaved-Notch1 expression in the OSCC.

The direct target genes of Notch signalling are Hes and Hey families of basic helix-loop-helix transcriptional suppressors (Bianchi et al. 2006). The cleaved notch (Notch

intracellular domain) interacts with the transcriptional suppressor RBP-J and converts it to activator, which activates Hes and Hey transcription (Iso et al. 2003). It was reported that activated Notch1 induces Hes1 and Hey transcription (Meier-Stiegen et al. 2010). Our data show upregulation of Hes1 in H357 and BICR56 and Hey1 in H357 cell lines, this result is in agreement with previous study that reported overexpression of Hes1 and Hey1 in OSCC cell lines (Hijioka et al. 2010). In light of the correlation between Notch1 and Hes1 and Hey1 genes, we performed qRT-PCR analysis for Hes1 and Hey1 for the same cell lines. Our results show negative correlation between Hes1 and Notch1 expression and Hey1 and Notch1 expression, however, it was statistically not significant. The OSCC cell lines with wild type Notch1 expression, show high Notch1 expression at RNA level with low Hes1 and Hey1 expression, for example BICR31 cell line showed very high Notch1 expression, but low Hes1 and very low Hey1 expression. Whilst, OSCC cell lines with mutated Notch1, H357 and BICR56 cell lines, have low Notch1 expression and high Hes1 and Hey1 expression. This is in contrast to other published studies, for example Notch1 knockdown using siRNA led to suppressed Hes1 and Hey1 expression which means there is a positive correlation between Notch1 expression and Hes1 and Hey1expression (Sakamoto et al. 2012; Yoshida et al. 2013). However, the negative correlation presented in our work may be related to the mutation in the Notch1/RBP-J site which lead to loss of Notch1 activation of the target genes and consequently inhibiting protein synthesis. This lead to up-regulation of Notch1 target genes through negative feedback loop, involving Hes1 and Hey1 genes (Meier-Stiegen et al. 2010). Accordingly, it can be suggested that Notch1 mutation leads to up-regulation of Hes1 and Hey1 repressor genes.

Work presented in Chapter 3 was concerned with the expression of Epsin3 in OSCC cell lines. Interestingly, our results revealed that the cell lines with high Epsin3 expression show high Notch1 expression at RNA and protein level. To identify the correlation between Notch1 and Epsin3 expression in the OSCC, a Person's product-moment test was carried out. Although there was no correlation at RNA level, the results revealed a strong positive correlation between Notch1 and Epsin3 expression at protein level. The previous studies confirmed that loss of Epsins impaired Notch signalling (Chen et al. 2009) and silencing of Epsin1 and 3 in vitro, lead to downregulation of Notch signalling in human keratinocytes (Di Giacomo et al. 2013). Collectively, Notch1 protein is positively correlated to Epsin3 protein expression in

OSCC, this suggests that Epsin3 is the trigger of Notch pathway. Further investigation of Notch1 and Epsin3 expression in tissue samples is needed to confirm this finding.

In summary, this chapter describes the differential expression of Notch1 in the OSCC cell lines. It was highly expressed in BICR31 cell line. Notch1 protein cannot be detected in H357 and BICR56 cell lines suggesting that Notch1 may be mutated in these OSCC cell lines. Speculatively, therefore this variation of expression lead us to hypothesise that Notch1 may have oncogenic and tumour suppressor functions in OSCC. Additionally, Notch1 did not show significant correlation with its target gene, Hes1 and Hey1 in OSCC. Interestingly, Notch1 has a positive correlation to Epsin3 expression in OSCC.

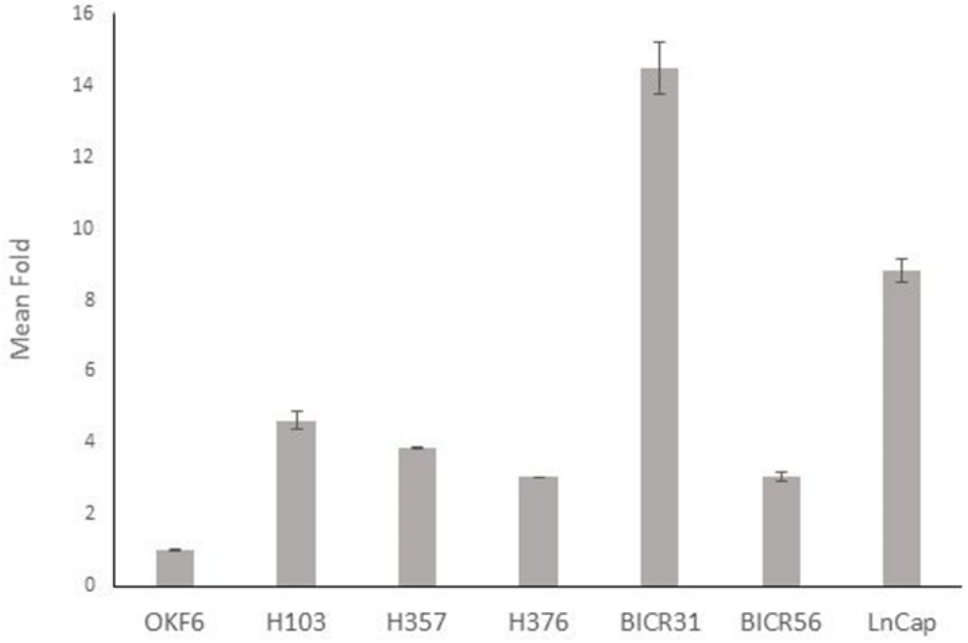

Figure 4.1:Notch1 gene expression in cell lines by quantitative RT-PCR.

The cells were cultured at $5x10^5$ in 6 well plate. RNA was extracted (three independent experiments) using reverse transcriptase (Applied Biosystems, USA). The final concentration of the cDNA template was 100ng/µl. Relative Notch1 mRNA transcription was determined using the $2^{-\Delta\Delta ct}$ method by using GAPDH as the reference gene. The data are expressed relative to GAPDH mRNA levels measured in the all cell lines and normalised to the OKF6 cell line. Data are shown as mean ±SD (n=3). BICR31 cell line showed highest levels of Notch1 compared to the other cell lines ($p<0.001$). OKF6 cells had significantly lower Notch1 transcripts than the other cell lines ($p<0.001$). Significance measured by one-way ANOVA followed by Bonferroni post hoc test.

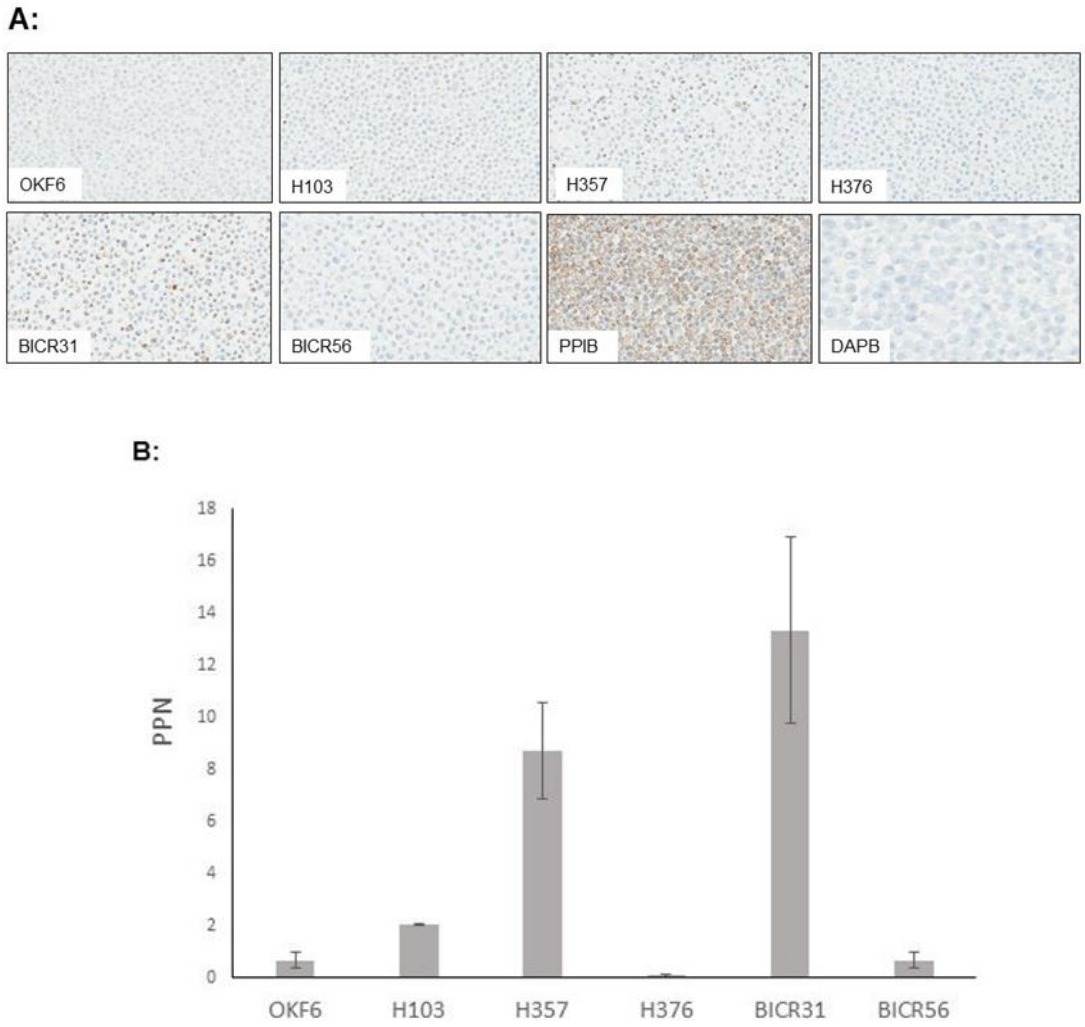

Figure 4.2:Notch1 gene expression in cell lines by RNA in situ hybridisation

A) The cell lines showed differential expression of Notch1 RNA. The BICR31 and H357 cell lines show moderate signals, while the signals from OKF6, H103, H376 and BICR56 were very weak. The positive control (PPIB) was strongly positive and the negative control (DAPB) did not show any signal (Original magnification x20).

B) The mean percentage positive nuclei (PPN) of Notch1 RNA signals was significantly different between the cell lines. The BICR31 cell line was significantly higher than OKF6, H103, H376 and BICR56 ($p<0.001$). H357 showed significantly higher PPN values than OKF6, H103 and BICR56 ($P<0.01$) and H367 ($P<0.001$). The PPN stated as the mean of three fields ±SD. Significance measured by one-way ANOVA followed by Bonferroni post hoc test.

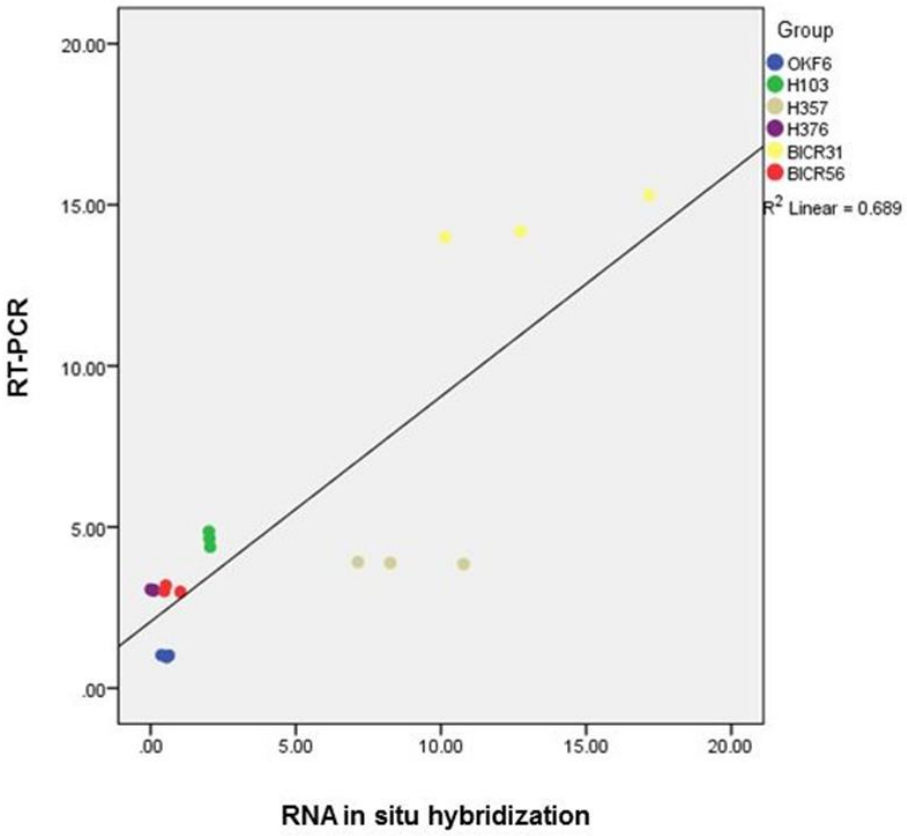

Figure 4.3: Relationship between expression levels of Notch1 RNA analysed by qRT-PCR and in situ hybridization.

Figure show the correlation between expression levels of Notch1 RNA analysed by qRT-PCR and Notch1 RNA in situ hybridization in OSCC, OKF6 cell lines analysed by bi-variate analysis followed by Pearson product-moment test. The addition of trend-line indicate significant correlation ($p<0.001$).

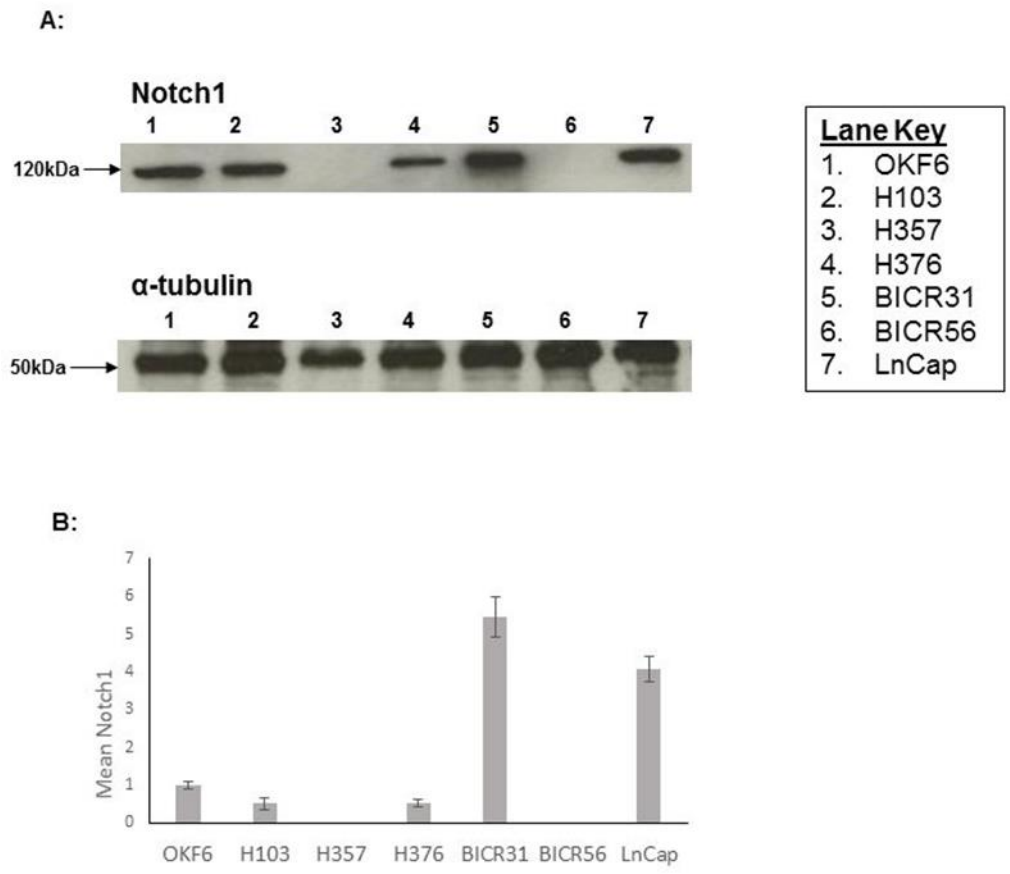

Figure 4.4: Representative Western blot showing expression of Notch1 and reference protein alpha-tubulin in the panel of the cell lines.

A) Cells were cultured in 6 well plate in a maintenance medium to ~90% confluence. Protein was extracted using RIPA buffer plus inhibitor, as described in Materials and Methods section. 20µg of protein were electrophoresed on 12.5% SDS-PAGE gel and transferred to PVDF membrane. The membrane incubated with antibodies against the Notch1 (1:1000) and α-tubulin (1:2000). The secondary antibody was horseradish-peroxidase. Notch1 protein detected at 120kDa and alpha-tubulin at 55kDa. Bands were visualized by chemiluminiscence (ECL) detection reagents (GE Healthcare).

B) Densitometry (Genetool from SynGen UK.) was adjusted for the background optical density of the X-ray film and normalized to α-tubulin protein. The results were expressed the intensity of Notch1 bands (sample from triplicate independent experiments for each cell lines). Notch1 protein expression stated as mean ±SD, n=9. Notch1 expression was significantly higher in BICR31 and LnCap cell lines than the other cell lines ($p<0.001$). Significance measured by one-way ANOVA followed by Bonferroni post hoc test.

.

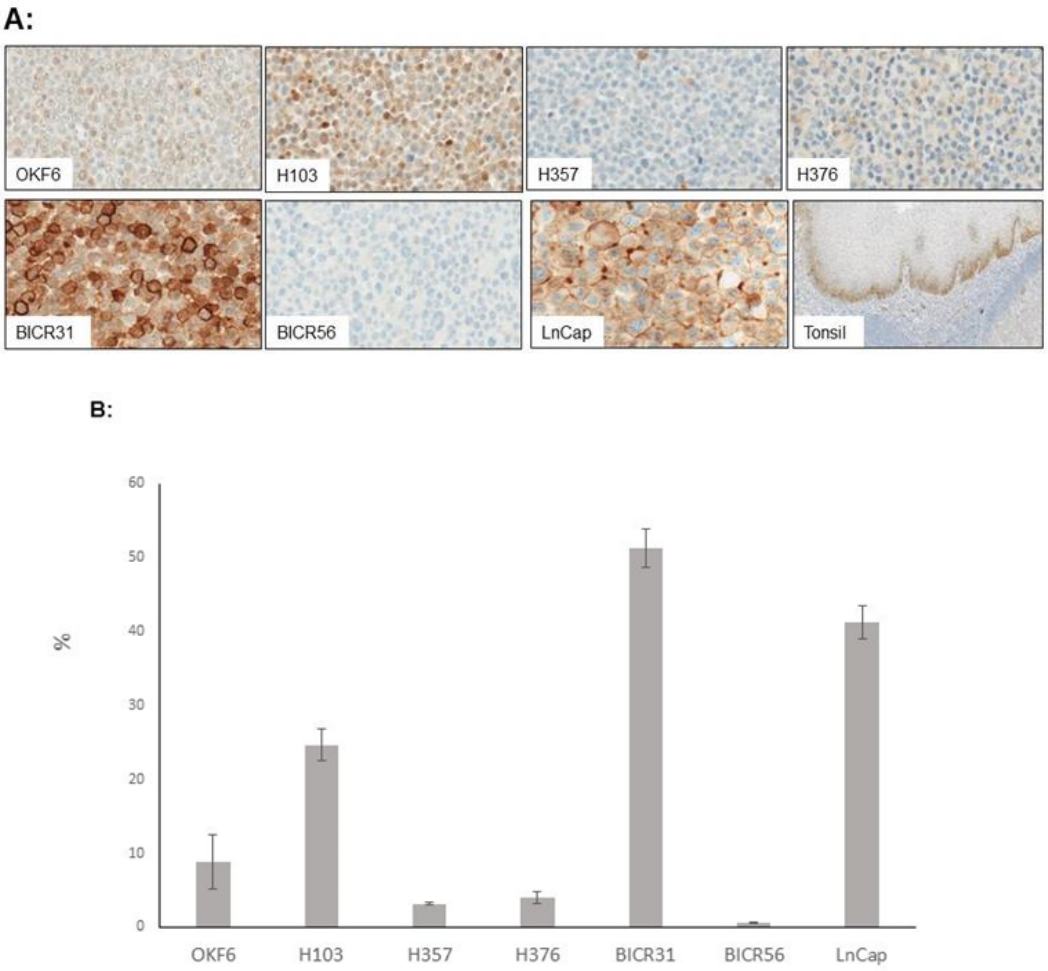

Figure 4.5: Notch1 protein expression by immunocytochemistry in cell lines and normal tonsil tissue.

A) The OKF6 and panel of cell lines showed membrane staining of Notch1 protein with different intensities at immunocytochemistry. Images taken at x20 magnification. Normal tonsil tissue showed strong staining of squamous epithelium. Image taken at x10 magnification.

B) The mean percentage positive cells was calculated for each cell line. The expression of Notch1was significantly higher in BICR31 cell line compared to all other cell lines ($p<0.001$). The LnCap cell line was significantly higher than OKF6, H103, H357, H376 and BICR56 ($p<0.001$). The H103 cell line showed higher significant expression than OKF6, H357, H376 and BICR56 cell line ($p<0.001$). The percentage of positive staining stated as mean ±SD n =3. Significance measured by one-way ANOVA followed by Bonferroni post hoc test.

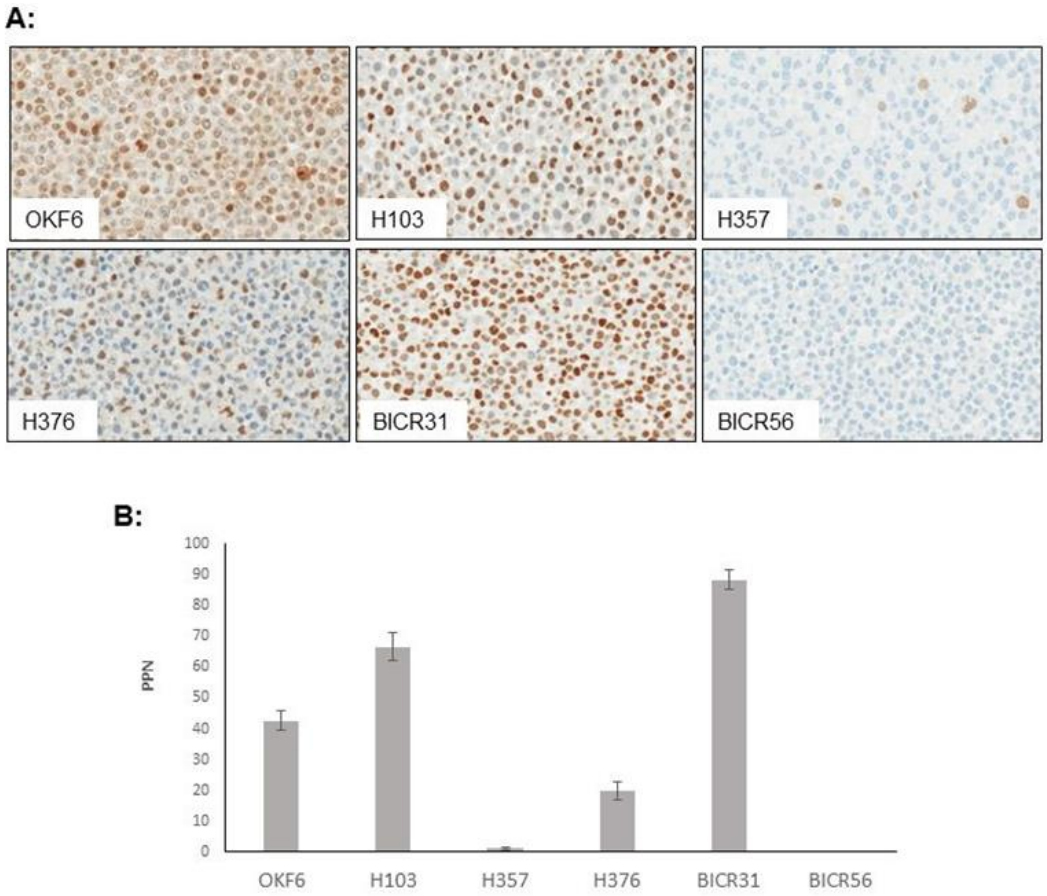

Figure 4.6: c-Notch1 protein expression by immunocytochemistry in cell lines

A) The OKF6 and panel of OSCC-derived cell lines showed nuclear staining of c-Notch1 protein with different intensities at immunocytochemistry. Images taken at x20 magnification.

B) Quantitation the mean of percentage positive nulei was calculated for each cell line. The expression of c-Notch1was significantly higher in BICR31 cell line compared to all other cell lines ($p<0.001$). The H103 cell line was significantly higher than OKF6, H357, H376 and BICR56 ($p<0.001$). The H357 and BICR56 cell lines showed lower significant expression compared to OKF6, H103, H376 and BICR31 ($p<0.001$). The percentage of positive staining stated as mean ±SD n =3. Significance measured by one-way ANOVA followed by Bonferroni post hoc test.

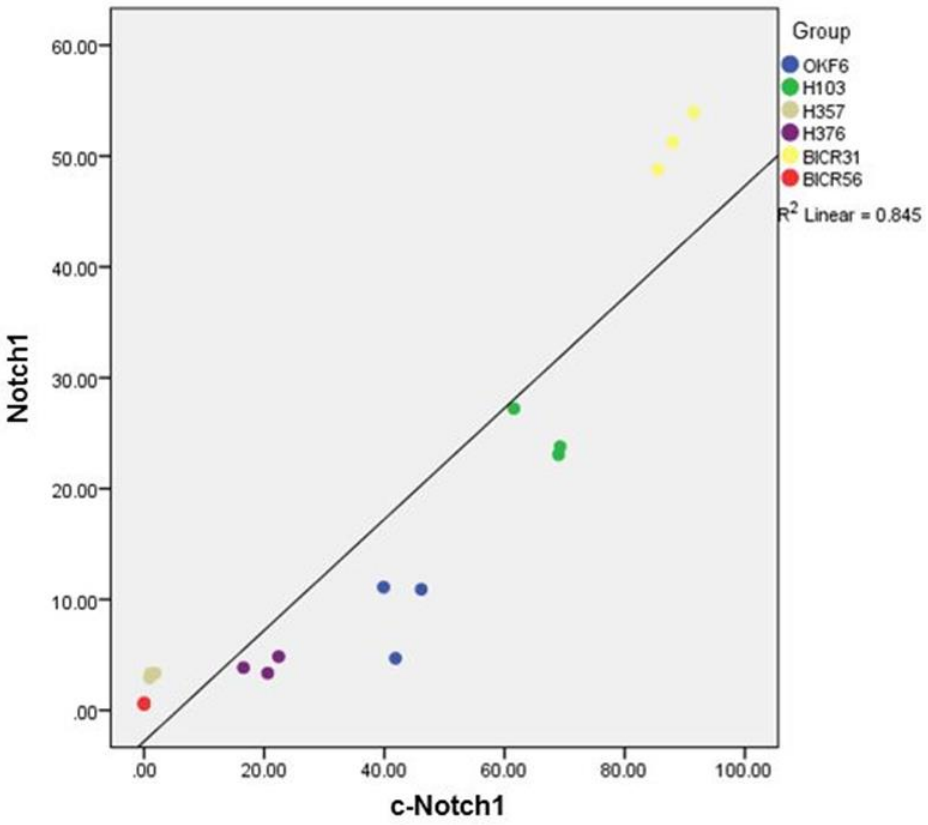

Figure 4.7: Relationship between expression levels of Notch1 protein and c-Notch1 protein analysed by immunocytochemistry.

Figure show the correlation between expression levels of Notch1 and c-Notch1 protein analysed by immunocytochemistry in OSCC, OKF6 cell lines analysed by bi-variate analysis followed by Pearson's product-moment test. The addition of trend-line indicate significant correlation ($p<0.001$).

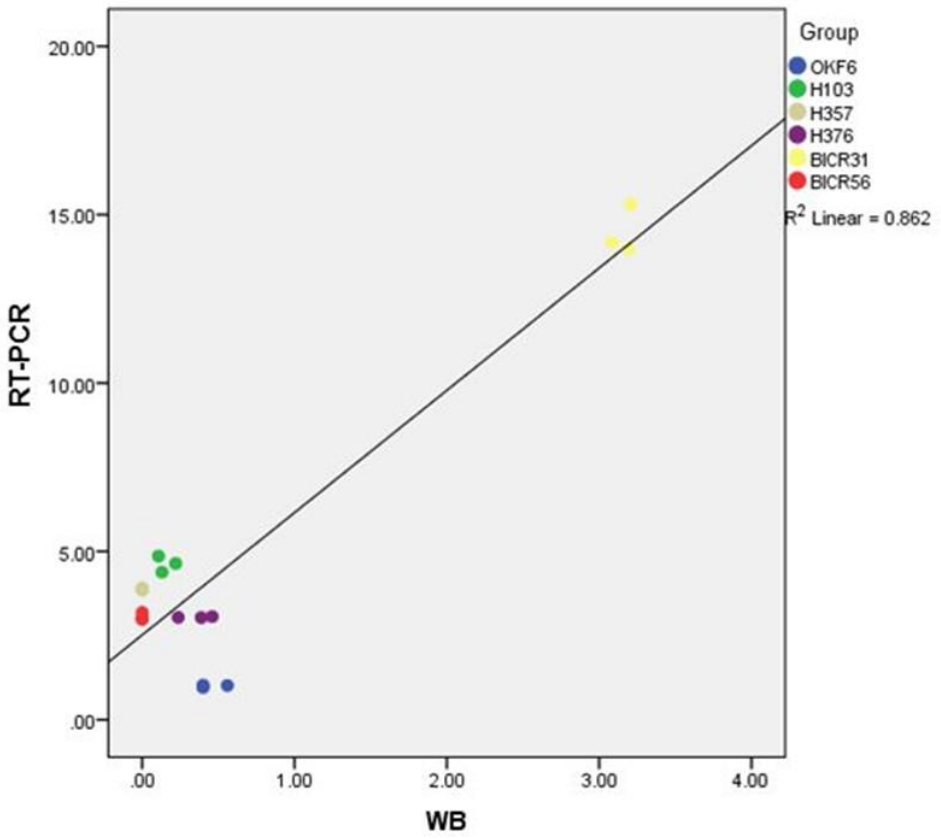

Figure 4.8: Relationship between expression levels of Notch1 RNA analysed by qRT-PCR and Notch1 protein analysed by Western blot.

Figure show the correlation between expression levels of Notch1 RNA and Notch1 protein analysed by WB in OSCC, OKF6 cell lines analysed by bi-variate analysis followed by Pearson's product-moment test. The addition of trend-line indicate significant correlation ($p<0.001$).

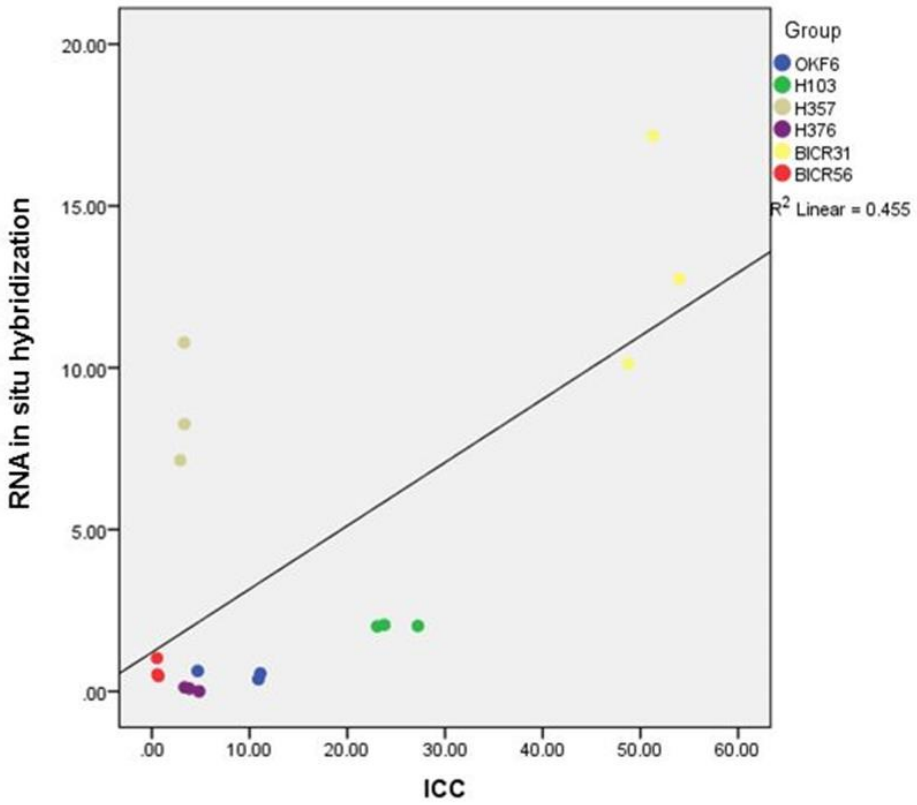

Figure 4.9: Relationship between expression levels of Notch1 RNA in situ hybridization and Notch1 protein analysed by immunocytochemistry.

Figure show the correlation between expression levels of Notch1 RNA in situ hybridization and Notch1 protein analysed by WB in OSCC, OKF6 cell lines analysed by bi-variate analysis followed by Pearson's product-moment test.The addition of trend-line indicate significant correlation ($p<0.001$).

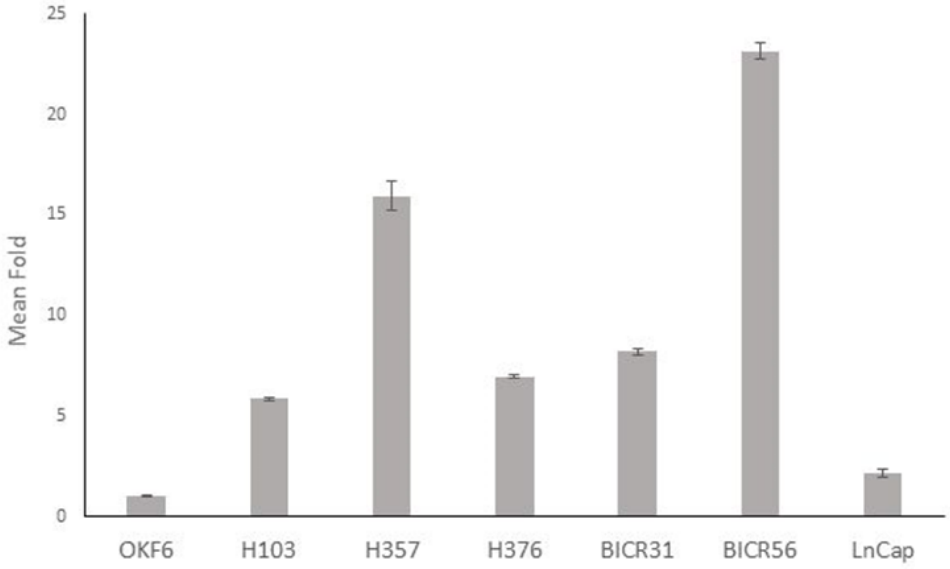

Figure 4.10: Hes1 gene expression in cell lines by quantitative RT-PCR.

The cells were cultured at $5x10^5$ in 6 well plate. RNA was extracted (three independent experiments) using reverse transcriptase (Applied Biosystems, USA). The final concentration of the cDNA template was 100ng/µl. Relative Hes1 mRNA expression was determined using the $2^{-\Delta\Delta ct}$ method by using GAPDH as the reference gene. The data are expressed relative to GAPDH mRNA levels measured in the all cell lines and normalised to the OKF6 cell line. Data are shown as mean ±SD (n=3). BICR56 cell line showed high significant Hes1 expression compared to all OSCC-derived and OKF6 cell lines ($p<0.001$). The H357 cell line had significantly higher expression compared to the OKF6, H103, H367, BICR31 and LnCap ($p<0.001$). The expression in the BICR31 cell lines was significantly higher than OKF6, H103 and LnCap ($p<0.001$) and H376 ($p<0.01$). The OKF6 cell line had significantly lower expression compared to the H103 and H376 ($p<0.001$) and LnCap ($p<0.5$). Significance measured by one-way ANOVA followed by Bonferroni post hoc test.

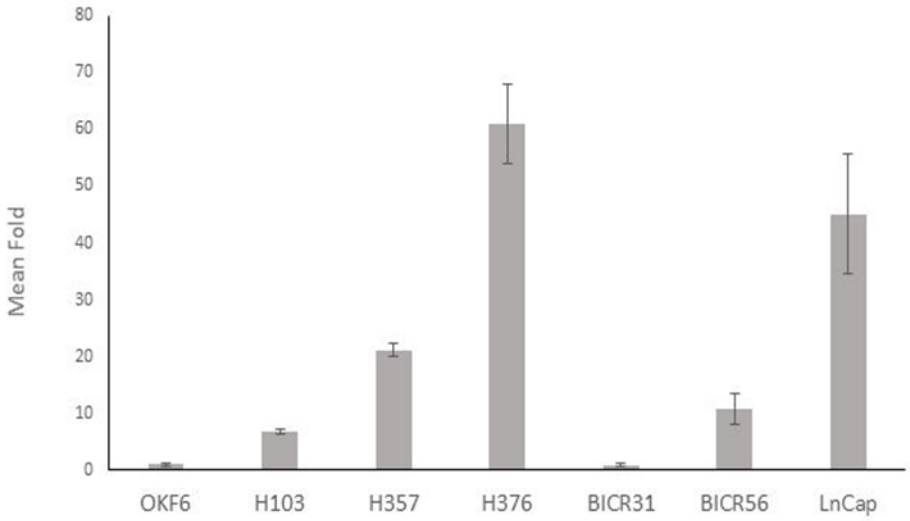

Figure 4.11: Hey1 gene expression in cell lines by quantitative RT-PCR.

The cells were cultured at $5x10^5$ in 6 well plate. RNA was extracted (three independent experiments) using reverse transcriptase (Applied Biosystems, USA). The final concentration of the cDNA template was 100ng/µl. Relative Hey1 mRNA expression was determined using the $2^{-\Delta\Delta ct}$ method by using GAPDH as the reference gene. The data are expressed relative to GAPDH mRNA levels measured in the all cell lines and normalised to the OKF6 cell line. Data are shown as mean ±SD (n=3). The H376 cell line showed the higher significant difference than OKF6, H103, H357, BICR31 and BICR56 ($p<0.001$) and LnCap ($p<05$). The LnCap had higher significant expression compared to the OKF6, H103, BICR31 and BICR56 ($P< 0.001$) and H357 ($p\leq 0.01$). The H357 was significantly higher than OKF6 and BICR31 ($p< 0.05$). Significance measured by one-way ANOVA followed by Bonferroni post hoc test.

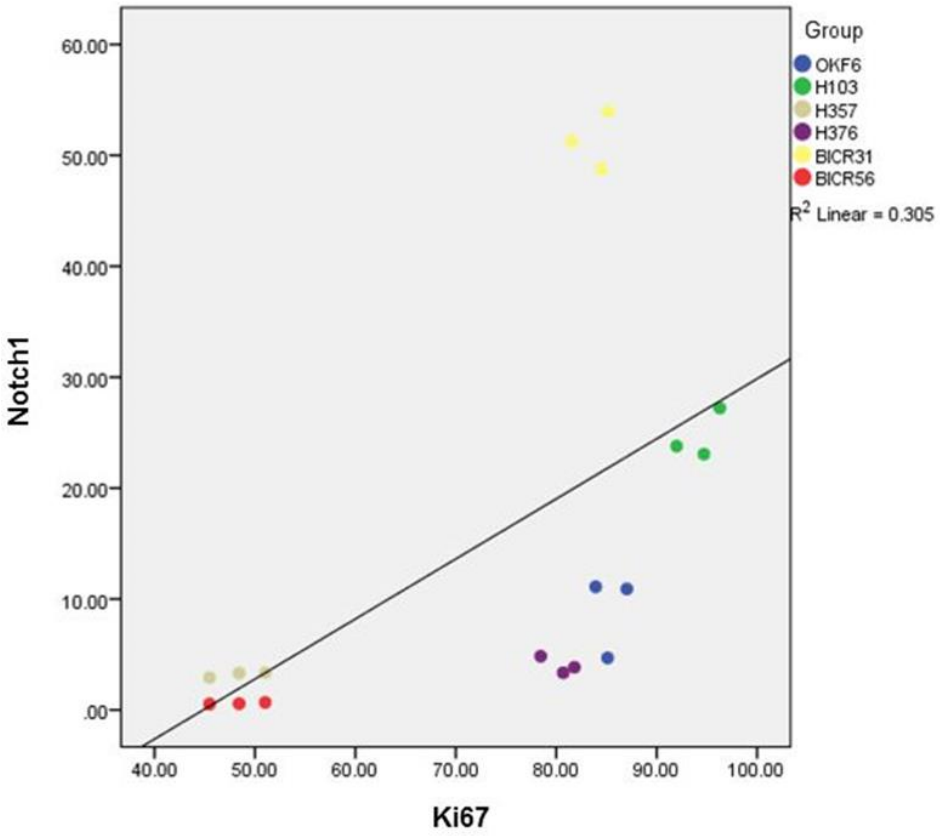

Figure 4.12: Relationship between of Notch1 protein expression levels and the Ki67 proliferation index.

Figure show the correlation between Notch1 protein and the Ki67 proliferation index, the data analysed by bi-variate correlation analysis followed by Person's product-moment test. The addition of trend-line indicate a significant correlation ($p<0.05$).

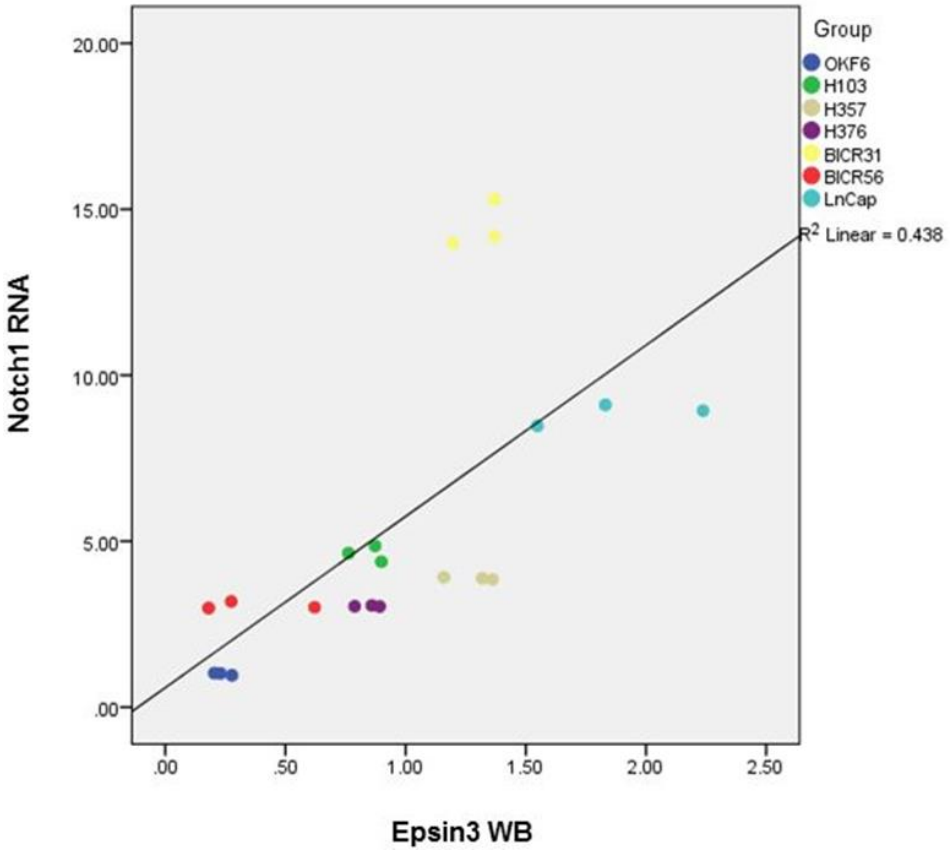

Figure 4.13: Relationship between expression levels of Notch1 RNA and Epsin3 protein analysed by Western blot.

Figure show the correlation between expression level of Epsin3 protein and Notch1 RNA expression level in OSCC, OKF6 and LnCap cell lines analysed by bi-variate analysis followed by Pearson's product-moment test. The addition of trend-line indicate significant correlation ($p<0.01$).

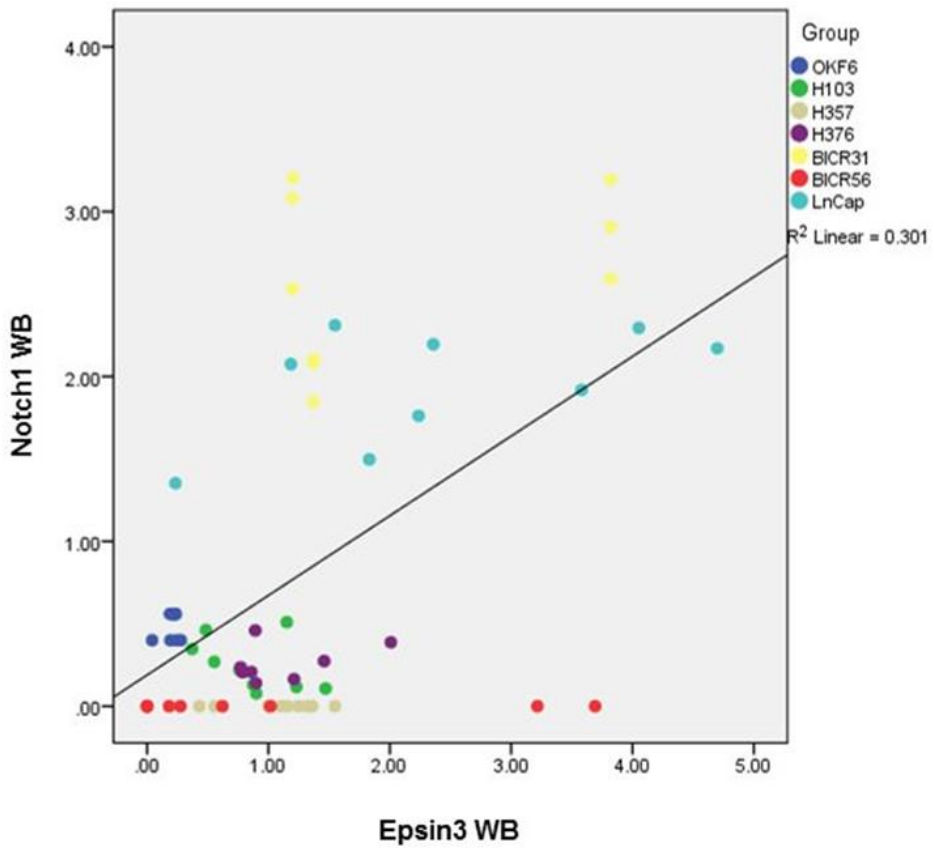

Figure 4.14: Relationship between expression levels of Notch1 protein and Epsin3 protein analysed by Western blot.

Figure show the correlation between expression levels of Epsin3 protein and Notch1 protein in OSCC, OKF6 and LnCap cell lines analysed by bi-variate analysis followed by Pearson's product-moment test. The addition of trend-line indicate significant correlation ($p<0.001$).

Chapter 5 **Epsin3 transfection experiments in selected oral cancer cell lines**

5.1 Introduction

Work presented in the Chapters 3 and 4 identified that the level of expression of Epsin3 and Notch1 in the OSCC cell lines was different. The results in Chapter 4 confirmed there was a significant correlation between Epsin3 and Notch1 expression at protein level in the OSCC cell lines; some cells with high Epsin3 expression level showed high Notch1 expression level.

Notch signalling is an unconventional pathway because it occurs during cell-cell contact, and because the membrane receptor proteins also act as transcription factors. Moreover, both ligands and receptors are exposed to different post-translational modifications that regulate their quantity and quality, these modification include: proteolysis, glycosylation, trafficking and ubiquitination. The endocytosis of ligands and receptors, which usually require ubiquitination, is needed for the pathway to function. Accordingly, dysregulation of ubiquitination events may lead to Notch signal disruption (Moretti and Brou 2013). Epsin3 is one of the endocytic adaptor protein family members important in endocytosis, the process which leads to internalization of plasma membrane proteins and plays a crucial role in the regulation of several signalling pathways. It has long been known that the endocytosis process results in attenuation of signals by internalizing activated ligand-receptor complexes, for example, the Epidermal Growth Factor: Epidermal Growth Factor Receptor tyrosine kinase complex. However, endocytosis can also activate cell signalling pathways, such as the Notch signalling pathway. Significantly, previous studies have reported that the Epsin family contributes to Notch activation by regulating the endocytosis of the Notch ligands in the signal-sending cell (Sen et al. 2012).

In mammals, activation of Notch signalling requires engagement of Notch receptor with its ligands, Jagged (Jagged 1 and 2) and Delta-like ligand (Capaccione and Pine 2013). The endocytosis of ligands on the signal-sending cell induce cleavage of Notch receptors and thus activating Notch in the signal-receiving cell (see Chapter1 Figure 1.1). There are different explanation why ligands needs to be endocytosed to activate Notch signalling. Ligand/Notch receptor binding leads to formation of an intercellular bridge between the sending and receiving cell, that is stressed by endocytosis of the ligand, resulting in conformational changes in the Notch that induce

S2 and S3 cleavage of Notch (Parks et al. 2000). In mammalian cells, trans-endocytosis of the Notch Extracellular Domain (NECD) by ligands in the sending cell play a role in Notch activation. The Notch receptors at the plasma membrane are heterodimers which remain associated after S1 cleavage that keep Notch inactive. Ligand binding with Notch receptor followed by endocytosis leads to dissociation of heterodimer and physical removal of the NECD subunit. Consequently, the Notch Intracellular Domain (NICD) will be exposed to proteolytic activity of ADAM resulting in S2 cleavage, followed by γ-secretase activity resulting in S3 cleavage to produce active NICD that is directed to the nucleus (Nichols et al. 2007).

Another study proposed that the activation takes place after internalization of the ligands, where the ligands enter a recycling pathway and are expose to the enzymatic processing converting them from an inert to an active form and recycling to the cell surface to confer signalling activity (Wang and Struhl 2004). Another model proposed that recruitment of ligands to the coated pits result in clustering and repackaging of the ligands on the cell surface (Le Borgne and Schweisguth 2003). Return of the ligands to the surface of signal-sending cell might keep them in high quantity to lengthen Notch activation and sustain signalling. In order to be endocytosed in the signal-sending cell, the ligands need to be mono-ubiquitinated and thereby targeted to special internalization pathway which are mediated by Epsin family. The previous studies have established that E3-ubiquitin ligase, Neutralized (Neur) and Mind bomb (Mib) are required for ligands ubiquitination to induce endocytosis which is required for signal activation (Weinmaster and Fischer 2011). Thus, Epsin proteins, through its ubiquitinated motifs, mediates endocytosis of mono-ubiquitinated ligands on the signal-sending cell. Hence, ubiquitinated ligands need to be internalized through a special Epsin dependent pathway to activate Notch signalling (Wang and Struhl 2004). Epsin recruits ubiquitinated ligands to the clathrin-coated pits which allow recycling of these proteins, otherwise they may degraded following internalization and are targeted to lysosomes (Chen and De Camilli 2005). Other studies reported that double knockout of Epsin1 and 2 in mice embryo leads to impairment of Notch signalling and reduction of Notch primary target genes, which results in developmental defects in the embryos (Chen et al. 2009). These findings support the role of Epsin as endocytic adapter protein in Notch signalling activation. Accordingly, we propose that Epsin3 is required for Notch signalling activation and absence of this protein may result in downregulation

of Notch signalling. On this basis, overexpression of Epsin3 was carried out in vitro, in addition to siRNA mediated knockdown of Epsin3.

5.2 Aims

To examine the role of Epsin3 in activating the Notch pathway and to determine if the level of Epsin3 mRNA and protein levels lead to change in Notch signals in OSCC cell lines.

To achieve this aim we investigated the effectiveness of overexpression and siRNA knockdown of Epsin3 on the Notch1 receptor in selected OSCC cell lines.

5.3 Results

5.3.1 Selection of OSCC cell lines for transient transfection of mammalian cells

The results presented in Chapter 3 and Chapter 4 revealed that the OSCC cell lines have different levels of Epsin3 and Notch1 expression. Accordingly, we selected the following cell lines for overexpression of Epsin3 due to their differing levels of endogenous expression of Epsin3 and Notch1 mRNA and protein (Table 5.1). Increased expression of Epsin3 was confirmed in each cell line at both RNA and protein levels. The effect of overexpression of Epsin3 on Notch1 RNA and protein levels was examined in each cell line. For knockdown of Epsin3 the BICR31 cell line was chosen as it showed high endogenous Epsin3 expression and had detectable levels of Notch1 at the RNA and protein level (Table 5.1).

	Endogenous mRNA		Protein	
Cell lines	**Epsin3**	**Notch1**	**Epsin3**	**Notch1**
H103	**Low**	**High**	**Low**	**High**
H357	**High**	**Low**	**High**	**Not detected**
BICR31	**High**	**High**	**High**	**High**
BICR56	**Low**	**Low**	**Low**	**Not detected**

Table 5.1: The endogenous expression of Epsin3 and Notch1 mRNA and protein in the selected cell lines.

5.3.2 Overexpression of Epsin3 in H103, H357, BICR31 and BICR56 cell lines

The selected cell lines were cultured for three passages in T75 flasks. Then the cells were grown in 6 well plates at $4x10^5$ cells/well. The cultured cells were transfected with 1µg of human Epsin3 expression vector (Lenti ORF clone of Human Epsin 3 (EPN3), Myc-DDK-tagged, 10µg OriGene) or 1µg of empty vector (p3XFLAG-CMVTM-10 expression vector, Sigma) and incubated for 24 hours (Section 2.5.1). The RNA and protein were extracted for each cell line. The level of Epsin3 expression in the transfected cells was determined using semi-quantitative RT-PCR, qRT-PCR and Western blotting.

5.3.3 RT-PCR analysis of Epsin3 RNA expression in the transfected cell lines

RNA was extracted from each of the cell lines and cDNA was prepared using Moloney Murine Leukaemia Virus, the final concentration of RNA was 1µg (Section 2.3.4). Semi-quantitative RT-PCR analysis was then performed to assess the expression of Epsin3 after transfection (Section 2.3.5). The housekeeping gene GAPDH was used to normalize the expression of Epsin3. An initial experiment contained treated (transfected) cells, untreated (untransfected) control cells and empty vector transfected controls. RT-PCR showed that untreated controls and empty vector transfected control cells had similar Epsin3 expression. While transfection cells with 1µg of Epsin3 expression vector resulted in an increase in the level of Epsin3 expression in these treated cell lines (Figure 5.1A). All the cell lines transfected with Epsin3 showed higher Epsin3 expression compared to untreated control (untransfected) and empty vector transfected control cells (Figure 5.1B). The increase in Epsin3 expression was most apparent in the H103 and BICR56 cell lines, which had the lowest endogenous Epsin3 RNA. These initial results indicate the successful transfection in the selected cell lines. Subsequently, additional assays were performed to confirm these results.

5.3.4 Quantitative RT-PCR analysis of Epsin3 expression in the transfected cell lines

The cDNA samples were prepared using reverse transcriptase (Applied Biosystems, USA) (Section 2.3.4). The required volume of QuantiFast SYBR Green PCR Master Mix (QIAGEN, Germany) was used (Section 2.3.6). The Log2 mean fold was calculated for treated samples and compared with the values of mean fold of untreated samples. All cell lines which were transiently transfected with Epsin3 showed significantly higher level of Epsin3 expression compared with untreated cell lines. (H103, $p<0.001$. H357, $p<0.01$. BICR31 and BICR56, $p<0.05$). (Figure 5.2).

5.3.5 Levels of Epsin3 protein quantification in the transfected cell lines by Western blot

The expression of Epsin3 protein in the transiently transfected cell lines was analysed using Western blot. The cell lysate was thawed and protein concentration was measured using Bradford protein Assay (Section 2.3.8). For each sample, 20µg protein sample was loaded to the 12.5% (v/v) SDS-PAGE gel. After electrophoresis, the gel was transferred to the PVDF membrane for 50 minutes. The membrane was incubated

with the blocking solution for 1 hour. The membrane of each cell line was incubated with Epsin3 antibody (1:50 dilution, Table 2.5) overnight while shaking at 4˚C. The membrane was then washed and incubated with the secondary anti-rabbit antibody (1:10,000 dilution, Table 2.5) for one hour at room temperature. The membrane was washed and visualised using chemiluminiscence (ECL) detection reagents and radiograph film. The membrane stripped and re-incubated with primary alpha-tubulin antibody (1:2000 dilution, Table 2.5) for 1 hour at room temperature while shaking and then washed, before incubation incubated with the secondary anti-rabbit antibody (1:10,000 dilution, Table 2.5) for one hour at room temperature. Then the membrane was washed and visualised using chemiluminiscence (ECL) detection reagents and radiograph film was taken. Levels of Epsin3 protein expression mirrored expression levels quantified at the RNA level. Levels of Epsin3 expression was significantly increased between the treated and untreated cell lines (Figure 5.3A). The transfected H103 cells showed significantly higher level of Epsin3 expression than untreated cells ($p<0.001$), transfected H357 compared to untreated cells ($p<0.01$), and transfected BICR31 compared with untreated cells ($p<0.05$). Although expressed at a low level, a visual increase in Epsin3 expression was observed in transfected BICR56 cells, this did not reach significance on densitometry (Figure 5.3B).

5.3.6 Investigation of the effect of increase Epsin3 expression on Notch1 level in transfected cell lines

To test the effect of overexpression of Epsin3 by plasmid transfection on the Notch signalling pathway, the level of Notch1 expression was examined in the cell lines which were transfected with Epsin3 plasmid. The expression was investigated at both RNA and protein levels. The correlation between Epsin3 and Notch1 expression level in transfected cell lines was calculated.

Quantitative RT-PCR analysis of Notch1 expression in the transfected cell lines

The cDNA samples of transfected cell lines, H103, H357, BICR31 and BICR56 were prepared using reverse transcriptase (Applied Biosystems, USA) (Section 2.3.4). The final concentration of the cDNA template was 100ng/µl. The samples were sent to University of Malaya, Kuala Lumpur, Malaysia and the qRT-PCR was performed, and results were analysed. The mean fold was calculated using Δct values. Notch1 showed differential expression levels in the cell lines tested. For three the cell lines the level of Notch1 expression was significantly lower in the Epsin3 transfected cells than in the un-transfected cell line controls, H103, BICR31 ($p<0.05$) and BICR56 ($p<0.01$). By

contrast, H357 cells showed the opposite effect; the level of Notch1 expression was significantly higher in the Epsin3 transfected cells than in the untransfected cell controls (Figure 5.4).

Levels of Notch1 protein quantification in the transfected cell lines by Western blot

The molecular weight of Notch1 protein is 120kDa and Epsin3 is 68kDa, so the same membranes prepared for Epsin3 expression analysis were used to perform Western blot analysis for Notch1 without the need for stripping. Each membrane was incubated with blocking solution for 1 hour while shaking at room temperature. The Notch1 antibody was applied to each membrane (1:1000, Table 2.5) and incubated overnight while shaking at 4˚C. The next day the membrane was washed 3 times for 15 minutes, then incubated with secondary anti-rabbit antibody (1:10,000, Table 2.5) for 1hour. After washing, the membrane was visualised using chemiluminiscence (ECL) detection reagents and radiograph film was taken. There was visual decrease in the level of Notch1 expression in the Epsin3 transfected H103 and BICR31 cells compared with untreated controls. Notch1 was not detected in H357 or BICR56 cells (Figure 5.5A). Levels of expression were compared with alpha-tubulin expression in the same samples (5.3.5.). The Notch1 expression level was significantly downregulated in the transfected H103 and BICR31 cell lines, compared with the untreated cells ($p<0.001$, $P<0.01$) respectively. The results were consistent with the qRT-PCR findings (Figure 5.5B).

5.3.7 Knockdown of the Epsin3 gene in BICR31 cell line

The BICR31 cell line expresses relatively high Epsin3 at both RNA and protein level (Table 5.1). Accordingly, it was selected for transient knockdown of Epsin3 using siRNA technology. The cells were grown in 6 well plates seeded at a density of $4x10^5$ cells/well until they reached 90% confluency. At this stage 10nM of siRNA (Santa Cruz Biotechnology, Germany) was applied for each transfection using GeneJammer transfection reagent. For control experiments, 10nM of siRNA (scrambled) (Santa Cruz Biotechnology, Germany) was used (Section 2.5.2). After 72 hours, RNA and protein were collected from cells and stored in -80˚C for future work.

5.3.8 RT-PCR analysis of Epsin3 expression in the siRNA knockdown BICR31cells

RNA was extracted from the cell line and cDNA prepared using Moloney Murine Leukaemia Virus, the final concentration of RNA was 1µg (Section 2.3.4). Semi-

quantitative RT-PCR analysis was performed to assess the expression of Epsin3 after knockdown. The housekeeping gene GAPDH was used to normalize the expression of Epsin3. Incubation of the BICR31 cells for 72 hours with siRNA sequence designed to target Epsin3, resulted in a reduction in Epsin3 expression of 69% (Figure 5.6A), when compared with siRNA (scrambled) control. The expression level of Epsin3 in the siRNA transfected cells was significantly lower than cells transfected with scrambled sequence ($p<0.01$) (Figure 5.6B).

5.3.9 Levels of Epsin3 protein quantification in siRNA knockdown BICR31 cells by Western blot

The protein lysis of BICR31 transfected cells was thawed and the concentration was measured using Bradford Assay (Section 2.3.8). The final concentration of protein used was 20µg. After gel running, the protein samples were transferred to the PVDF membrane, and it was incubated with antibodies against Epsin3 [(1:50) dilution, overnight and alpha-tubulin (1:2000) dilution for 1 hour (Table 2.5)]. The membrane was then visualised using chemiluminiscence detecting reagent and then radiograph film was taken (Figure 5.7A). The level of expression of Epsin3 protein was reduced in the cells transfected with 10nM siRNA (68.5%, compared with siRNA scrambled control). The difference was significant ($p<0.05$) (Figure 5.7B). This result was similar to the result obtained by semi-quantitative RT-PCR analysis.

5.3.10 Levels of Notch1 protein quantification in Epsin3 knockdown BICR31 cells by Western blot

To detect the level of Notch1 protein expression in the BICR31 cell line after transient knockdown of the Epsin3 with siRNA, Western blot analysis was carried out. The same membrane prepared for detection of Epsin3 protein expression in the above experiment was used (5.3.9). The membrane was re-probed and incubated with Notch1 antibody (1:1000) overnight. After visualisation of the membrane using chemiluminiscence detecting reagent, radiograph film was taken. The effect of reducing Epsin3 mRNA expression on the Notch1 signalling pathway was inconclusive (Figure 5.8A).The Epsin3 siRNA caused a 20% reduction in Notch1 expression, however, the reduction was not statistically significant ($p>0.05$) (Figure 5.8B).

5.4 Discussion

The results presented in Chapter 4 revealed that the expression of Epsin3 protein shows a positive correlation with expression of Notch1 protein in some OSCC cell lines, based on this we hypothesized a mechanistic relationship between Epsin3 and Notch1 and therefore investigated the effect of changing levels of Epsin3 expression on the Notch1 expression in the OSCC cell lines. Epsin3 gene was increased using a transient transfection of human Epsin3 expression vector (Origene) in the selected OSCC cell lines. The knock on effect on the expression of Notch1 was measured at both the RNA and protein level after transfection. Significant increase in Epsin3 expression was confirmed at RNA and protein level. Significant decrease in Notch1 RNA expression was observed in the transfected H103, BICR31 and BICR56 cell lines in response to an increase in Epsin3 levels in these cells. However, H357 cell line, showed an opposite results that the expression level of Notch1 RNA was significantly elevated in cells overexpressing Epsin3. Similar to RNA, Notch1 protein expression showed significant reduction in the transfected H103 and BICR31 cells compared to untreated control. However, Notch1 protein was not detected in H357 and BICR56 transfected cells. H357 and BICR56 cells have a mutation in the Notch1 gene in the EGF-like binding domain (Mutvei et al. 2015; Yap et al. 2015). In the presence of wild type Notch1 these observations suggest that overexpression of Epsin3 attenuates significantly the expression level of Notch1. The consequence would be disruption of endocytosis of Notch1 by overexpression of Epsin3 resulting in significant reduction of Notch1 receptor expression, which would lead to downregulation of the signal.

Our present data suggest that Epsin3 is required for Notch activation and increased levels of Epsin3 result in significant reduction of Notch1 receptor expression at both RNA and protein levels. The possible explanation of these results would related to the structure of Epsin. Epsin contains several motifs, the N-terminal homology domain (ENTH), which interact with phosphatidylinositol 4, 5 bisphosphate [PtdIns (4,5)P2] which activates the binding of Epsin to the plasma membrane (Itoh et al. 2001), the C-terminal homology contains: NPF (asparagine-proline-phenylalanine), DPW which are known as asparate-proline-tryptophan and clathrin-binding motifs, these motifs are involved in linking clathrin-coat proteins such as Ap-2, Eps15 and clathrin heavy chain. In between these two motifs there is UIM that is required for Epsin ubiquitination (Chen et al. 1998; Wendland 2002). Several studies report that disruption of any of these motifs result in an inhibition of clathrin-mediated endocytosis. For example the UIM of

Epsin1 is required to interact with ubiquitinated EGF to activate endocytosis, and using a mutant UIM of Epsin1 lead to impairment of the interaction between Epsin1 and ubiquitinated EGF, moreover overexpression of ENTH-UIM fragment of Epsin1, resulting in an inhibition of internalization of EGF if ubiquitination of EGF is inhibited (Kazazic et al. 2009).

In agreement, microinjection of CV-1 cells (Normal African Green Monkey Kidney Fibroblast Cells) with affinity-purified anti-epsin antibodies result in blockage the internalization of EGF. Moreover, overexpression of DPW motifs (Asp-Pro-Trp) of Epsin results in an inhibition of clathrin-mediated endocytosis (Chen et al. 1998). Likewise, overexpression of mutated Epsin (with deletion of ENTH), but not wild type Epsin, inhibits internalization of EGF (Itoh et al. 2001). This inhibition possibly occurs due to sequestration of AP-2 and clathrin by DPW motif that lead to non-specific inhibition of endocytosis, as the Eps15/AP-2 interaction is essential for receptor-mediated endocytosis, disruption of this interaction inhibits the formation of plasma membrane-coated pits, consequently inhibits endocytosis (Benmerah et al. 1998). Other explanation that overexpression of mutant ENTH made it unable to bind to the PtdIns (4, 5) P2 which is essential to induce clathrin-mediated endocytosis. These results suggest that overexpression of Epsin may have a dominant-negative effect on clathrin-mediated endocytosis which in turn, would result in a reduction of Notch1 expression. Collectively, we can hypothesize that overexpression of Epsin inhibit the internalization of EGF and block the endocytosis of ligand-receptor complex, the prerequisite step for Notch signal activation.

Interestingly, these findings are comparable with our present data that show significant reduction of Notch1 expression in the OSCC cell lines transfected with Epsin3 plasmid. However, we did not explored in the current study which site or motif of Epsin3 are overexpressed. Down regulation of Notch signalling in OSCC was reported previously indicating the tumour suppressor function of Notch. For example, Notch signalling in keratinocytes induces differentiation by activation p21, the major target of TP53 activity, and deletion of Notch1 in vivo lead to reduce p21 levels (Rangarajan et al. 2001). Additionally, impaired Notch1 expression may lead to abnormal cell differentiation in pre-cancers and cancers, indicating that Notch signalling has a role in squamous epithelium differentiation (Yugawa et al. 2010). Moreover, Duan et al. (2006) study showing that overexpression of NICD (active form of Notch signalling) in tongue carcinoma cell line causes cell cycle arrest, suppression of cell growth and

induction of apoptosis. Recently, Nowell and Radtke (2017), demonstrated that squamous cell carcinoma (SCC) development and progression usually associated with loss of Notch signalling.

Surprisingly, the H357 cell line which has mutated Notch1 mainly with the EGF motif (Yap et al. 2015) did not show the same result, with the expression level of Notch1 being significantly elevated after transfection with Epsin3 in these cells. In agreement, transfection of a mutant EGFR cell line (Y1045F) with a plasmid encoding ENTH-UIM part of Epsin1 showed higher EGFR internalization compared to the wild type EGFR (wt-EGFR) cell line (Kazazic et al. 2009). In addition, EGF internalization in the Y1045F cell line was not sensitive to non-clathrin internalization inhibitors (Sigismund et al. 2005). This result indicates that ligand-receptor endocytosis may occurs independently of EGF ubiquitination and may reflect development of compensatory mechanisms leading to internalization of EGF and finally ligand-receptor endocytosis. Speculatively, therefore the EGF mutation may explain the elevation of Notch1 expression at the RNA level through this mechanism. However, at the protein level, Notch1 was not detected in either H357 or BICR56 cell lines. In H357 this is indicative of a truncated mutation of Notch1 leading to loss of its expression (Yap et al. 2015), similarly, a truncation mutation in BICR56 (Mutvei et al. 2015) could also explain this lack of Notch1 expression.

The BICR31 OSCC cell line was transfected with human Epsin3 siRNA with the aim to establish Epsin3 knockdown in these cells, and investigate whether Epsin3 inhibition affects level of Notch1 expression. The knockdown resulted in a reduction of Epsin3 expression in BICR31 cells approximately 69% at both RNA and protein level. The cell lysate, after SDS-PAGE, was immunoblotted with an antibody specific against Notch1. However, the Epsin3 knockdown resulted in a reduction of Notch1 expression of only about 20% which was not statistically significant, however the possible biological significance of fall in protein expression of about 20% cannot be ignored. Preliminary results from our work indicate that Epsin3 knockdown did not affect endocytosis of the ligand-receptor. Our present results are consistent with previous data showing that EGF internalization was reduced by about 15-30% in Hela cells transfected with Epsin1 siRNA (Huang et al. 2004). Likewise, Sigismund et al. (2005), stated that individual knockdown of Epsin1 had no effect on the EGF internalization in Hela cells . Simultaneously, Sigismund performed triple Eps15/Eps15R/epsin knockdown and Huang performed double Eps15/Eps15R knockdown, both experiment resulting in

EGF internalization inhibition. Furthermore, double Epsin1/2 knockout in mice lead to impairment of Notch signalling (Chen et al. 2009). Taken together, with these results, our finding suggest that siRNA-mediated Epsin3 knockdown was not sufficient to inhibit completely EGF endocytosis, suggesting existence of other ubiquitin-binding proteins which may compensate and produce endocytosis and internalization of EGRR, or that Epsin3 is working with other family members. Thus Notch1 expression did not appear to be inhibited. However, Kazazic et al. (2009), reported that siRNA-mediated Epsin1 knockdown inhibits internalization of EGF in both wt-EGFR and Y1045F-EGFR cell lines, and so this may be a variant specific process.

In summary, data presented in this chapter suggest that the disruption of Epsin3 expression affects the endocytosis of ligand-receptor and may lead to disturbance of Notch1 expression. Hence, overexpression of Epsin3 results in significant reduction of Notch1 expression in OSCC cell lines, except for those that have or may have a Notch1 mutation. Although siRNA-mediated Epsin3 knockdown in the OSCC cell line did not resulted in complete inhibition of Epsin3, there was minor reduction on Notch1 expression, we speculate that Epsin3 activates Notch signalling in OSCC via interaction between its UIM and ubiquitinated EGFR which mediate ligand-receptor endocytosis, the crucial step for Notch signal activation. These results lead us to conclude that expression level of Epsin3 in the OSCC may be considered as a biomarker for oral squamous cell carcinoma that may be mirrored in in vivo samples. Further work should investigate the level of Epsin3 expression in tissue samples, including normal, dysplasia and OSCC, and its relation with malignant progression.

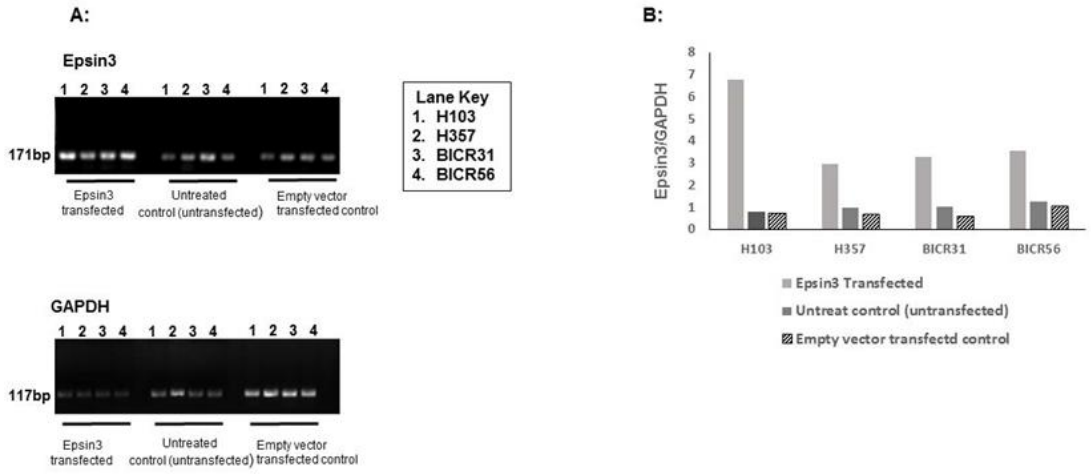

Figure 5.1: Levels of Epsin3 mRNA in the OSCC cell lines transfected with human Epsin3 expression vector, untreated cells and cells transfected with empty vector.

A) Bands were generated by RT-PCR from RNA samples extracted from cells grown in the presence of either 1µg of human Epsin3 expression vector (OriGene) under standard conditions or 1µg of empty vector (Sigma, p3XFLAG-CMVTM-10 Expression vector) or untransfected cells, for 24 hours. All cells were lysed and cDNA was prepared by reverse transcription for each cell line. Representative gel image showing Epsin3 expression (expected at 171bp) and the reference gene GAPDH (expected at 117bp).

B) Relative levels of Epsin3 in cells transiently transfected with either 1µg Epsin3 expression vector or 1µg of empty vector or untransfected cells. The levels were obtained by measuring the band intensity on a gel, using Gene Snap software and GAPDH in the same sample. Relative levels are shown for one individual PCR reaction analysed.

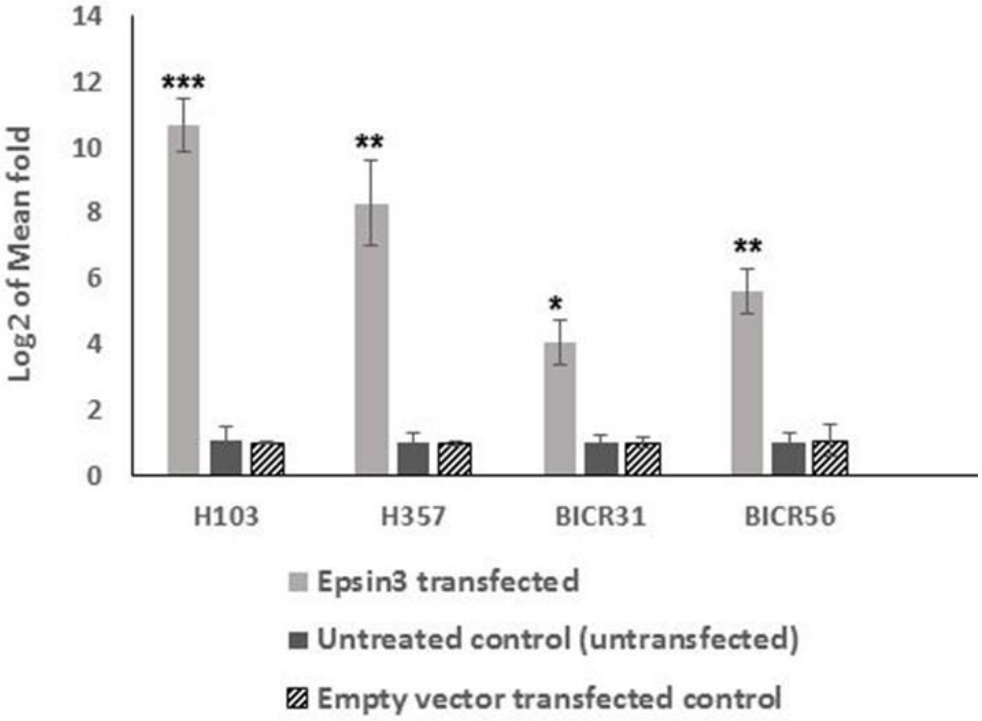

Figure 5.2: Levels of Epsin3 mRNA in the OSCC cell lines after transient transfection with human Epsin3 expression vector

OSCC cell lines (H103, H357, BICR31 and BICR56) were transfected with either 1µg of human Epsin3 expression vector (OriGene) under standard conditions or 1µg of empty vector (Sigma, p3XFLAG-CMVTM-10 Expression vector) or untransfected cells or 24 hours. Cells were lysed and cDNA was prepared by reverse transcription. qRT-PCR was used to assess Epsin3 gene expression. Relative Epsin3 expression was determined using the 2-ΔΔCt method using the GAPDH as a reference gene. Data are shown as mean ±SD (n=9). All transfected cell lines have significantly higher level of Epsin3 expression compared with untreated cells, ***=p<0.001, **=p<0.01 *=p<0.05 compared to untreated negative control. Significance measured by Paired Samples t-test.

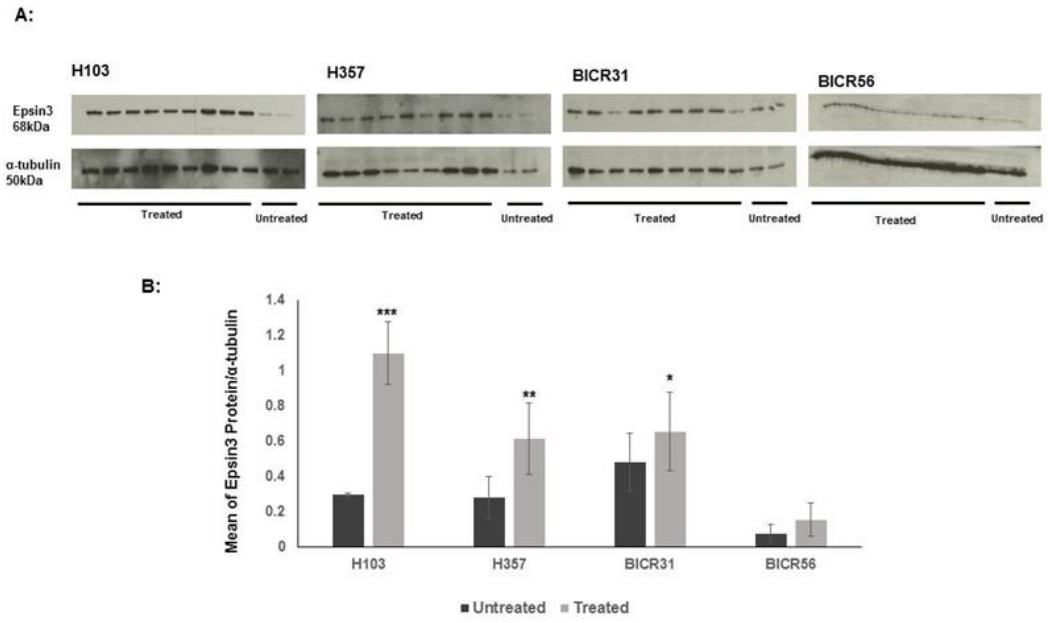

Figure 5.3: Expression of Epsin3 protein in the OSCC cell lines after transfected with human Epsin3 expression vector

OSCC cell lines (H103, H357, BICR31 and BICR56) were treated with 1µg of human Epsin3 expression vector (OriGene) for 24 hours. Cells were lysed and prepared for SDS-PAGE. Extracts were immunoblotted with antibodies against Epsin3 (1:50) and α-tubulin (1:2000).

A) Representative images showing level of Epsin3 expression was visually higher in treated cell lines compared with untreated cells.

B) Densitometry was adjusted for the background optical density of the radiographic film and normalised to α-tubulin. Data are shown as mean ±SD (n=9) from three independent experiments, the band intensity analysis revealed that the level of Epsin3 expression was significantly higher in treated H103, H357 and BICR31 cell lines than untreated cells, ***=$p<0.001$, **=$p<0.01$, *=$p<0.05$. There was no significant difference between the treated and untreated samples from the BICR56 cell line. Significance measured by Paired Samples t-test.

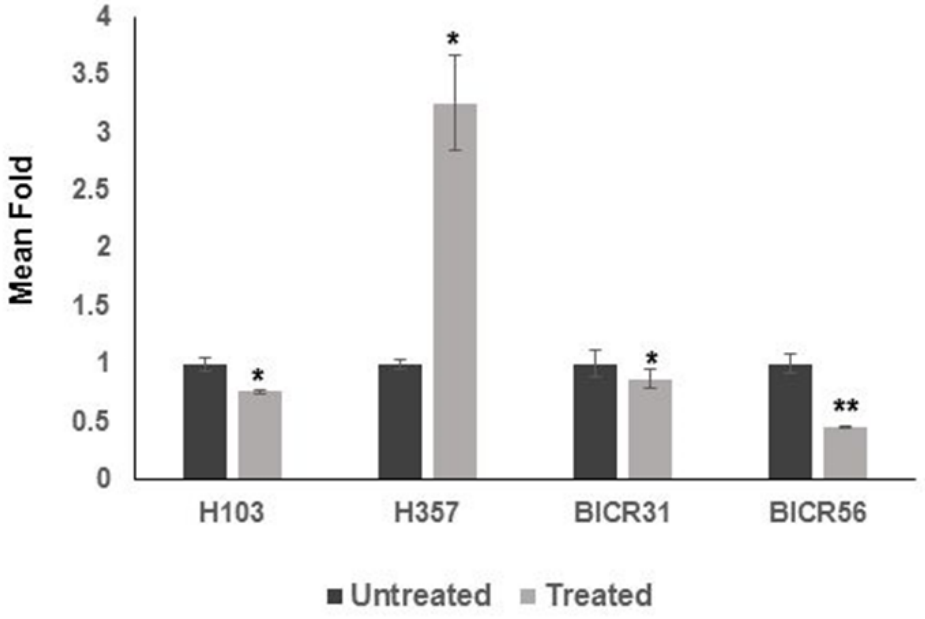

Figure 5.4: Levels of Notch1 mRNA in the OSCC cell lines after transient transfection with human Epsin3 expression vector

OSCC cell lines (H103, H357, BICR31 and BICR56) were transfected with 1µg of human Epsin3 expression vector (OriGene) for 24 hours. Cells were lysed and cDNA was prepared by reverse transcription. qRT-PCR was used to assess Notch1gene expression. Relative Notch1 expression was determined using the $2^{-\Delta\Delta Ct}$ method using the GAPDH as a reference gene. Data are shown as mean ±SD (n=3). The transfected H103, BICR31, and BICR56 cell lines with increased expression of Epsin3 (treated) had significantly lower Notch1 expression than untreated cells. By contrast, the transfected (treated) H357 cell line had significantly higher level of Notch1 expression compared to untreated cells. **=p<0.01, *=p<0.05. Significance measured by Paired Samples t-test.

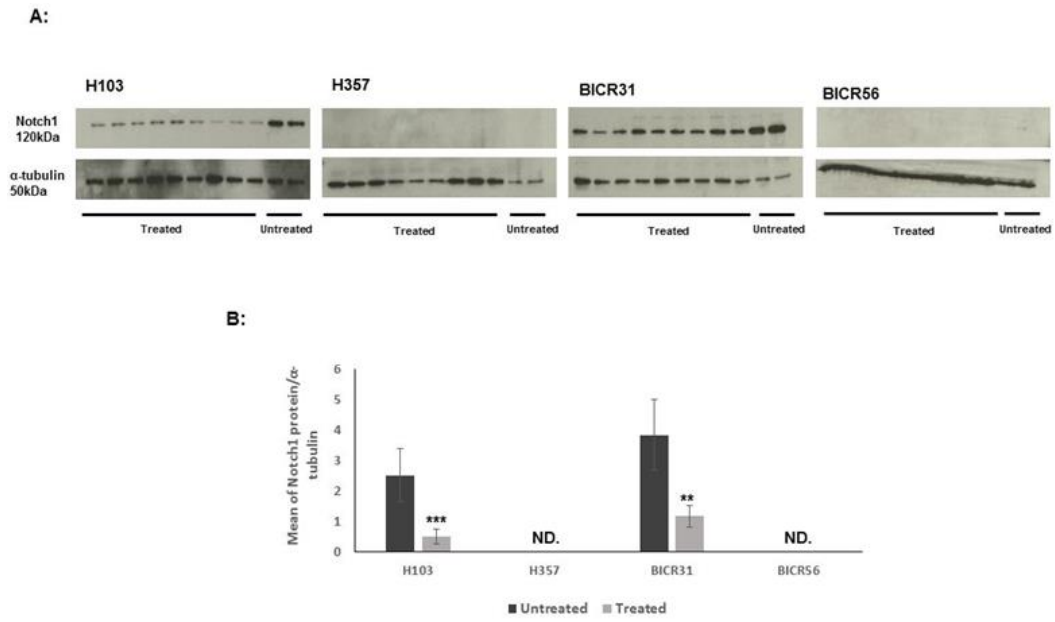

Figure 5.5: Expression of Notch1 protein in the OSCC cell lines after transfected with human Epsin3 expression vector.

OSCC cell lines (H103, H357, BICR31 and BICR56) were treated with 1µg of human Epsin3 expression vector. Cells were lysed and prepared for SDS-PAGE. Extracts were immunoblotted with antibodies against Notch1 (1:1000) and α-tubulin (1:2000).

A) Representative images of WBs showing that the level of Notch1 expression was lower in the H103 and BICR31 transfected cells by comparison with the untreated cell lines controls. No Notch1 protein could be detect in the H357 and BICR56 cells.

B) Densitometry was adjusted for the background optical density of the radiographic film and normalised to α-tubulin. Data are shown as mean ±SD (n=9) from three independent experiments, the band intensity analysis revealed that the level of Notch1 expression was significantly lower in the transfected (treated) H103, and BICR31 cell lines compared with the untreated cells, ***=$p<0.001$, **=$p<0.01$. Significance measured by Paired Samples t-test. ND: not detected.

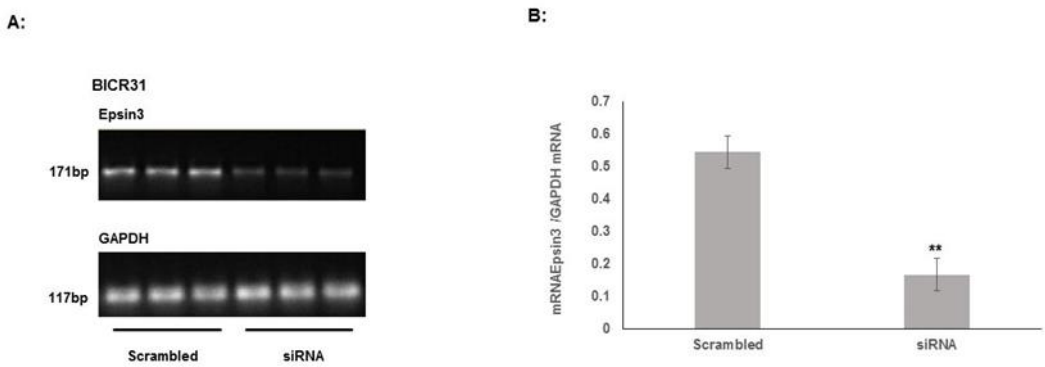

Figure 5.6: Levels of Epsin3 mRNA in the BICR31 cell line after transient knockdown of Epsin3 with siRNA.

Bands were generated by semi-quantitative RT-PCR from RNA samples extracted from cells grown in the presence of 10nM Epsin3 siRNA. For negative control, 10nM of scrambled sequence was used. Cells were lysed and cDNA was prepared by reverse transcription.

A) Representative gel images showing that Epsin3 expression was lower in the cells transfected with Epsin3 siRNA by comparison with the controls, which were transfected with the scrambled sequence. Similar band intensities for the reference gene GAPDH was observed, indicating the quantities of RNA in the samples were the same.

B) Densitometry analysis of relative Epsin3 mRNA levels expressed as a ratio of GAPDH mRNA levels. The expression was significantly lower in the transfected cells compared with scrambled, **=$p<0.01$. Significance measured by Paired Samples t-test.

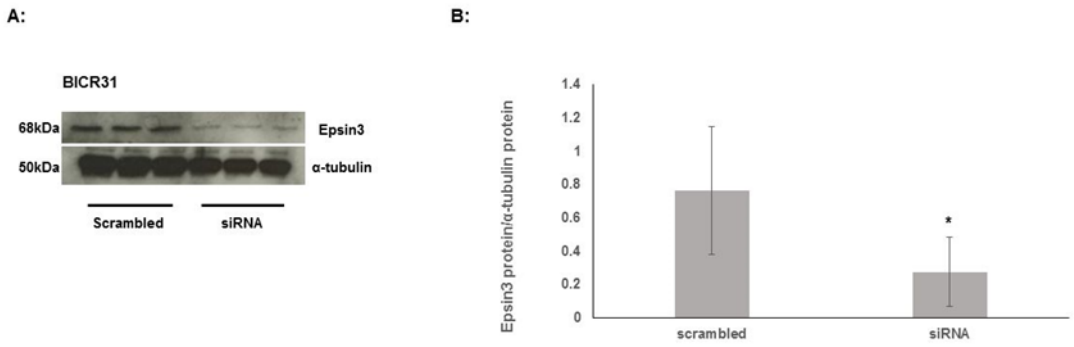

Figure 5.7: Expression of Epsin3 protein in the BICR31 cell line after transient knockdown of Epsin3 with siRNA.

BICR31 cells were treated with 10nM Epsin3 siRNA, and 10nM scrambled sequence. Cells were lysed and prepared for SDS-PAGE. Extracts were immunoblotted with antibodies against Epsin3 (1:50) and α-tubulin (1:2000).

A) Representative images of WB showing the level of Epsin3 expression was reduced in cells transfected with Epsin3 siRNA (expected band at 68 kDa). Both siRNA and scrambled samples have the same band intensity for the reference protein α-tubulin (expected band at 50kDa).

B) Densitometry was adjusted for the background optical density of the radiographic film and normalised to α-tubulin. Data are shown as mean ±SD (n=3). The expression was significantly lower in the siRNA samples than scrambled, *=$p<0.05$. Significance measured by Paired Samples t-test.

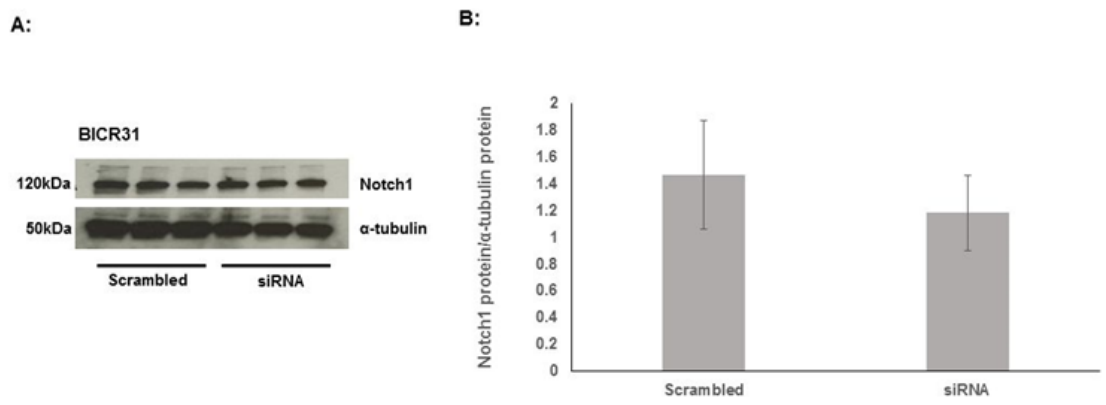

Figure 5.8: Expression of Notch1 protein in the BICR31 cell line after transient knockdown of Epsin3 with siRNA.

BICR31 cells were treated with 10nM Epsin3 siRNA, and 10nM scrambled sequence. Cells were lysed and prepared for SDS-PAGE. Extracts were immunoblotted with antibodies against Notch1 (1:1000) and α-tubulin (1:2000).

A) Representative images of WB showing the level of Notch1 expression was visually the same in cells transfected with Epsin3 siRNA and scrambled (expected band at 120kDa). Both siRNA and scrambled samples have the same band intensity for the reference protein α-tubulin (expected band at 50kDa).

B) Densitometry was adjusted for the background optical density of the radiographic film and normalised to α-tubulin. Data are shown as mean ±SD (n=3). There is no significant difference between the band intensity in the siRNA transfected cells and scrambled. Significance measured by Paired Samples t-test.

Chapter 6 **Expression of Epsins and Notch1 in normal oral mucosa, oral epithelial dysplasia and oral squamous cell carcinoma**

6.1 Introduction

Work presented in Chapters 3 and 4 characterised the expression of Epsins and Notch1 in OSCC-derived cell lines and immortalised normal oral keratinocytes. The results revealed a positive correlation between Epsin3 protein and Notch1 protein levels. However, work presented in Chapter 5 demonstrated that when Epsin3 expression was increased by plasmid transfection of cells with functional Notch1, Notch1 levels were decreased. In order to examine these findings, the expression profiles of Epsin1 and 2 (ZZ3), Epsin3 and Notch1 have examined in tissue from a well characterised cohort of patients with oral epithelial dysplasia and oral squamous cell carcinoma (OSCC), normal oral mucosa was used as a comparator

6.1.1 Tissue sample characteristics

Oral epithelial dysplasia samples were graded using a binary classification into high-grade and low-grade lesions (Kujan et al. 2006). OSCCs were staged using the 'Tumour, Node, Metastasis' (TNM) classification developed by the International Union Against Cancer (L.H. Sobin 2009), only patients with early disease (Stage I and II) OSCC were included in this study.

6.1.2 Epsin1, 2 and 3 proteins expression in tissues

Epsin1 and 2 (ZZ3) have the same domain architecture, with similar protein binding parts and both are enriched in brain. They are both involved in the clathrin-mediated endocytosis process (Rosenthal et al. 1999). Epsin3 is expressed in the parietal cells of stomach and skin keratinocytes during wound healing (Spradling et al. 2001; Ko et al. 2010). Epsin proteins play a critical role in regulation of different signalling pathways by internalization of membrane proteins such as Notch receptors, EGFR protease-activating receptor and VEGFR2 (Kazazic et al. 2009; Chen et al. 2011). Consequently, dysregulation of Epsins may adversely affect important cellular processes. For example, double knockout of Epsin1 and 2 resulted in developmental defects in mice embryos, which is caused by inhibition of Notch signaling (Chen et al. 2009).

Epsins expression may upregulated or downregulated in cancer. Epsin1 and 2-upregulation is involved in endocytosis of VEGFR2, which induces vascularization of

tumour tissues. Deletion of both Epsin1 and 2 in endothelial cells of mice resulted in blocking VEGFR2 receptor degradation and increase VEGFR2 signaling which result in formation of aberrant non-functional vessels preventing tumour growth in lung carcinoma (LLC) cells and melanoma cells (mouse skin cancer cell line B16F10, colorectal tumour, and adenocarcinoma of mouse prostate cancer) (Pasula et al. 2012). Overexpression of Epsin1 and 2 have been reported to be related to increased proliferation, invasion and metastasis of cancer cells through activation Notch signalling (Tessneer et al. 2013). Wang et al. (2006), reported that the expression level of Epsin3 is elevated in a human lung non-small-cell carcinoma cell line. Recently, Epsin3 expression was found to be downregulated in gastric cancer. Moreover, Epsin3 may act as a target of TP53 a key mediator of apoptosis (Mori et al. 2017). These findings suggest that Epsin3 may perform diverse roles in carcinogenesis. To date, the expression profile and potential role of Epsins in oral squamous cell carcinoma has not been described**.**

6.1.3 Notch1 protein expression in tissues

Notch1 expression has been reported to be upregulated in different human cancers including malignant melanoma, breast cancer and lung adenocarcinoma (Hoek et al. 2004; Balint et al. 2005; Stylianou et al. 2006; Donnem et al. 2010). In OSCC the expression level of Notch1 is variable. There are studies that have found Notch1 upregulated in OSCC (Yoshida et al. 2013; Gokulan and Halagowder 2014), whereas other have shown reduced Notch1 expression (Sakamoto et al. 2012).

6.2 Aims

1. To investigate Epsin and Notch1 protein expression in human tissues samples of oral epithelial dysplasia and early stage OSCC.
2. To correlate the expression levels of these proteins with the clinico-pathological features and clinical outcomes.

6.3 Results

6.3.1 Dysplasia group: patient characteristics and histological grade of epithelial dysplasia

A total of 79 tissue samples from patients with oral epithelial dysplasia were included in this study. The majority (63.3%) of patients were male and the mean of age was 58 years-old (range 30-94 years-old). The majority of cases presented on the floor of the mouth (39%) and lateral border of the tongue (29%). Smaller proportions affected the buccal mucosa, gingiva/alveolar ridge, or palate. The majority (62.5%) of patients had an adverse clinical outcome, which included local recurrence, new lesion formation and malignant transformation. Twenty-two of the 79 dysplasias in the study underwent malignant transformation to OSCC (Figure 6.1). Kaplan-Meier time to event analysis did not detect any significant difference between patient sex (males vs. female) and age (young vs. old) with regards to clinical outcome ($p>0.05$ data not shown). There were slightly more high-grade oral epithelial dysplasias than low grade lesions (56% vs 44%).

Kaplan-Meier time to event analysis demonstrated that high grade oral epithelial dysplasias were more likely to have an adverse outcome by comparison with low grade lesions (Log Rank Mantel Cox analysis $p<0.01$) (Figure 6.2A). However there was no significance difference in the rate of malignant transformation (Log Rank Mantel Cox analysis $p>0.05$), (Figure 6.2B).

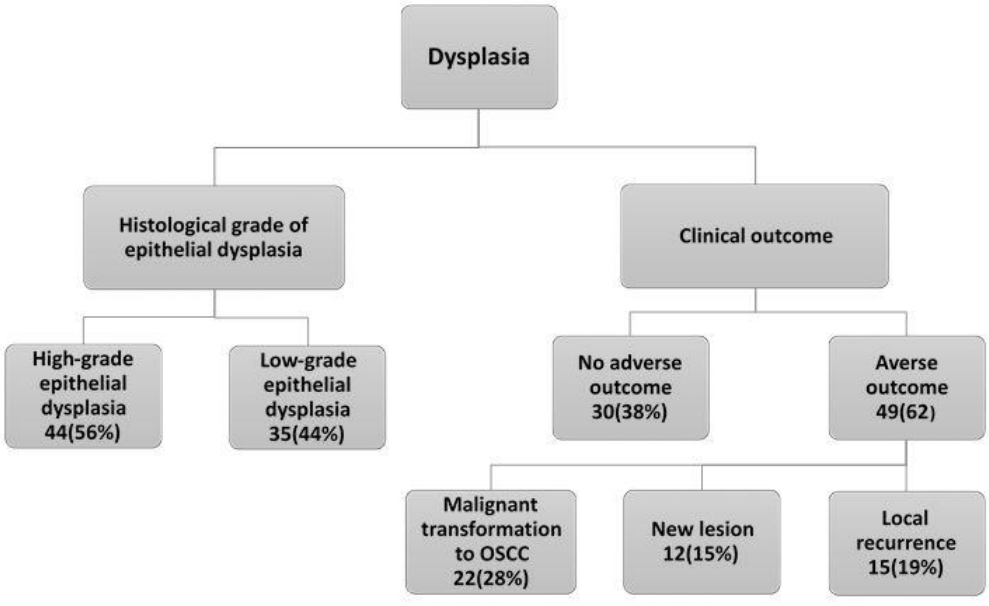

Figure 6.1Characteristics of the group of cases with dysplasia (n = 79).

6.3.2 Early-stage OSCC group: patient characteristics, mucosal subsite, pStage, and histological differentiation

A total of 31 tissue samples from patients with early-stage OSCC were included in this study. There were slightly more males than females (55% vs 45%males; male: female ratio1.2:1). The mean age was 64.8 years-old (range: 34-93 years-old). The majority of cases presented on the lateral border of the tongue and floor of mouth. Smaller proportions as affected the buccal mucosa, gingiva/alveolar ridge, or palate. Histologically, moderately differentiated OSCC was the commonest group (Table 6.1).The majority of cases were at Stage I (81%), the carcinoma were less than 2cm in maximum dimension and had not spread to lymph nodes or distant organs.

Clinical outcomes of patients diagnosed with early-stage OSCC

The majority (22 of 31; 71%) of patients were alive and disease free at the end of the study. The mean overall survival time was 52 months. The mean disease-free survival time was 45.7 months.

Nine patients died during the study period. Six of these patients died free from disease. The remaining three patients died from disease; two had recurrent disease (Table 6.1).

Characteristic	Number (%)
Histological grade of differentiation	
• Well differentiated	5 (16)
• Moderately differentiated	25 (81)
• Poorly differentiated	1 (3)
Clinical outcome :	
Alive	22 (71)
• Free from disease	22 (71)
• With disease	0
Deceased	9 (29)
• Free from disease	6 (19)
• With disease	3 (10)

Table 6.1Characteristics of the group of cases with OSCC (n=31).

Oral epithelial dysplasia cases that transformed to OSCC were also included in the study. There were 18 OSCC available, fifteen of the cases were either Stage I/Stage

II cancers and were added to the 31 cases described above. Three were Stage IV which were not included in the analysis.

Kaplan-Meier analysis did not detect any difference in the disease free survival and overall survival for the Stage I and Stage II OSCC (Figure 6.3A, B) respectively

6.3.3 Expression profile of ZZ3 protein

The ZZ3 antibody detects Epsin1 and Epsin2 and was optimised for immunohistochemistry by staining sections of formalin-fixed paraffin-embedded (FFPE) normal tonsil. The tonsil showed strong membrane and cytoplasmic staining of squamous epithelium, endothelium and lymphoid follicles (Chapter 3 Figure 3.7A). The samples from the patient cohort generally showed weak staining with the majority of samples being negative (Figure 6.4). By comparison with the normal samples, there were more cases with no staining in the dysplasia and OSCC samples, however, the differences were not statistically significant ($p>0.05$; Figure 6.5).

6.3.4 Expression profile of Epsin3 protein

The anti-Epsin3 antibody was optimised for immunohistochemistry by staining sections of normal tonsil. The tonsil show membrane and cytoplasmic staining of squamous epithelium and endothelium (Chapter 3 Figure 3.8A).

Expression profile of Epsin3 in the oral dysplasia

Seventy-four dysplastic tissue samples were examined for Epsin3 expression. Normal oral epithelium showed weak to moderate expression. Oral epithelial dysplasia and OSCC showed variable Epsin3 expression ranging from weak to strong (Figure 6.6). Epsin3 protein expression was measured using an H score [the product of the staining intensity (0-3) and the proportion of cells stained (0-100%); range 0-300]. Samples were assigned to a binary ‘high Epsin3’ or ‘low Epsin3’ category according to whether Epsin3 expression was either above or equal to or below 100. Epsin3 protein expression was higher in dysplastic epithelium relative to the normal epithelium (Figure 6.6), there was a significant difference between the expression levels in the normal and oral dysplasia ($p<0.001$). Cases of high-grade epithelial dysplasia show significantly higher expression level of Epsin3 compared to the low-grade dysplasia ($p<0.05$). Dysplasia with adverse outcomes (i.e. local recurrence, new lesion formation, malignant transformation) had a significantly higher Epsin3 expression than dysplasia with no adverse outcome ($p<0.001$) (Figure 6.7). The expression was also significantly

higher in dysplastic tissues that underwent malignant transformation relative to cases which did not transform into cancer ($p<0.01$) (Figure 6.7). Nevertheless, Kaplan-Meier analysis did not detect a significant difference between Epsin3 high vs. Epsin3 low group over time ($p>0.05$; Log Rank Mantel Cox test; Figure 6.8).

Expression profile of Epsin3 in early-stage oral squamous cell carcinoma

Thirty-one samples of early stage OSCC (T1 & T2), in addition to nine cases of dysplasia that underwent malignant transformation to OSCC were selected for analysis of Epsin3 expression level.

Epsin3 protein expression was generally higher in the majority of OSCC compared to the normal epithelium (Figure 6.6). The H score was significantly higher in the OSCC compared to the normal tissues ($p<0.0001$). There was no significant difference between the OSCC and dysplasia samples ($p>0.05$) (Figure 6.9).

Expression of Epsin3 in early-stage OSCC with adverse clinical outcomes (i.e. local recurrence and death from disease) had no significant difference from cases with no adverse outcome (i.e. cases which had no recurrence and were alive and disease-free), ($p>0.05$) (Figure 6.9). Kaplan-Meier analysis did not detect any significant differences between Epsin3-high and Epsin3-low cases, with regards to disease free survival and overall survival ($p>0.05$) (Figure 6.10).

6.3.5 Expression profile of Notch1 protein

The Notch1 antibody was optimised for immunohistochemistry by staining sections of normal tonsil. The tonsil show membrane and cytoplasmic staining of squamous epithelium and endothelium (Chapter 4 Figure 4.5A).

Expression profile of Notch1 in the oral dysplasia

Seventy-four dysplastic tissue samples were examined for of Notch1 expression. Normal epithelium showed weak to moderate Notch1 expression in the basal keratinocytes (Figure 6.11 a & b). Oral epithelial dysplasia showed variable Notch1 expression, some samples showed similar staining intensity to normal epithelium, whereas others there was no staining (Figure 6.11 c & d). Notch1 expression was categorised as either positive (some staining observed) or negative (no staining). Notch1 was expressed in the majority of normal samples (92%), but fewer dysplasia samples (58%; Figure 6.12), which was statistically significantly different ($p<0.01$).

Cases with high-grade epithelial dysplasia show significantly lower numbers of Notch1 positive cases compared to low-grade epithelial dysplasia ($p<0.05$). Dysplasia with adverse outcomes had a significantly lower Notch1 expression than dysplasia with no adverse outcome (i.e. local recurrence, new lesion formation, malignant transformation; $p<0.001$). There was no significant difference in the proportion of Notch1 negative cases between dysplasia that did not transformed and those that underwent malignant transformation ($p>0.05$; Figure 6.12). Kaplan-Meier time to event analysis showed that cases with loss of Notch expression were more likely to transform to OSCC ($p<0.001$; Log Rank Mantel Cox test; Figure 6.13).

Expression profile of Notch1 in early-stage oral squamous cell carcinoma

Thirty-one samples of early stage oral squamous cell carcinoma (pT1, pT2), in addition to nine cases of dysplasia that underwent malignant transformation were examined for Notch1 protein expression by immunohistochemistry.

Notch1 expression was variable in OSCC and was categorised as either positive or negative (Figure 6.11). The majority of OSCC had lost Notch1 expression by comparison to normal epithelium (Figure 6.14) and the difference was significant ($p<0.001$). However, there was no significant difference in the proportion of Notch1 positive/negative cases oral epithelial dysplasia and OSCC ($p>0.05$; Figure 6.14). There was no significant difference in Notch expression between OSCC with adverse clinical outcomes (i.e. local recurrence and death from disease) and those with no adverse outcome ($p>0.05$; Figure 6.14).

Kaplan-Meier survival analysis did not detect any difference in disease free survival or overall survival time between Notch1 positive and Notch1 negative cases ($p>0.05$; Log Rank Mantel Cox test; Figure 6.15).

6.3.6 RNA in situ hybridization

Notch1 RNA in situ hybridization was optimised for the cell lines in (Chapter 4.Section 4.3.2). The signals detected in the tissue samples were very weak/barely perceptible and heterogeneous, but showed similar trends to that described for Notch1 immunohistochemistry. Generally, normal samples were positive and dysplastic

epithelium and OSCC samples were negative, however, the signals were too weak and heterogeneous to reliably assess across the sample cohort.

6.3.7 Relationship between Epsin3 and Notch1 expression levels in the oral epithelial tissues

The relationship between Epsin3 and Notch1 expression level in the oral dysplasia and OSCC tissues was analysed by Pearson's chi-square test. The analysis revealed a significant correlation between Epsin3 and Notch1 in both the dysplasia and OSCC ($P<0.001$, ch2 value 42, 1d.f. and $p<0.001$, ch2 value 21.4, 1d.f.) respectively. Epsin3 expression was conversely correlated with Notch1 expression. Dysplasia and OSCC cases have high Epsin3 expression, showed low or negative Notch1 expression.

6.4 Discussion

Work presented in Chapter 3 and 4 was concerned with assessing the expression levels of Epsin1, 2 and 3, and Notch1 proteins in the panel of OSCC cell lines. The results revealed the differential of expression levels of these proteins in the cell lines. Moreover, the effect of Epsin3 expression level on the Notch1 expression level was confirmed in Chapter 5. Based on these observations, work presented in this chapter highlighted the expression levels of these proteins in the oral tissues including normal, dysplasia and OSCC.

6.4.1 Patient characteristics, epithelial dysplasia grade and OSCC differentiation

In the present study, most of the patients with dysplasia/early-stage OSCC were in their 6th to 7th decades and most of them consumed alcohol and tobacco. There was no difference in the sex ratio. The grade of epithelial dysplasia does not accurately predict clinical outcomes, particularly the risk of malignant transformation (Dost et al. 2014). Our results revealed a significant correlation between clinical outcome (recurrence, new lesion formation and malignant transformation) and grade of dysplasia. However, there was no significant correlation between grade of epithelial dysplasia and malignant transformation. By contrast, the previous studies reported that the risk of malignant transformation to cancer was significantly related to grade of oral dysplasia (Mehanna et al. 2009; Warnakulasuriya et al. 2011). In our study, the data analysis confirmed that the demographic profile of the patients including age and sex did not correlate with clinical outcome (Diajil et al. 2013). A previous study reported that the grade of differentiation of OSCC cases has a relationship with survival rate (Arduino et al. 2008). By contrast, our analysis did not detect a significant correlation, but this could be due to the small number of cases that have been used in our study.

6.4.2 Expression of ZZ3 protein

The endocytic adapter proteins Epsin1 and 2 play an important role in clathrin-mediated endocytosis. They have a critical role and demonstrate redundancy (compensation), because single deletion of either Epsin1 or 2 in mice did not result in a phenotype defect, while double knockout of both Epsin1 and 2 results in embryonic lethality (Chen et al. 2009). Dysregulation of Epsin1 and 2 in cancer has been reported in several studies, through their function of the internalization of ubiquitinated receptors of different pathways. Disturbance of receptors internalization may result in up or down

regulation of signalling; thus lead to disturbance of cell proliferation, differentiation and migration. Epsin1 and 2 are enriched in the brain tissue (Chen et al. 2009). Our data revealed generally low levels of ZZ3 (Epsin1 and 2) in normal epithelium, epithelial dysplasia and OSCC with no significant difference between them. By contrast, upregulation of Epsin1 and 2 was observed in human prostate cancer tissues compared to normal prostate tissue analysed by IHC (Tessneer et al. 2013) and also in colorectal adenocarcinoma tissues compared to normal colon tissues (Chang et al. 2015) . Other studies demonstrate the role of Epsin1 and 2 in tumour angiogenesis and reported that deletion of endothelial Epsin1 and 2 may lead to tumour growth regression by formation of aberrant vasculature , suggesting the activating function of Epsin1 and 2 in cancer (Pasula et al. 2012). However, none of these studies included squamous epithelium and OSCC. It is therefore difficult to accurately compare our data with the results of these studies. Nonetheless, downregulation of Epsin1 and 2 in dysplasia and OSCC tissues may result in deficient endocytosis of signalling receptors. Impaired endocytosis of signalling receptors may be associated with cancer, since it can lead to activated and uncontrolled signalling. Therefore, dysregulation of adaptor proteins required for receptor downregulation can be oncogenic and lead to tumour development (Crosetto et al. 2005). For example, Epsin1 is responsible for regulation of EGFR signalling through endocytosis and degradation of EGFR (Kazazic et al. 2009). Overexpression of EGFR was reported in the OSCC (Grandis and Tweardy 1993). Therefore, downregulation of Epsin1 in dysplasia and OSCC in our study may resulted in loss of EGFR down-regulation, hence, the EGFR signalling becomes constitutive. However, although Epsin1 and 2 expression in dysplasia and OSCC was less than normal tissue, there was no significant difference between them. To date, the profile of Epsin1/Epsin2 expression in oral dysplasia and OSCC tissues has not been described and the exact role of Epsin1 and 2 in OSCC is yet to be determined.

6.4.3 Expression of Epsin3 protein

The other endocytic adaptor protein which are involved in the clathrin-mediated endocytosis is Epsin3. Our results revealed that the expression level of Epsin3 was differential in the OSCC cell lines. Upregulation of Epsin3 has been documented in skin keratinocytes during wound healing. Epsin3 was expressed mainly in migrating keratinocyte cells and absent in differentiating cells. Epsin3 was found to be down-regulated in intact skin (Spradling et al. 2001). These observation suggest that Epsin3 has a crucial function in cell proliferation and migration. Similarly, up-regulation of

Epsin3 has been associated with invasiveness of the tumour cells and its overexpression enhance migration and invasion of fibrosarcoma cells (Coon et al. 2010; Coon et al. 2011). Our data shows Epsin3 upregulation in the oral dysplasia and OSCC compared to the normal oral tissues, the expression was higher in cases with high grade of epithelial dysplasia compared with low grade dysplasia. Moreover, dysplasia with adverse outcome had higher expression levels than cases with no adverse outcome. The previous observation is relevant to our results considering up-regulation of Epsin3 in epithelial tissues that underwent pathological changes (i.e. dysplasia and OSCC) (Spradling et al. 2001). By contrast, recently Mori et al. (2017), reported that Epsin3 was down-regulated in gastric cancer tissue compared to normal tissues. Epsin3 has involved in DNA damage-induced apoptosis suggesting that Epsin3 may induce apoptosis of oncogenic proteins through endocytosis such as CD44, KLK6, EPHA3 and RORI1; anti-apoptotic membrane proteins. Hence, down-regulation of Epsin3 may causes apoptosis resistance. Furthermore, the expression level of Epsin3 in gastric cancer tissues did not correlate with overall survival. Our results also show that Epsin3 overexpression does not correlated with clinical outcome. This may indicate that Epsin3 is not associated with progression of the disease. However, the small sample size of OSCC involved in present study may influence the results and make them unreliable.

6.4.4 Expression of Notch1 protein

The Notch pathway is altered in HNSCC and several studies reported its dual role. Notch can have either an oncogenic or tumour suppressor effect. Work presented in Chapter 4 was concerned with measuring the expression levels of Notch1 receptor protein in the OSCC cell lines. Observations from previous studies demonstrated that squamous cell carcinoma development and progression is associated with loss of Notch signalling (Nowell and Radtke 2017). Results presented in Chapter 4 revealed absence of Notch1 protein expression in two of OSCC cell lines. To support our findings in the cell lines, we examined the expression of Notch1 protein in oral tissues including normal, dysplasia and OSCC. Our data shows down-regulation of Notch1 protein in dysplasia and OSCC compared to normal tissues. Interestingly, down-regulation of Notch1 in premalignant and OSCC tissues was reported in previous study by IHC (Sakamoto et al. 2012) and by genomic analysis (Agrawal et al. 2011; Stransky et al. 2011; Pickering et al. 2013).

Furthermore, our results demonstrate that cases of dysplasia with adverse outcome have significantly lower Notch1 expression than cases with no adverse outcome and cases with reduction of Notch1 expression are more likely to undergo malignant transformation than cases with high Notch1 expression. Sakamoto et al. (2012), reported that Notch1 expression was down-regulated in regenerative epithelia, suggesting that down-regulation of Notch1 expression is a mechanism switching epithelial cells from normal and mature to an activated and immature state. Impaired Notch1 expression may led to abnormal cell differentiation in cancers and pre-cancers, indicating that Notch signalling has a role in squamous epithelial differentiation (Yugawa et al. 2010). Thus reduction of Notch1 expression may contribute to the pathogenesis of dysplasia by ceasing terminal differentiation with the formation of immature epithelium. Additionally, overexpression of cleaved Notch1, the active form of Notch signalling; lead to suppression of cell growth in tongue carcinoma cell line (Duan et al. 2006; Pickering et al. 2013). Pickering et al. (2013), indicated that activation of Notch1 lead to arrest in the G1 phase and over activation of cleaved Notch1 lead to cease of cells proliferation and senescent. Notch signalling in epidermis and keratinocytes induces cell cycle arrest and terminal differentiation, which aids to eliminate cancer stem cells and tumour-initiating cells (Wilson and Radtke 2006; Koch and Radtke 2007). It was reported that Notch signalling in keratinocytes induces differentiation by activation p21, the major target of TP53 activity, and deletion of Notch1 in vivo lead to reduce p21 levels (Rangarajan et al. 2001).Taken together, these results support the hypothesis that Notch signalling has a tumour suppressive function in OSCC.

Our analysis shows downregulation of Notch1 in dysplasia and OSCC. This is in contrast to previous studies that show an oncogenic role for the Notch pathway in OSCC, for example upregulation of Notch signalling molecules, such as Notch1 and Notch3 receptors, was reported in human tongue carcinoma, the expression was higher in tongue carcinoma than adjacent non-neoplastic tongue tissues and Notch1 expression level is positively correlated with lymph node metastasis and invasion (Joo et al. 2009; Zhang et al. 2011). Similarly, expression of Notch1, Notch2, Jagged1, Hes1 and Hey1 was upregulated in OSCC tissues compared to the normal and dysplasia and blocking of Notch signalling using γ-secretase inhibitor effectively reduce tumour growth in vitro (Hijioka et al. 2010). These results are in agreement with the observation from Yoshida et al. (2013), who reported that Notch1 expression was localized to

invasive OSCC, in addition, Notch1 knockdown and use of γ-secretase inhibitor prevent cell proliferation in vitro.

Furthermore, Gokulan and Halagowder (2014), demonstrated that Notch signalling components, cleaved Notch1 and Hes1; were significantly increased from normal to dysplasia to OSCC. Collectively, all the previous observations indicate that Notch signalling may have a tumour suppressive or oncogenic role in HNSCC. Loss-of-function mutations of Notch signalling are frequent in HNSCC, indicating its tumour suppressive function. Nonetheless, observations that revealed overexpression of Notch signalling in the HNSCC are obtained from in vitro studies using human HNSCC cells, which cannot accurately delineate the processes that arise during development of the tumour in vivo (Nowell and Radtke 2017).

Interestingly, our data showed that the expression level of Notch1 in the tissues sample was correlated with expression of Epsin3, suggesting that Epsin3 can play a critical role in Notch signalling activation.

In summary, the expression levels of ZZ3 (Epsin1/Epsin2) in the tissues did not show a difference between normal epithelium, epithelial dysplasia and OSCC. All the tissue samples had low ZZ3 staining, indicating that Epsin1 and 2 endocytic adaptor proteins are expressed less in oral epithelial tissues. Whereas Epsin3 expression was up-regulated in dysplasia and OSCC relative to normal tissues, and dysplasia with adverse outcome had significantly higher Epsin3 expression compared to cases with no adverse outcome. This is consistent with studies of high Epsin3 expression in the immature and undifferentiated keratinocytes and Epsin3 expression is more associated with the epithelial cells that undergo pathological changes. This result may indicate a role of Epsin3 as a potential tumour biomarker, although up-regulation of Epsin3 in OSCC does not correlate with clinical outcome.

Notch1 expression was down-regulated in dysplasia and OSCC relative to normal epithelium. Furthermore, dysplasia transformed to OSCC had a significant correlation with low Notch1 expression. These findings are concordant with previously published studies of Notch1 expression in OSCC, and support the hypothesis that Notch signalling has a tumour-suppressor function in OSCC.

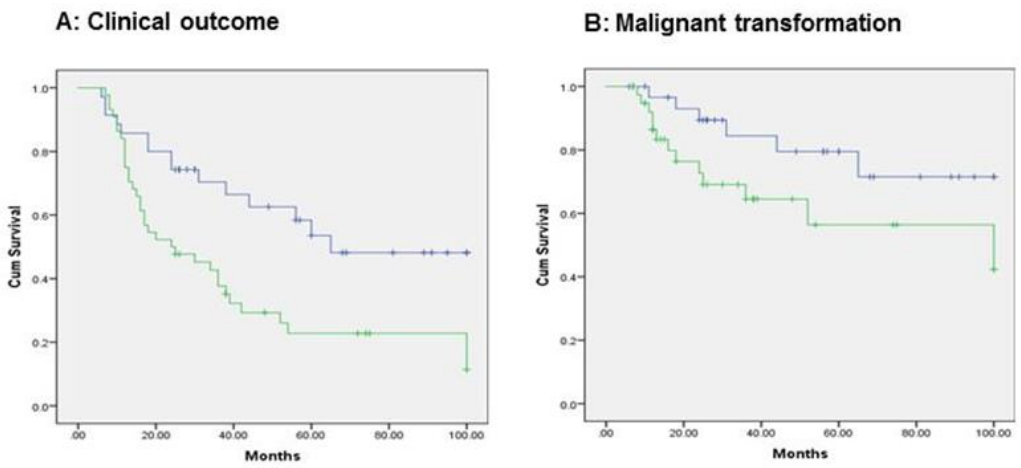

Figure 6.2: Kaplan Meier time to event analysis comparing low and high grade epithelial dysplasia for clinical outcome and malignant transformation.

Colour index: blue line: low grade epithelial dysplasia (n=35), green line: high grade epithelial dysplasia (n=44).

A) Lesions with high grade epithelial dysplasia were more likely to experience an adverse clinical outcome (recurrence, new lesion formation and malignant transformation) compared to lesions with low high grade of epithelial dysplasia ($p<0.01$, Log Rank Mantel-Cox test).

B) Lesions with high grade epithelial dysplasia were more likely to undergo malignant transformation than those with low grade dysplasia, but the difference was not statistically significant ($p>0.05$, Log Rank Mantel-Cox test).

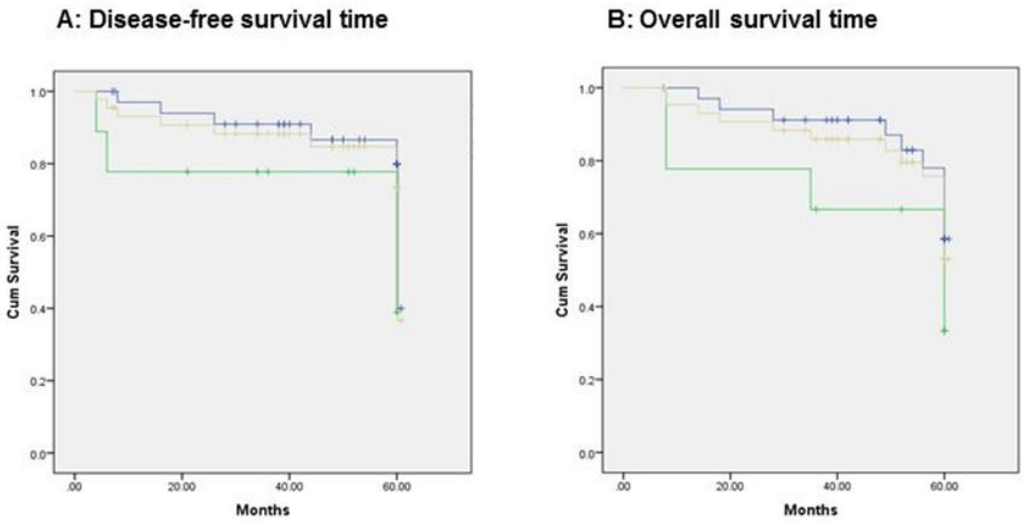

Figure 6.3: Kaplan-Meier survival curve analysis comparing Stage I and Stage II OSCC for disease free survival and overall survival.

Colour index: blue line: Stage I (n=36); green line: Stage II (n=10); yellow line: Stage I & Stage II combined. Patients with Stage I tumours had a better DFS and OS than Stage II tumours, but the difference was not statistically significant ($p>0.05$, Log Rank Mantel-Cox test).

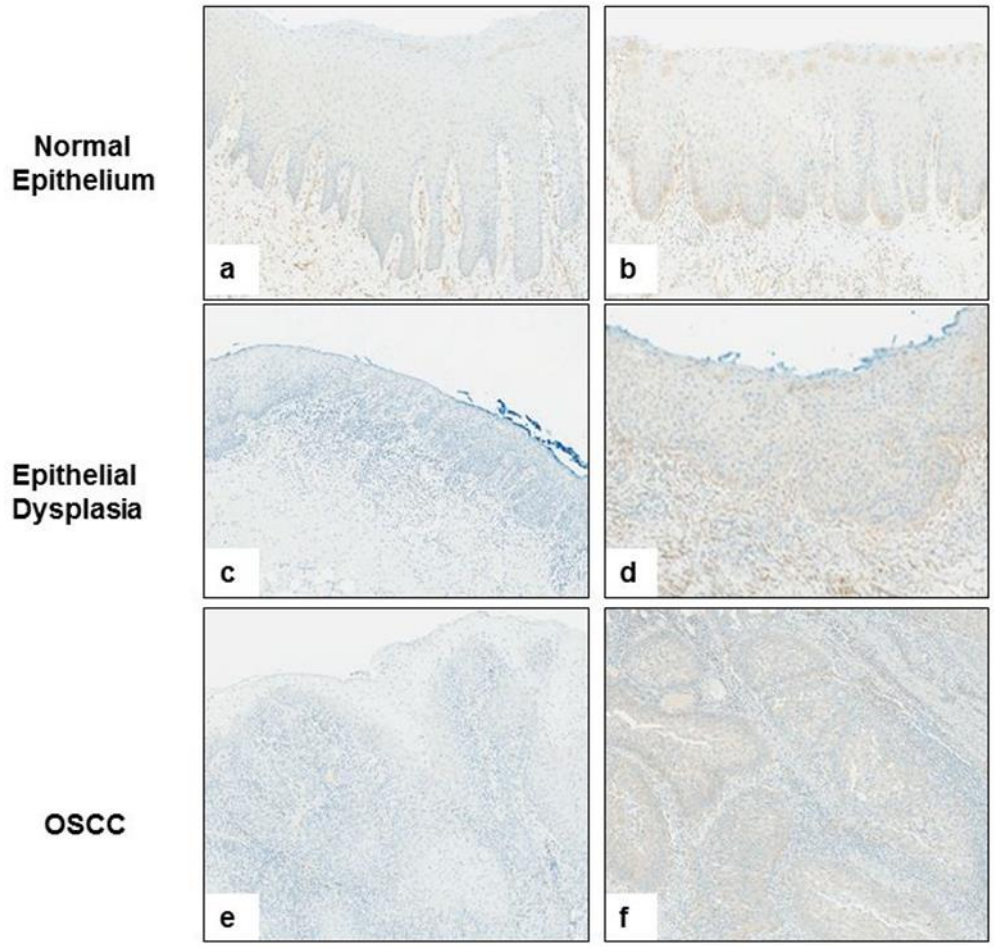

Figure 6.4: Expression profile of ZZ3 in normal epithelium, epithelial dysplasia and OSCC tissues.

Normal epithelium was either negative **(a)** or showed very weak cytoplasmic staining **(b)**. Epithelial dysplasia and OSCC showed a similar ZZ3 profile to normal epithelium, some were negative whereas others showed some weak staining **(c-f).** Images taken at 5x magnification.

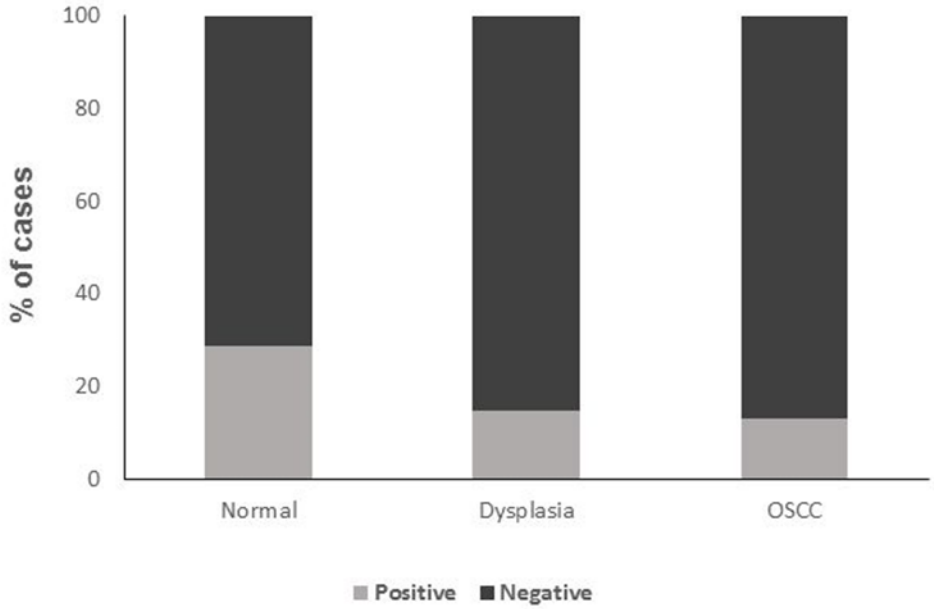

Figure 6.5: Percentage of cases with negative and positive ZZ3 staining for normal epithelium, epithelial dysplasia and OSCC tissues samples.

The majority of cases did not show any ZZ3 expression. There was no significant difference in the proportion of case that were ZZ3 positive between the normal epithelium (n=21) and epithelial dysplasia (n=74) ($p>0.05$, Independent T-test), and normal epithelium and OSCC (n=31) ($p>0.05$, Independent T-test).

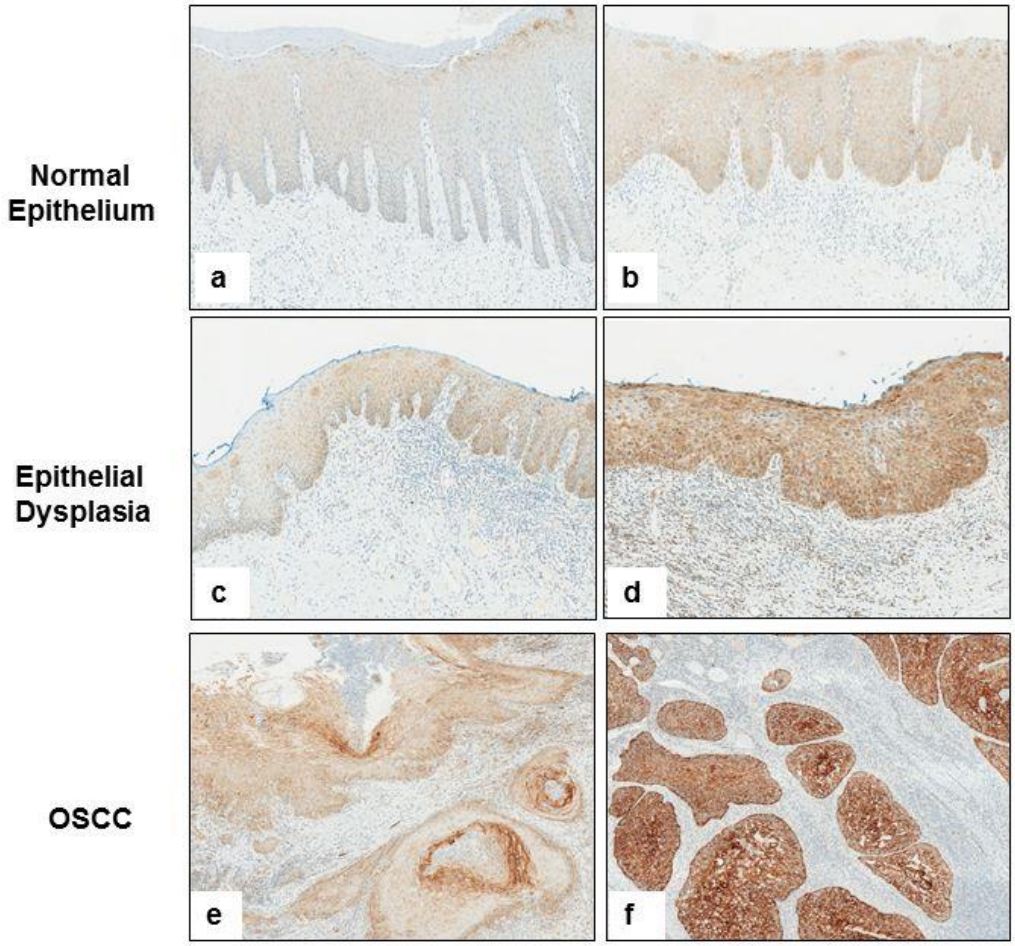

Figure 6.6: Expression profile of Epsin3 in normal epithelium, epithelial dysplasia and OSCC tissues.

Normal epithelium showed weak **(a)** to moderate **(b)** cytoplasmic staining with Epsin3. Epithelial dysplasia and OSCC showed variable Epsin3 expression ranging from weak to strong **(c-f)**. Images taken at 5x magnification.

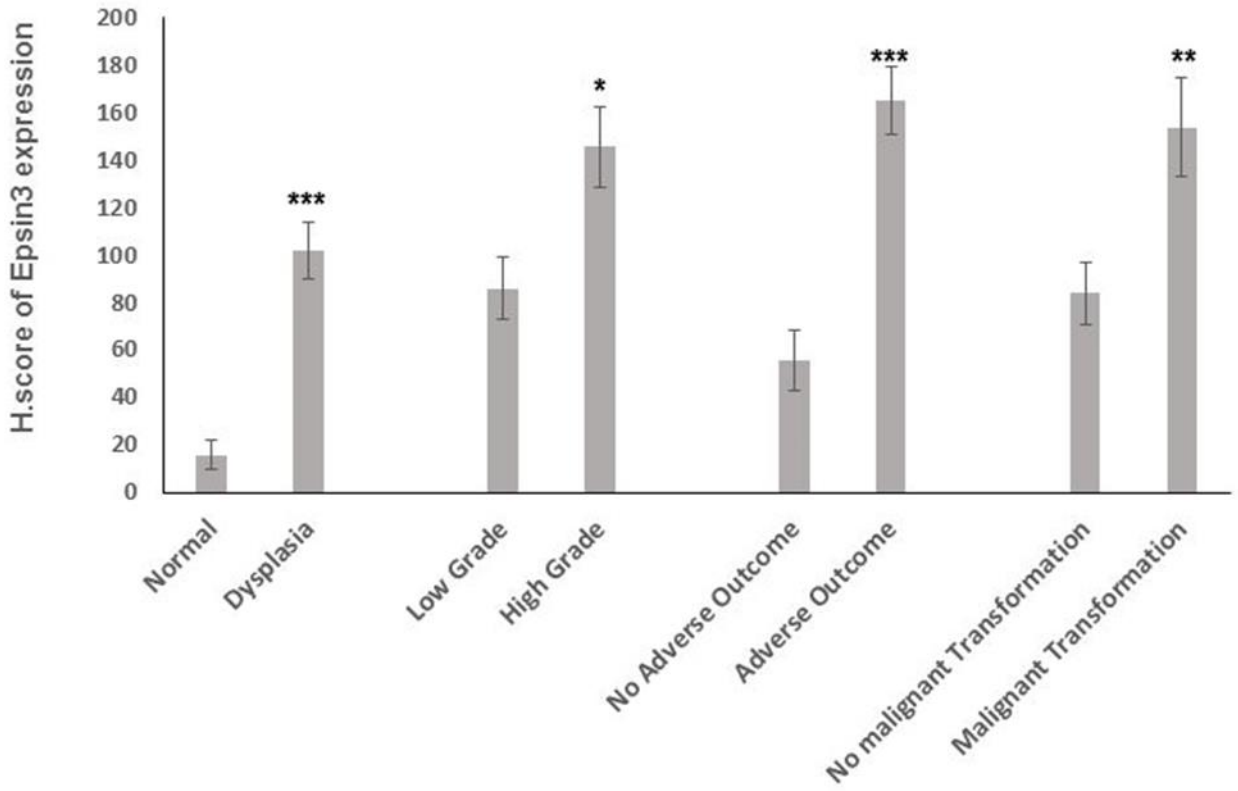

Figure 6.7: Comparison of the Epsin3 expression profile in normal epithelium and oral dysplasia stratified according to epithelial dysplasia (binary classification) grade and clinical outcome.

Epsin3 was significantly higher in epithelial dysplasia relative to normal epithelium ($p<0.001$). Cases with high-grade epithelial dysplasia had a significantly higher Epsin3 expression than the cases with low-grade epithelial dysplasia ($p<0.05$). Dysplasias with an adverse clinical outcome had significantly higher Epsin3 expression than dysplasias with no adverse clinical outcome ($p<0.001$). Dysplasias that underwent malignant transformation had a higher Epsin3 expression than cases that did not transform ($p<0.01$). Significance measured by Mann-Whitney U test.

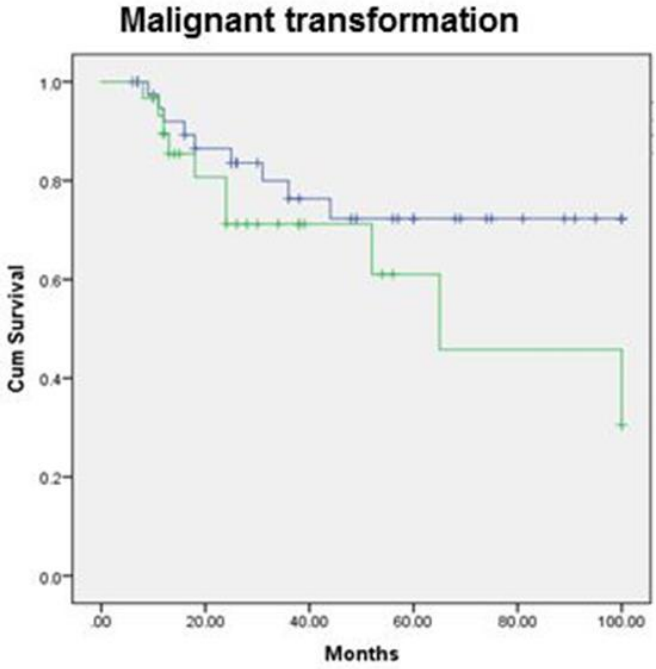

Figure 6.8: Kaplan Meier time to event analysis showing correlation between Epsin3 expression and malignant transformation.

Colour index: blue line: low Epsin3, green line: high Epsin3. Kaplan-Meier time to event analysis showed that lesions with high Epsin3 (H score >100) were more likely to undergo malignant transformation than lesions with low Epsin3 expression, however, the difference was not statistically significant (Log Rank Mantel-Cox test $p>0.05$).

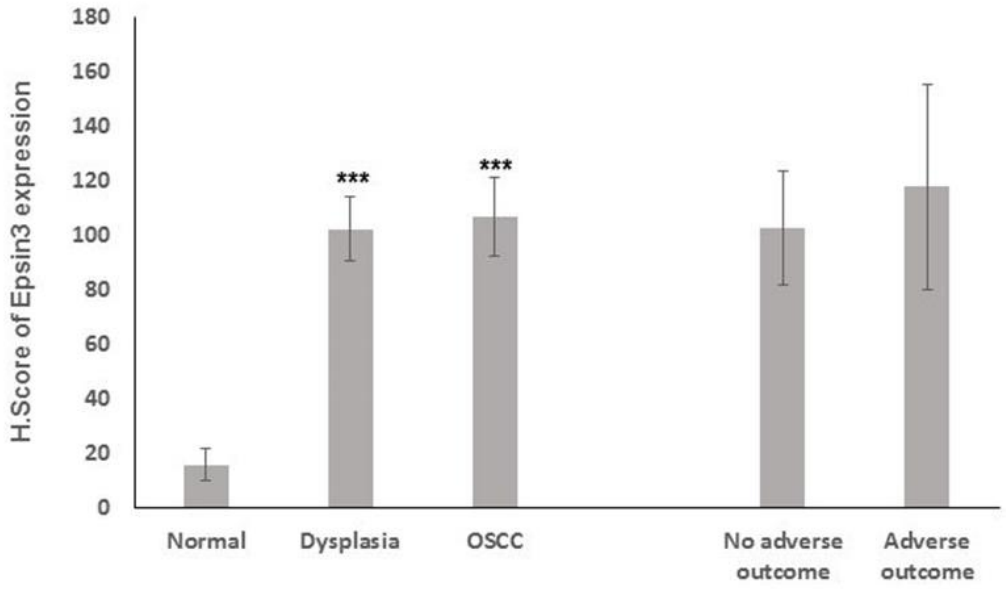

Figure 6.9: Comparison of the Epsin3 expression profiles in normal epithelium, epithelial dysplasia and OSCC.

Epsin3 expression was significantly higher in epithelial dysplasia and OSCC compared to the normal epithelium ($p<0.001$). There was no significant difference between epithelial dysplasia and OSCC ($p>0.05$). There was no significant difference in Epsin3 expression between the OSCC with no adverse clinical outcome those cases with adverse clinical outcome (i.e. disease recurrence and death) ($p>0.05$). Significance measured by Mann-Whitney U test.

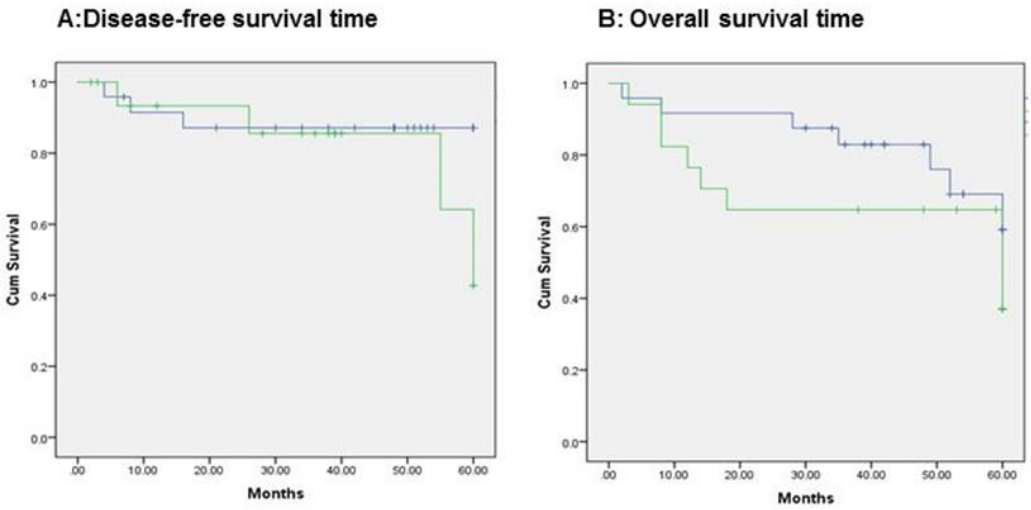

Figure 6.10: Kaplan Meier survival curve analysis showing correlation between Epsin3 expression levels and clinical outcome in OSCC cases.

Colour index: blue line: low Epsin3 expression, green line: high Epsin3 expression. Kaplan-Meier survival curves showed that there was no statistically significant difference in disease-free survival (A; $p>0.05$) or overall survival (B; $p>0.05$) for OSCC with high (H score > 100) or low Epsin3 expression. Significance measured by Log Rank Mantel-Cox test.

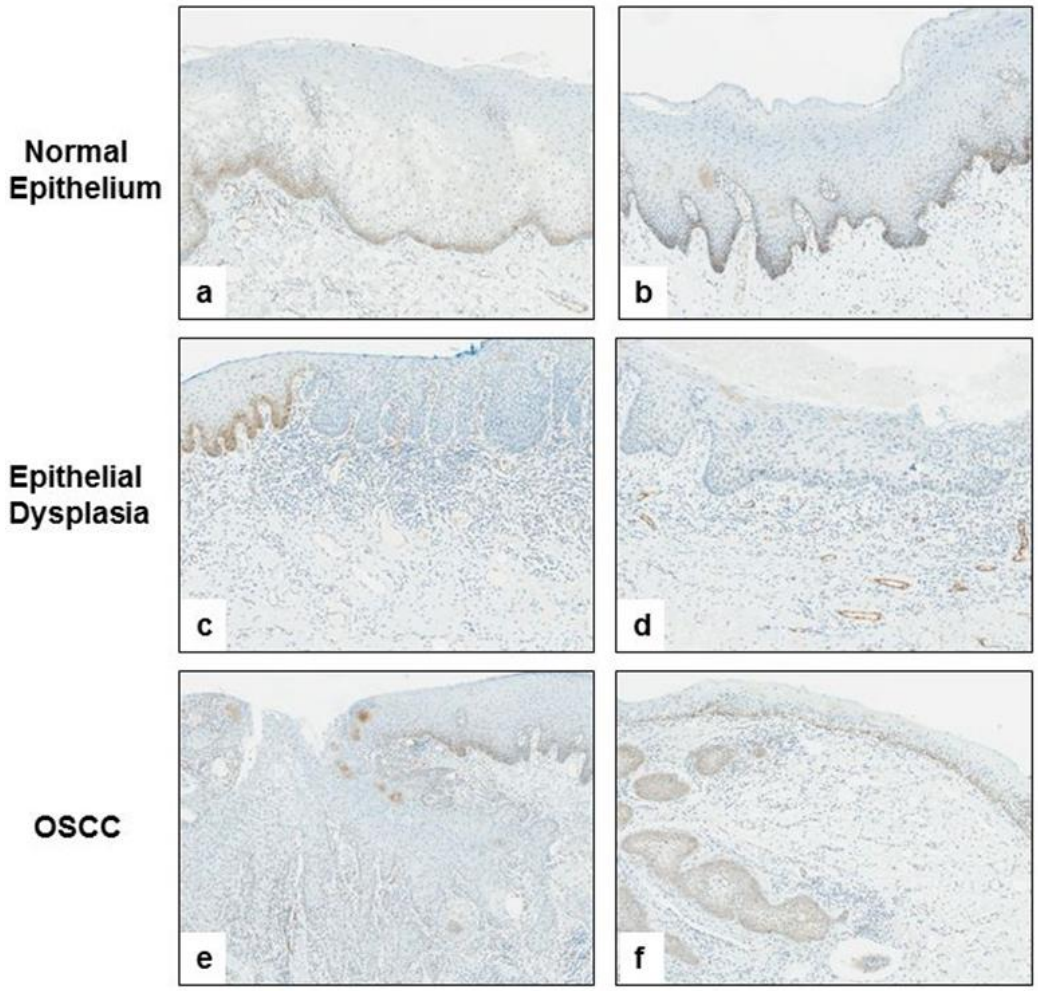

Figure 6.11: Expression profile of Notch1 in normal epithelium, epithelial dysplasia and OSCC tissues.

Normal epithelium showed weak to moderate cytoplasmic staining for Notch1 in the basal keratinocytes **(a & b).** Oral epithelial dysplasia and OSCC showed variable expression form ranging from weak staining to negative **(c-f)**. Images taken at 5x magnification.

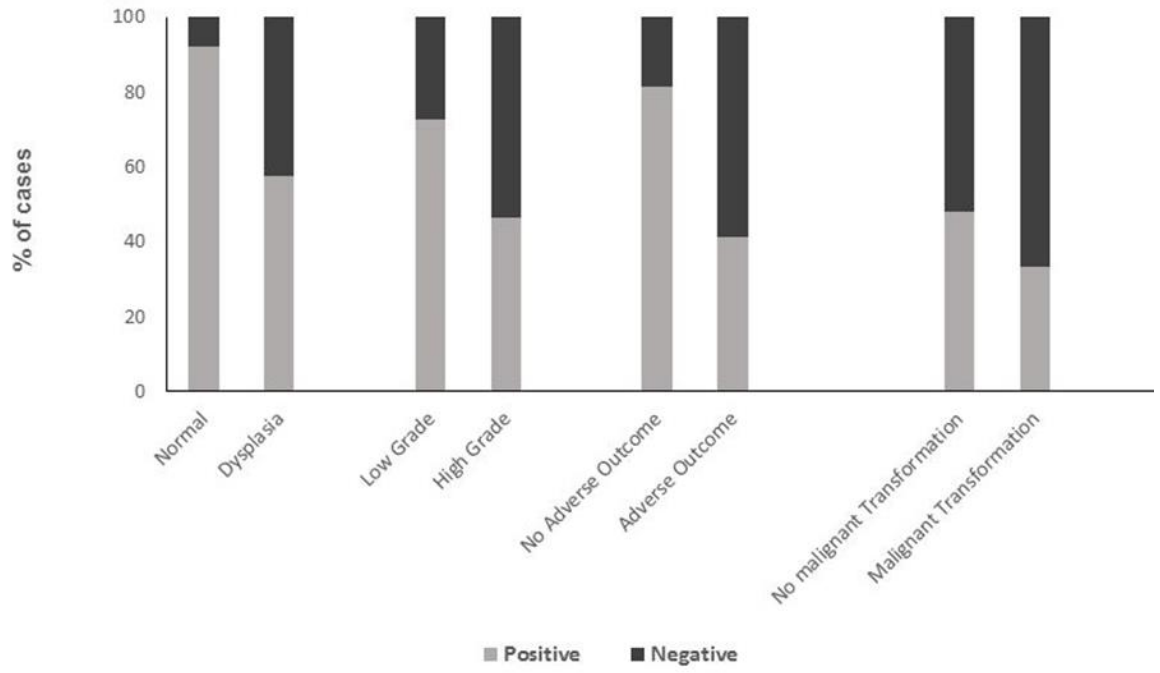

Figure 6.12: Comparison of the proportion of Notch1 positive vs. Notch1 negative samples for normal epithelium and oral epithelial dysplasia, then stratified according to dysplasia grade and clinical outcome.

The majority (90%) of oral mucosa samples expressed Notch1 in the basal layers of the epithelium. By comparison with the normal samples, fewer oral epithelial dysplasias expressed Notch1 ($p<0.01$). Cases with high grade epithelial dysplasia had fewer Notch1 positive cases than low grade lesions ($p<0.05$). Dysplasias with adverse clinical outcome had fewer Notch1 positive cases than dysplasias with no adverse clinical outcome ($p<0.001$). Dysplasias that underwent malignant transformation had fewer Notch1 positive samples than cases with no malignant transformation ($p>0.05$). Significance measured by Mann-Whitney U test.

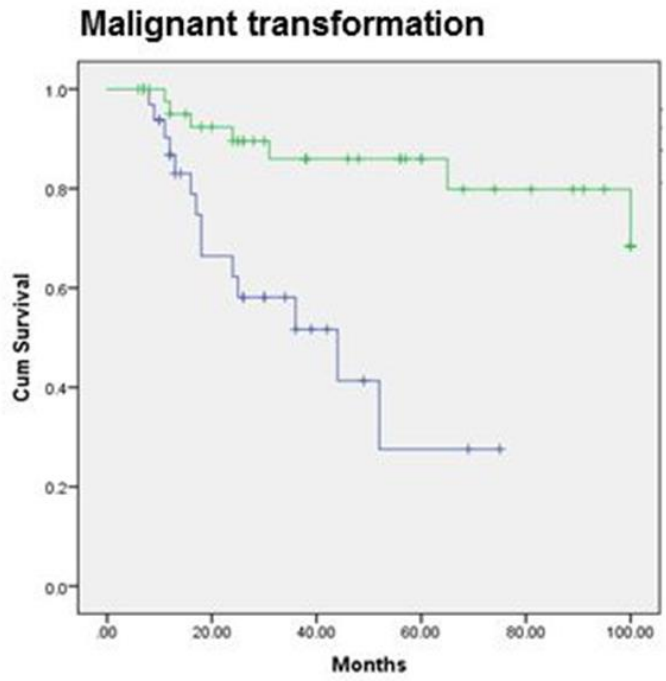

Figure 6.13: Kaplan Meier time to event analysis showing correlation between Notch1 expression and malignant transformation.

Colour index: blue line: no Notch1 expression (negative), green line: Notch1 expression (positive). Kaplan-Meier time to event analysis showed that cases of epithelial dysplasia that showed loss of Notch1 expression were more likely to undergo malignant transformation than cases that retained some Notch expression ($p<0.001$). Significance measured by Log Rank Mantel-Cox test.

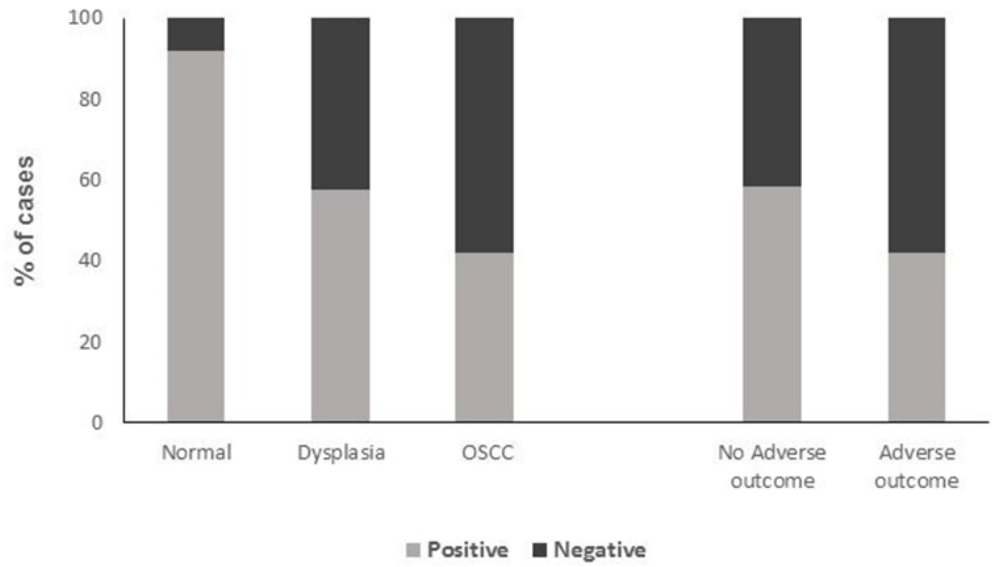

Figure 6.14: Comparison of the proportion of Notch1 positive vs. Notch1 negative samples for normal oral epithelium, oral epithelial dysplasia and OSCC. The OSCC were then stratified according to clinical outcome.

The percentage of Notch1 positive cases was significantly higher in normal epithelium compared to epithelial dysplasia and OSCC ($p<0.01$, $p<0.001$) respectively. There was no significant difference between epithelial dysplasia and OSCC ($p>0.05$). There was no significant difference in Notch1 positivity between the OSCC with no adverse clinical outcome and those cases with adverse clinical outcome (i.e. disease recurrence and death) ($p>0.05$). Significance measured by Mann-Whitney U test.

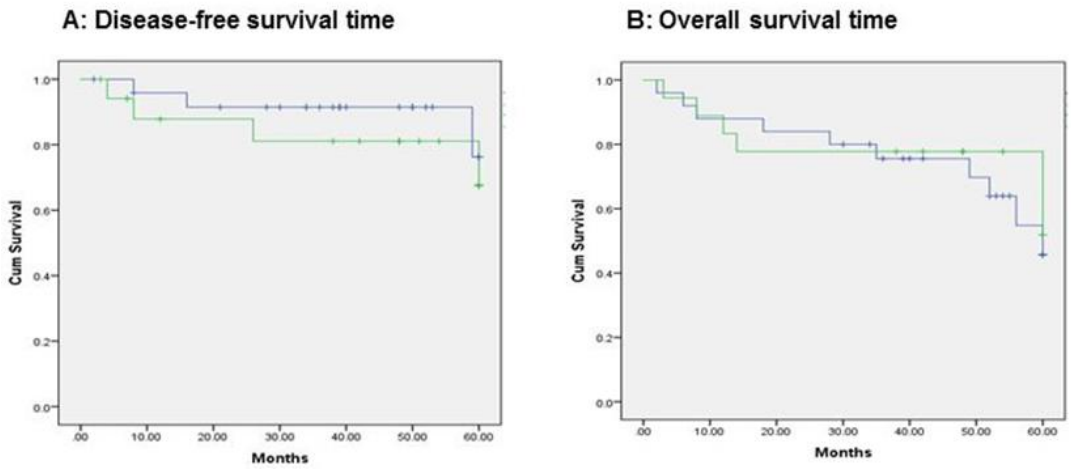

Figure 6.15: Kaplan Meier survival curve analysis showing correlation between Notch1 expression levels and clinical outcome in OSCC cases.

Colour index: blue line: no Notch1 expression (negative), green line: Notch1 expression (positive). Kaplan-Meier survival curve analysis showed that Notch1 expression in early-stage OSCC did not correlate with clinical outcome measured in terms of either **A)** disease-free survival ($p>0.05$) or **B)** overall survival ($p>0.05$). Significance measured by Log Rank Mantel-Cox test.

Chapter 7 **General discussion**

7.1 Introduction

Head and neck cancer accounts for 3% of all new cases of cancer in the UK (Cancer Research UK, 2014) with oral squamous cell carcinoma (OSCC) representing greater than 90% of all oral cancer types (Johnson et al. 2011). It is a major global healthcare problem (Jemal et al. 2011) with late diagnosis and formation of secondary tumours being the main causes for poor survival rates (McGurk et al. 2005; Tsou et al. 2007). Prevention, by elimination of risk factors, and early detection, by the identification of oral potentially malignant disorders and diagnosis of early stage OSCC are the keys to improving outcomes for patients (Amagasa 2011). Oral health care professionals are trained to recognized oral potentially malignant disorders, but assessing the risk of developing OSCC for individual patients is imprecise. Biopsy and histopathological examination is the most common method for risk assessment, however, this method lacks sensitivity (Mehrotra and Gupta 2011) and cannot accurately predict which lesion will progress to cancer (Kujan et al. 2009). There is a need to development new tools for diagnosis and treatment stratification. Recently, several molecular biomarkers have been identified, loss of heterozygosity of TP53 and EGFR but, as yet, none are validated as reliable biomarkers for oral cancer detection (Nylander et al. 2000; Varun et al. 2014). This study sought to examine the potential diagnostic utility/functional significance of each of the biomarkers evaluated; Epsin and Notch1. A subsidiary aim was to investigate the effect of Epsin on the Notch signalling.

7.2 Key findings

7.2.1 Expression of Epsin1 and 2 in OSCC cell lines and dysplasia and OSCC tissues.

Epsin1 and 2 proteins are upregulated in human breast adenocarcinoma and prostate cancer (Pawlowski et al. 2009; Tessneer et al. 2013). To date, the expression levels of these two adaptor proteins has not been examined in oral carcinogenesis.

Our analysis showed that the expression levels of Epsin1 mRNA and protein was high in the OSCC cell lines, however, there was no significant difference between expression in the OSCC cell lines and an immortalized normal oral keratinocyte line. Levels of Epsin2 were not detectable in the OSCC and the positive control LnCap cell line at both mRNA and protein levels, when analyzed by Western blot. This finding suggests that Epsin2 is not expressed in the oral keratinocytes or is not expressed at

a high enough level to be detected using these techniques. Alternatively, there may have been methodological issues preventing the detection of Epsin2, such as the primer design and the antibody used for Western blot. A polyclonal antibody that detects Epsin1 and 2 (ZZ3) showed high expression in all the cell lines including normal oral keratinocytes however based on the other techniques, the expression probably represents Epsin1 rather than Epsin2 protein levels. High levels of Epsin1 in our OSCC cell lines is comparable with a previous study that reported the overexpression of adapter proteins Epsin in cancer such as lung fibrosarcoma and breast adenocarcinoma (Pawlowski et al. 2009; Coon et al. 2010).

By contrast, the tissues samples in our study showed reduced levels of ZZ3 staining in oral epithelial dysplasia and OSCC samples versus normal oral epithelium, however, the differences were not significant. (Chapter 6). It is possible that dysregulation of adaptor proteins may result in impairment of receptor internalization and consequently prolong the signalling (Crosetto et al. 2005). For example, degradation of EGFR and termination of EGFR signalling is mediated by Epsin1 protein (Kazazic et al. 2009), hence, downregulation of Epsin1 inhibits EGFR internalization which is reported to be upregulated in OSCC (Grandis and Tweardy 1993). Reduced levels of Epsin1 and 2 in our samples is in contrast to the previous studies that show upregulation of Epsin1 and 2 in human prostate cancer tissues compared to normal prostate tissue (Tessneer et al. 2013) and colorectal adenocarcinoma tissues compared with normal colon tissues (Chang et al. 2015) . A possible explanations for this discrepancy is that these studies did not include OSCC tissues, and used specific Epsin1 and 2 antibodies. It is therefore difficult to compare our data with the results of the previous study meaningfully. On balance, our findings support the view that Epsin1 and 2 have low expression in the OSCC tissues, agreeing with the authors of a previous study reporting that Epsin1 and 2 proteins are predominantly expressed in normal brain tissue, but not other tissue (Chen et al. 1998; Rosenthal et al. 1999; Chen et al. 2009).

7.2.2 *Expression of Epsin3 in the OSCC cell lines and dysplasia and OSCC tissues.*

Our analysis show that Epsin3 expression is variable between OSCC cell lines and three of OSCC cell lines had consistently higher Epsin3 expression than normal oral keratinocytes across all methods (Chapter 3). Interestingly, Spradling et al. (2001) reported that mRNA isolated from chronic cutaneous wounds, basal cell carcinoma, and ulcerative colitis show high levels of Epsin3 mRNA expression, whereas Epsin3 mRNA was not detected in normal skin.

Up-regulation of Epsin3 *in vitro* has been documented previously in human lung non-small-cell carcinoma cell line, EKVX,(Wang et al. 2006). It was reported that Epsin3 has a role in the invasion and migration of cancer cells through interaction of Epsin N-terminal homology (ENTH) domain with N terminus of the RalBP1 (Ral-Binding Protein), which causes inhibition of GAPs (GTPase Activating Protein) and accumulation of GTPase. As a result the signal transduction is prolonged leading to increased cell migration (Coon et al. 2010).

Our analysis shows that Epsin3 protein had a heterogeneous expression profile in both oral epithelial dysplasia and OSCC tissue samples (Chapter 6). There was a significantly increased level of expression of Epsin3 protein relative to the normal epithelium, however, Epsin3 protein expression did not show a significant difference between oral epithelial dysplasia and OSCC. No correlation was identified between level of Epsin3 protein expression and clinical outcome in OSCC.

Our results also show a positive correlation between Epsin3 protein expression and grade of epithelial dysplasia (Chapter 6). Dysplasia with adverse outcomes had a significantly higher Epsin3 expression than dysplasia with no adverse outcome, and cases that underwent malignant transformation had significantly higher expression level. This suggests that Epsin3 may have the clinical utility as a biomarker for identifying cases of oral epithelial dysplasia at risk of undergoing malignant transformation. By contrast, a recent study showed downregulation of Epsin3 expression in gastric cancer tissue compared with normal tissue. The authors reported that Espin3 protein regulates apoptosis of oncogenic proteins by endocytosis process and therefore, downregulation of Epsin3 may induce apoptosis resistance (Mori et al. 2017). However, Epsin3 function may differ between tissue types and further work to investigate the functional role of Epsin3 is required.

7.2.3 Expression of Notch1 in the OSCC cell lines and dysplasia and OSCC tissues.

Notch signalling has a dual role in cancer. In OSCC, Notch signalling was reported to have both oncogenic and tumour suppressor functions. Notch signalling is reported to be mutated in the head and neck squamous cell carcinoma, and most of these mutations are found in the Notch1 receptor (Nowell and Radtke 2017).

This study examined the expression levels of Notch1 in OSCC cell lines and tissues. Our analysis showed upregulation of Notch1 mRNA in OSCC cell lines (Chapter 4). Previous *in vitro* studies have shown that Notch1 is up-regulated in OSCC (Hijioka et al. 2010; Zhang et al. 2011). However, Notch1 protein expression analyzed by Western blot and ICC showed differential expression levels in the OSCC cell lines (Chapter 4). Notch1 protein was not detected in H357 and BICR56 cell lines, consistent with previously reported Notch1 mutations in these cell lines, the mutations lead to production of a truncated protein (Mutvei et al. 2015; Yap et al. 2015). Loss-of-function mutation in Notch pathway members has been reported previously in head and neck squamous cell carcinoma (SCC) (Agrawal et al. 2011; Stransky et al. 2011), cutaneous SCC, lung SCC and oesophageal SCC (Wang et al. 2011; Pickering et al. 2014; Song et al. 2014b; South et al. 2014). Most of these mutations occur in the Notch receptor domain resulting in formation of non-functioning truncated proteins suggesting a tumour suppressor role of Notch signalling (Nowell and Radtke 2017).

Effective Notch signalling promotes cell cycle arrest and differentiation, which limits the risk of developing tumour initiating cells and cancer stem cells (Wilson and Radtke 2006; Koch and Radtke 2007). Active Notch signalling regulates maturation and stimulates differentiation of squamous epithelia (Blanpain and Fuchs 2009; Yugawa et al. 2010), and reduction of Notch signalling leading to impairment of differentiation of squamous cell carcinoma cells and increased activity and proliferation of stem cells (Lefort et al. 2007). Moreover, Notch signalling induce growth suppression and differentiation of keratinocytes in vitro through activation of p21, which promotes cell cycle arrest, and deletion of Notch1 in primary culture of keratinocytes results in loss of normal growth control and formation of epidermal hyperplasia and increased proliferation by inhibition of several differentiation markers (Rangarajan et al. 2001).Taken together, these results highlight the tumour suppressor function of Notch signalling in squamous cell carcinoma.

Our analysis revealed downregulation of Notch1 protein in oral epithelial dysplasia and OSCC tissue samples (Chapter 6). Dysplastic cases with adverse outcome have significantly lower Notch1 expression than cases with no adverse outcome, and cases that underwent malignant transformation showed lower expression than non-transformed cases. Interestingly, Sakamoto et al. (2012), reported that knockdown of Notch1 in epithelial cell culture result in formation of dysplastic stratified epithelium and an immunohistochemical study showed that downregulation of Notch1 led to abnormal differentiation of basal cells and formation of immature epithelium.

By contrast, elevated Notch1 in oral cancer has been demonstrated previously (Hijioka et al. 2010; Zhang et al. 2011) and upregulation of Notch1 expression found to be correlated with the invasiveness of OSCC (Yoshida et al. 2013), indicating the oncogenic role of Notch signalling in the OSCC

This discussion highlights the dual role of Notch signalling in head and neck SCC. The possible explanation of this behavior is that HNSCC is a heterogeneous disease, and the majority of OSCC are genetically unstable and have large copy number alteration with loss of heterozygosity, however genetically stable OSCC has been identified with minimal copy number of alteration and loss of heterozygosity (Hunter et al. 2006; Pickering et al. 2013). Consequently, Notch signalling might act as a tumour suppressor in genetically stable OSCC, while in genetically unstable OSCC Notch functions as oncogenic (Yap et al. 2015).

Active Notch signalling is responsible for stimulation of transcription of Hes1 and Hey1 genes (Meier-Stiegen et al. 2010). Our data confirm that Hes1 and Hey1 genes are overexpressed in some of OSCC cell lines (Hijioka et al. 2010), yet, Notch1 expression levels in the OSCC cell lines was negatively correlated with expression levels of Hes1 and Hey1 genes (Chapter 4). This is in contrast to the previous studies that show Notch1 expression is positively correlated with Hes1 and Hey1 expression in the OSCC cell lines (Sakamoto et al. 2012; Yoshida et al. 2013). Loss of Notch1 protein expression in two of OSCC cell lines, due to mutations, may have led to upregulation of Hes1 and Hey1 target genes through a negative feedback loop (Meier-Stiegen et al. 2010).

Present results showed that Notch1 protein expression in the OSCC cell lines correlated with expression level of Epsin3 protein (Chapter 4). Interestingly, a previous

study demonstrated that silencing of Epsin3 resulted in an inhibition of Notch signalling in human keratinocytes (Di Giacomo et al. 2013). However, knockdown of Epsin3 in the OSCC cell line did not significantly affect the expression levels of Notch1, this is likely to be due to incomplete reduction of Epsin3 expression in the OSCC cells. By contrast, in our experiments overexpression of Epsin3 in the OSCC cell lines resulted in a significant reduction in the expression levels of Notch1 in three of the OSCC cell lines. This result was comparable with our immunohistochemical analysis of oral cancer tissues which showed upregulation of Epsin3 and downregulation of Notch1 with significant correlation between the expression levels of both proteins in these tissue samples. In our model system, we propose that elevated levels of Epsin3 leads to internalization and ubiquitination of Notch1, which in turn results in a reduction of Notch1 receptors at the cell surface and loss of Notch signalling. As a consequence, Notch1 downstream targets will be suppressed leading to loss of control of cell proliferation, apoptosis and migration, which are all hallmarks of cancer. An alternative explanation is that when Epsin is overexpressed the internalization of ligand-receptor complexes at EGFR like repeat is inhibited (Itoh et al. 2001; Kazazic et al. 2009). Internalization of this complexes is an essential process for Notch activation (Wang and Struhl 2005) and therefore, disturbance or inhibition of internalization of ligand-receptor complexes may lead to inhibition of Notch signalling.

7.3 Concluding and future work

In conclusion, the work presented in this thesis has made novel contributions to the understanding of the role of Epsins in oral squamous cell carcinoma and their relationship with the Notch signalling pathway. Specifically, Epsin3 protein was found to be upregulated in OSCC cell lines, oral epithelial dysplasia tissue samples and OSCC tissue samples, suggesting that Epsin3 may have a critical role in oral carcinogenesis. In addition, the findings reveal that Notch1 protein was either reduced or completely lost during the development of oral cancer, supporting the hypothesis that Notch signalling has a tumour suppressor function. The results have also shown a positive correlation between expression levels of Epsin3 protein and Notch1 mRNA, and Epsin3 protein and Notch1 protein in OSCC cell lines.

Based on the present findings, areas of future research would include:

1. It would be interesting to sequence the Notch1 gene to determine the location and type of mutation in the H357 and BICR56 cell lines.
2. Results revealed that transient overexpression of Epsin3 in OSCC cell lines resulted in marked reduction in the expression levels of Notch1 (Chapter 5). It would be interesting to determine the functional significance of these molecular changes by examining cellular viability, proliferation, apoptosis, migration and invasion. Ideally, these experiments would require the generation of stable transfectants, possibly using a highly efficient Lentivirus transfection method. Cellular viability and proliferation could be measured using the MTT assay or, fluorescence-activated cell sorting (FACS) analysis gated for cell cycle analysis. Apoptosis could be assessed using Tunnel assay, Caspase 3, Annexin V, and M30. Cell migration could be assessed using scratch assays. Cell invasion could be assessed using organotypic models as previously described (Jenei et al. 2011).
3. It would also be interesting to investigate the effect of Epsin3 overexpression on cell behaviour *in vivo*. This could be assessed by using an orthotopic mouse model of tumourigenesis. Stably transfected cells with high levels of Epsin3 could be inoculated into the floor of the mouth of nude mice and tumour development, invasion and metastasis could be assessed as previously described **(Jenei et al. 2011)** Epsin3 transfectants would be compared with vector only controls and parental cell lines.

Appendix A Presentations and scientific meetings

Mar. 2016: Newcastle University, Postgraduate Cancer Conference – The Discovery Museum. (Oral presentation)

"Expression of Epsin3 in oral cancer"

Apr. 2016: British Society of oral and Maxillofacial Pathology. Annual Scientific Meeting, Edinburgh (Oral presentation).

"Expression of Epsin3 in oral cancer"

Sep. 2016: European Congress on Head and Neck Oncology, Budapest, Hungary (Poster and oral presentation)

"Expression of Epsins in oral cancer"

References

Adepoju O, Wong A, Kitajewski A, Tong K, Boscolo E, Bischoff J, Kitajewski J, Wu JK. 2011. Expression of HES and HEY genes in infantile hemangiomas. Vascular cell 3(1):19.

Agrawal N, Frederick MJ, Pickering CR, Bettegowda C, Chang K, Li RJ, Fakhry C, Xie T-X, Zhang J, Wang J. 2011. Exome sequencing of head and neck squamous cell carcinoma reveals inactivating mutations in NOTCH1. Science 333(6046):1154-1157.

Aguilar RC, Longhi SA, Shaw JD, Yeh L-Y, Kim S, Schön A, Freire E, Hsu A, McCormick WK, Watson HA, et al. 2006. Epsin N-terminal homology domains perform an essential function regulating Cdc42 through binding Cdc42 GTPase-activating proteins. Proceedings of the National Academy of Sciences of the United States of America 103(11):4116-4121.

Ahle S, Mann A, Eichelsbacher U, Ungewickell E. 1988. Structural relationships between clathrin assembly proteins from the Golgi and the plasma membrane. The European Molecular Biology Organization journal 7(4):919.

Alani RM, Münger K. 1998. Human papillomaviruses and associated malignancies. Journal of clinical oncology 16(1):330-337.

Allen TD, Rodriguez EM, Jones KD, Bishop JM. 2011. Activated Notch1 induces lung adenomas in mice and cooperates with Myc in the generation of lung adenocarcinoma. Cancer research 71(18):6010-6018.

Allsopp RC, Vaziri H, Patterson C, Goldstein S, Younglai EV, Futcher AB, Greider CW, Harley CB. 1992. Telomere length predicts replicative capacity of human fibroblasts. Proceedings of the National Academy of Sciences 89(21):10114-10118.

Amagasa T. 2011. Oral premalignant lesions. International Journal of Clinical Oncology 16(1):1-4.

Arduino PG, Carrozzo M, Chiecchio A, Broccoletti R, Tirone F, Borra E, Bertolusso G, Gandolfo S. 2008. Clinical and histopathologic independent prognostic factors in oral squamous cell carcinoma: a retrospective study of 334 cases. Journal of Oral and Maxillofacial Surgery 66(8):1570-1579.

Artavanis-Tsakonas S, Matsuno K, Fortini ME. 1995. Notch signaling. Science 268(5208):225-232.

Artavanis-Tsakonas S, Rand MD, Lake RJ. 1999. Notch signaling: cell fate control and signal integration in development. Science 284(5415):770-776.

Awasthi S, Singhal SS, Awasthi YC, Martin B, Woo J-H, Cunningham CC, Frankel AE. 2008. RLIP76 and Cancer. Clinical Cancer Research 14(14):4372-4377.

Bache KG, Slagsvold T, Stenmark H. 2004. Defective downregulation of receptor tyrosine kinases in cancer. The European Molecular Biology Organization journal 23(14):2707-2712.

Bailey AM, Posakony JW. 1995. Suppressor of hairless directly activates transcription of enhancer of split complex genes in response to Notch receptor activity. Genes & development 9(21):2609-2622.

Balint K, Xiao M, Pinnix CC, Soma A, Veres I, Juhasz I, Brown EJ, Capobianco AJ, Herlyn M, Liu Z-J. 2005. Activation of Notch1 signaling is required for β-catenin–mediated human primary melanoma progression. Journal of Clinical Investigation 115(11):3166-3176.

Barnes L. 2005. Pathology and genetics of head and neck tumours IARC.

Benmerah A, Lamaze C, Bègue B, Schmid SL, Dautry-Varsat A, Cerf-Bensussan N. 1998. AP-2/Eps15 interaction is required for receptor-mediated endocytosis. The Journal of cell biology 140(5):1055-1062.

Beverly LJ, Felsher DW, Capobianco AJ. 2005. Suppression of p53 by Notch in lymphomagenesis: implications for initiation and regression. Cancer Research 65(16):7159-7168.

Bianchi S, Dotti MT, Federico A. 2006. Physiology and pathology of notch signalling system. Journal of cellular physiology 207(2):300-308.

Birajdar SS, Radhika M, Paremala K, Sudhakara M, Soumya M, Gadivan M. 2014. Expression of Ki-67 in normal oral epithelium, leukoplakic oral epithelium and oral squamous cell carcinoma. Journal of oral and maxillofacial pathology 18(2):169-176.

Blanpain C, Fuchs E. 2009. Epidermal homeostasis: a balancing act of stem cells in the skin. Nature reviews Molecular cell biology 10(3):207-217.

Bodnar AG, Ouellette M, Frolkis M, Holt SE, Chiu C-P, Morin GB, Harley CB, Shay JW, Lichtsteiner S, Wright WE. 1998. Extension of life-span by introduction of telomerase into normal human cells. science 279(5349):349-352.

Borggrefe T, Oswald F. 2009. The Notch signaling pathway: transcriptional regulation at Notch target genes. Cellular and molecular life sciences 66(10):1631-1646.

Bray SJ. 2006. Notch signalling: a simple pathway becomes complex. Nature reviews Molecular cell biology 7(9):678-689.

Brou C, Logeat F, Gupta N, Bessia C, LeBail O, Doedens JR, Cumano A, Roux P, Black RA, Israël A. 2000. A novel proteolytic cleavage involved in Notch signaling: the role of the disintegrin-metalloprotease TACE. Molecular cell 5(2):207-216.

Cabay RJ, Morton TH, Epstein JB. 2007. Proliferative verrucous leukoplakia and its progression to oral carcinoma: a review of the literature. Journal of Oral Pathology & Medicine 36(5):255-261.

Cancer Research UK,. 2014. [accessed on July 29th, 2017]. http://www.cancerresearchuk.org/cancer-info/cancerstats/keyfacts/.

Capaccione KM, Pine SR. 2013. The Notch signaling pathway as a mediator of tumor survival. Carcinogenesis 34(7):1420-1430.

Caulin C, Nguyen T, Longley MA, Zhou Z, Wang X-J, Roop DR. 2004. Inducible activation of oncogenic K-ras results in tumor formation in the oral cavity. Cancer research 64(15):5054-5058.

Chang B, Tessneer KL, McManus J, Liu X, Hahn S, Pasula S, Wu H, Song H, Chen Y, Cai X, et al. 2015. Epsin is required for Dishevelled stability and Wnt signalling activation in colon cancer development. Nature Communications 6:6380.

Chen B, Dores MR, Grimsey N, Canto I, Barker BL, Trejo J. 2011. Adaptor protein complex-2 (AP-2) and epsin-1 mediate protease-activated receptor-1 internalization via phosphorylation-and ubiquitination-dependent sorting signals. Journal of Biological Chemistry 286(47):40760-40770.

Chen H, Fre S, Slepnev VI, Capua MR, Takei K, Butler MH, Di Fiore PP, De Camilli P. 1998. Epsin is an EH-domain-binding protein implicated in clathrin-mediated endocytosis. Nature 394(6695):793-797.

Chen H, De Camilli P. 2005. The association of epsin with ubiquitinated cargo along the endocytic pathway is negatively regulated by its interaction with clathrin. Proceedings of the National Academy of Sciences of the United States of America 102(8):2766-2771.

Chen H, Ko G, Zatti A, Di Giacomo G, Liu L, Raiteri E, Perucco E, Collesi C, Min W, Zeiss C. 2009. Embryonic arrest at midgestation and disruption of Notch signaling produced by the absence of both epsin 1 and epsin 2 in mice. Proceedings of the National Academy of Sciences 106(33):13838-13843.

Chen S-F, Yu F-S, Chang Y-C, Fu E, Nieh S, Lin Y-S. 2012. Role of human papillomavirus infection in carcinogenesis of oral squamous cell carcinoma with evidences of prognostic association. Journal of Oral Pathology & Medicine 41(1):9-15.

Chial H. 2008. Proto-oncogenes to oncogenes to cancer. Nature Education 1(1):33.

Chitnis A, Henrique D, Lewis J, Ish-Horowicz D, Kintner C. 1995. Primary neurogenesis in Xenopus embryos regulated by a homologue of the Drosophila neurogenic gene Delta. Nature 375(6534):761-766.

Collins BM, McCoy AJ, Kent HM, Evans PR, Owen DJ. 2002. Molecular architecture and functional model of the endocytic AP2 complex. Cell 109(4):523-535.

Conway DI, Stockton DL, Warnakulasuriya KAAS, Ogden G, Macpherson LMD. 2006. Incidence of oral and oropharyngeal cancer in United Kingdom (1990–1999)—recent trends and regional variation. Oral Oncology 42(6):586-592.

Coon BG, Burgner J, Camonis JH, Aguilar RC. 2010. The epsin family of endocytic adaptors promotes fibrosarcoma migration and invasion. Journal of biological chemistry 285(43):33073-33081.

Coon BG, DiRenzo DM, Konieczny SF, Aguilar RC. 2011. Epsins' novel role in cancer cell invasion. Communicative & Integrative Biology 4(1):95-97.

Counter CM, Avilion AA, LeFeuvre CE, Stewart NG, Greider CW, Harley CB, Bacchetti S. 1992. Telomere shortening associated with chromosome instability is arrested in immortal cells which express telomerase activity. European Molecular Biology Organization 11(5):1921-1929.

Cremona O, De Camilli P. 2001. Phosphoinositides in membrane traffic at the synapse. Journal of cell science 114(6):1041-1052.

Crosetto N, Tikkanen R, Dikic I. 2005. Oncogenic breakdowns in endocytic adaptor proteins. Federation of European Biochemical Societies letters 579(15):3231-3238.

D'Souza B, Miyamoto A, Weinmaster G. 2008. The many facets of Notch ligands. Oncogene 27(38):5148-5167.

Dahmane N, Sánchez P, Gitton Y, Palma V, Sun T, Beyna M, Weiner H, i Altaba AR. 2001. The Sonic Hedgehog-Gli pathway regulates dorsal brain growth and tumorigenesis. Development 128(24):5201-5212.

Davies M, Paterson IC, Stone A, Huntley S, Patel V, Curtis R, Matthews JB, Pring M, Eveson JW, Prime SS. 1999. Loss of differentiation of 4NQO‐induced rat malignant oral keratinocytes correlates with metastatic dissemination and is associated with a reduced cellular response to TGF‐pi and an altered receptor profile. Journal of oral pathology & medicine 28(9):397-405.

Di Giacomo G, Sala E, Ruggiero L, Cremona O. 2013. Epsins in Notch skin activation. Italian Journal of Anatomy and Embryology 118(2):72.

Diajil A, Robinson CM, Sloan P, Thomson PJ. 2013. Clinical outcome following oral potentially malignant disorder treatment: a 100 patient cohort study. International journal of dentistry 2013.

Dickson MA, Hahn WC, Ino Y, Ronfard V, Wu JY, Weinberg RA, Louis DN, Li FP, Rheinwald JG. 2000. Human keratinocytes that express hTERT and also bypass a p16INK4a-enforced mechanism that limits life span become immortal yet retain normal growth and differentiation characteristics. Molecular and cellular biology 20(4):1436-1447.

Donnem T, Andersen S, Al‐Shibli K, Al‐Saad S, Busund LT, Bremnes RM. 2010. Prognostic impact of Notch ligands and receptors in nonsmall cell lung cancer. Cancer 116(24):5676-5685.

Dost F, Le Cao K, Ford PJ, Ades C, Farah CS. 2014. Malignant transformation of oral epithelial dysplasia: a real-world evaluation of histopathologic grading. Oral surgery, oral medicine, oral pathology and oral radiology 117(3):343-352.

Dreher D, Junod AF. 1996. Role of oxygen free radicals in cancer development. European Journal of Cancer 32(1):30-38.

Duan L, Yao J, Wu X, Fan M. 2006. Growth suppression induced by Notch1 activation involves Wnt-beta-catenin down-regulation in human tongue carcinoma cells. Biology of the Cell 98(8):479-490.

Eagle H. 1955. Propagation in a fluid medium of a human epidermoid carcinoma, strain KB. Experimental Biology and Medicine 89(3):362-364.

Edbauer D, Winkler E, Regula JT, Pesold B, Steiner H, Haass C. 2003. Reconstitution of γ-secretase activity. Nature cell biology 5(5):486-488.

Edington KG, Loughran OP, Berry IJ, Parkinson EK. 1995. Cellular immortality: a late event in the progression of human squamous cell carcinoma of the head and neck associated with p53 alteration and a high frequency of allele loss. Molecular carcinogenesis 13(4):254-265.

Engin F, Bertin T, Ma O, Jiang MM, Wang L, Sutton RE, Donehower LA, Lee B. 2009. Notch signaling contributes to the pathogenesis of human osteosarcomas. Human molecular genetics 18(8):1464-1470.

Eversole LR, Sapp JP. 1993. C-myc oncoprotein expression in oral precancerous and early cancerous lesions. European Journal of Cancer Part B: Oral Oncology 29(2):131-135.

Farah CS, McCullough MJ. 2007. A pilot case control study on the efficacy of acetic acid wash and chemiluminescent illumination (ViziLite™) in the visualisation of oral mucosal white lesions. Oral oncology 43(8):820-824.

Farah CS, McCullough MJ. 2008. Oral cancer awareness for the general practitioner: new approaches to patient care. Australian dental journal 53(1):2-10.

Feng J, Funk WD, Wang S-S, Weinrich SL. 1995. The RNA component of human telomerase. science 269(5228):1236.

Fischer A, Gessler M. 2007. Delta–Notch—and then? Protein interactions and proposed modes of repression by Hes and Hey bHLH factors. Nucleic acids research 35(14):4583-4596.

Fleming RJ. 1998. Structural conservation of Notch receptors and ligands. Seminars in Cell & Developmental Biology 9(6):599-607.

Gaidarov I, Keen JH. 1999. Phosphoinositide-AP-2 interactions required for targeting to plasma membrane clathrin-coated pits. Journal of Cell Biology 146(4):755-764.

Gale N, Blagus R, El-Mofty SK, Helliwell T, Prasad ML, Sandison A, Volavšek M, Wenig BM, Zidar N, Cardesa A. 2014. Evaluation of a new grading system for laryngeal squamous intraepithelial lesions—a proposed unified classification. Histopathology 65(4):456-464.

Gerhard DS, Wagner L, Feingold EA, Shenmen CM, Grouse LH, Schuler G, Klein SL, Old S, Rasooly R, Good P. 2004. The status, quality, and expansion of the NIH full-length cDNA project: the Mammalian Gene Collection (MGC). Genome research 14(10B):2121-2127.

Gokulan R, Halagowder D. 2014. Expression pattern of Notch intracellular domain (NICD) and Hes-1 in preneoplastic and neoplastic human oral squamous epithelium: their correlation with c-Myc, clinicopathological factors and prognosis in Oral cancer. Medical Oncology 31(8):1-10.

Goldstein JL, Anderson RGW, Brown MS. 1979. Coated pits, coated vesicles, and receptor-mediated endocytosis. Nature 279(5715):679-685.

Grachtchouk M, Mo R, Yu S, Zhang X, Sasaki H, Hui C-c, Dlugosz AA. 2000. Basal cell carcinomas in mice overexpressing Gli2 in skin. Nature genetics 24(3):216-217.

Grandal MV, Madshus IH. 2008. Epidermal growth factor receptor and cancer: control of oncogenic signalling by endocytosis. Journal of cellular and molecular medicine 12(5a):1527-1534.

Grandis JR, Tweardy DJ. 1993. Elevated levels of transforming growth factor α and epidermal growth factor receptor messenger RNA are early markers of carcinogenesis in head and neck cancer. Cancer research 53(15):3579-3584.

Greenwald I. 1998. LIN-12/Notch signaling: lessons from worms and flies. Genes & development 12(12):1751-1762.

Hallahan AR, Pritchard JI, Hansen S, Benson M, Stoeck J, Hatton BA, Russell TL, Ellenbogen RG, Bernstein ID, Beachy PA. 2004. The SmoA1 mouse model reveals that notch signaling is critical for the growth and survival of sonic hedgehog-induced medulloblastomas. Cancer research 64(21):7794-7800.

Hartenstein AY, Rugendorff A, Tepass U, Hartenstein V. 1992. The function of the neurogenic genes during epithelial development in the Drosophila embryo. Development 116(4):1203-1220.

Hayward P, Brennan K, Sanders P, Balayo T, DasGupta R, Perrimon N, Arias AM. 2005. Notch modulates Wnt signalling by associating with Armadillo/β-catenin and regulating its transcriptional activity. Development 132(8):1819-1830.

Hecht SS. 2003. Tobacco carcinogens, their biomarkers and tobacco-induced cancer. Nature Reviews Cancer 3(10):733-744.

Hijioka H, Setoguchi T, Miyawaki A, Gao H, Ishida T, Komiya S, Nakamura N. 2010. Upregulation of Notch pathway molecules in oral squamous cell carcinoma. International journal of oncology 36(4):817-822.

Ho MW, Risk JM, Woolgar JA, Field EA, Field JK, Steele JC, Rajlawat BP, Triantafyllou A, Rogers SN, Lowe D, et al. 2012. The clinical determinants of malignant transformation in oral epithelial dysplasia. Oral Oncology 48(10):969-976.

Hoek K, Rimm DL, Williams KR, Zhao H, Ariyan S, Lin A, Kluger HM, Berger AJ, Cheng E, Trombetta ES. 2004. Expression profiling reveals novel pathways in the transformation of melanocytes to melanomas. Cancer research 64(15):5270-5282.

Hopfer O, Zwahlen D, Fey MF, Aebi S. 2005. The Notch pathway in ovarian carcinomas and adenomas. British journal of cancer 93(6):709-718.

Horoszewicz JS, Leong SS, Chu TM, Wajsman ZL, Friedman M, Papsidero L, Kim U, Chai LS, Kakati S, Arya SK, et al. 1980. The LNCaP cell line--a new model for studies on human prostatic carcinoma. Progress in Clinical and Biological Research 37:115-132.

Howie NM, Trigkas TK, Cruchley AT, Wertz PW, Squier CA, Williams DM. 2001. Short-term exposure to alcohol increases the permeability of human oral mucosa. Oral Diseases 7(6):349-354.

Huang F, Khvorova A, Marshall W, Sorkin A. 2004. Analysis of clathrin-mediated endocytosis of epidermal growth factor receptor by RNA interference. Journal of Biological Chemistry 279(16):16657-16661.

Humayun S, Prasad VR. 2011. Expression of p53 protein and ki-67 antigen in oral premalignant lesions and oral squamous cell carcinomas: An immunohistochemical study. National Journal of Maxillofacial Surgery 2(1):38-46.

Hunter KD, Parkinson EK, Harrison PR. 2005. Profiling early head and neck cancer. Nature Reviews Cancer 5(2):127-135.

Hunter KD, Thurlow JK, Fleming J, Drake PJH, Vass JK, Kalna G, Higham DJ, Herzyk P, MacDonald DG, Parkinson EK. 2006. Divergent routes to oral cancer. Cancer research 66(15):7405-7413.

Iso T, Kedes L, Hamamori Y. 2003. HES and HERP families: multiple effectors of the Notch signaling pathway. Journal of cellular physiology 194(3):237-255.

Itoh T, Koshiba S, Kigawa T, Kikuchi A, Yokoyama S, Takenawa T. 2001. Role of the ENTH domain in phosphatidylinositol-4, 5-bisphosphate binding and endocytosis. Science 291(5506):1047-1051.

Jackson KA, Helston RM, McKay JA, O'Neill ED, Mathers JC, Ford D. 2007. Splice variants of the human zinc transporter ZnT5 (SLC30A5) are differentially localized and regulated by zinc through transcription and mRNA stability. Journal of Biological Chemistry 282(14):10423-10431.

Jarriault S, Le Bail O, Hirsinger E, Pourquié O, Logeat F, Strong CF, Brou C, Seidah NG, Israël A. 1998. Delta-1 Activation of Notch-1 Signaling Results inHES-1 Transactivation. Molecular and Cellular Biology 18(12):7423-7431.

Jehn BM, Bielke W, Pear WS, Osborne BA. 1999. Cutting edge: protective effects of notch-1 on TCR-induced apoptosis. The Journal of Immunology 162(2):635-638.

Jemal A, Bray F, Center MM, Ferlay J, Ward E, Forman D. 2011. Global cancer statistics. CA: a cancer journal for clinicians 61(2):69-90.

Jenei V, Nystrom ML, Thomas GJ. 2011. Measuring invasion in an organotypic model. Methods in Molecular Biology 769:223-232.

Johnson NW, Jayasekara P, Amarasinghe AAHK. 2011. Squamous cell carcinoma and precursor lesions of the oral cavity: epidemiology and aetiology. Periodontology 2000 57(1):19-37.

Joo Y-H, Jung C-K, Kim M-S, Sun D-I. 2009. Relationship between vascular endothelial growth factor and Notch1 expression and lymphatic metastasis in tongue cancer. Otolaryngology--Head and Neck Surgery 140(4):512-518.

Kandoth C, McLellan MD, Vandin F, Ye K, Niu B, Lu C, Xie M, Zhang Q, McMichael JF, Wyczalkowski MA. 2013. Mutational landscape and significance across 12 major cancer types. Nature 502(7471):333-339.

Kanojia D, Vaidya MM. 2006. 4-Nitroquinoline-1-oxide induced experimental oral carcinogenesis. Oral oncology 42(7):655-667.

Kao H-Y, Ordentlich P, Koyano-Nakagawa N, Tang Z, Downes M, Kintner CR, Evans RM, Kadesch T. 1998. A histone deacetylase corepressor complex regulates the Notch signal transduction pathway. Genes & development 12(15):2269-2277.

Kazazic M, Bertelsen V, Pedersen KW, Vuong TT, Grandal MV, Rødland MS, Traub LM, Stang E, Madshus IH. 2009. Epsin 1 is Involved in Recruitment of Ubiquitinated EGF Receptors into Clathrin‐Coated Pits. Traffic 10(2):235-245.

Kerr MC, Teasdale RD. 2009. Defining macropinocytosis. Traffic 10(4):364-371.

Kim J, Sebring A, Esch JJ, Kraus ME. 1996. Integration of positional signals and regulation of wing formation and identity by Drosophila vestigial gene. Nature 382(6587):133.

Kimble J, Simpson P. 1997. The LIN-12/Notch signaling pathway and its regulation. Annual review of cell and developmental biology 13(1):333-361.

Kimura K, Satoh K, Kanno A, Hamada S, Hirota M, Endoh M, Masamune A, Shimosegawa T. 2007. Activation of Notch signaling in tumorigenesis of experimental pancreatic cancer induced by dimethylbenzanthracene in mice. Cancer science 98(2):155-162.

Kiyono T, Foster SA, Koop JI, McDougall JK, Galloway DA, Klingelhutz AJ. 1998. Both Rb/p16INK4a inactivation and telomerase activity are required to immortalize human epithelial cells. Nature 396(6706):84-88.

Ko G, Paradise S, Chen H, Graham M, Vecchi M, Bianchi F, Cremona O, Di Fiore PP, De Camilli P. 2010. Selective high-level expression of epsin 3 in gastric parietal cells, where it is localized at endocytic sites of apical canaliculi. Proceedings of the National Academy of Sciences 107(50):21511-21516.

Koch U, Radtke F. 2007. Notch and cancer: a double-edged sword. Cellular and Molecular Life Sciences 64(21):2746-2762.

Kopan R. 2002. Notch: a membrane-bound transcription factor. Journal of cell science 115(6):1095-1097.

Krause CJ, Carey TE, Ott RW, Hurbis C, McClatchey KD, Regezi JA. 1981. Human squamous cell carcinoma: Establishment and characterization of new permanent cell lines. Archives of Otolaryngology 107(11):703-710.

Krauss M, Kinuta M, Wenk MR, De Camilli P, Takei K, Haucke V. 2003. ARF6 stimulates clathrin/AP-2 recruitment to synaptic membranes by activating phosphatidylinositol phosphate kinase type Iγ. The Journal of cell biology 162(1):113-124.

Kujan O, Oliver RJ, Khattab A, Roberts SA, Thakker N, Sloan P. 2006. Evaluation of a new binary system of grading oral epithelial dysplasia for prediction of malignant transformation. Oral oncology 42(10):987-993.

Kujan O, Glenny AM, Oliver R, Thakker N, Sloan P. 2009. Screening programmes for the early detection and prevention of oral cancer. Australian Dental Journal 54(2):170-172.

L.H. Sobin MKGaCW. 2009 TNM Classification of Malignant Tumours. Wiley-Blackwell and Union for International Cancer Control. Seventh Edition. ed.

Lacy PD, Piccirillo JF, Merritt MG, Zequeira MR. 2000. Head and neck squamous cell carcinoma: better to be young. Otolaryngology--Head and Neck Surgery 122(2):253-258.

Lai EC. 2004. Notch signaling: control of cell communication and cell fate. Development 131(5):965-973.

Langdon JD, Henk JM. 1995. Classification and staging. Malignant Tumours of the Mouth, Jaws and Salivary Glands 29(3):36-44.

Le Borgne R, Schweisguth F. 2003. Notch signaling: endocytosis makes delta signal better. Current biology 13(7):R273-R275.

Le Borgne R, Bardin A, Schweisguth F. 2005. The roles of receptor and ligand endocytosis in regulating Notch signaling. Development 132(8):1751-1762.

Lee SH, Hong HS, Liu ZX, Kim RH, Kang MK, Park N-H, Shin K-H. 2012. TNFα enhances cancer stem cell-like phenotype via Notch-Hes1 activation in oral squamous cell carcinoma cells. Biochemical and biophysical research communications 424(1):58-64.

Leemans CR, Braakhuis BJM, Brakenhoff RH. 2011. The molecular biology of head and neck cancer. Nature Reviews Cancer 11(1):9-22.

Leethanakul C, Patel V, Gillespie J, Pallente M, Ensley JF, Koontongkaew S, Liotta LA, Emmert-Buck M, Gutkind JS. 2000. Distinct pattern of expression of differentiation and growth-related genes in squamous cell carcinomas of the head and neck revealed by the use of laser capture microdissection and cDNA arrays. Oncogene 19(28):3220-3224.

Lefort K, Mandinova A, Ostano P, Kolev V, Calpini V, Kolfschoten I, Devgan V, Lieb J, Raffoul W, Hohl D. 2007. Notch1 is a p53 target gene involved in human keratinocyte tumor suppression through negative regulation of ROCK1/2 and MRCKα kinases. Genes & development 21(5):562-577.

Leong KG, Karsan A. 2006. Recent insights into the role of Notch signaling in tumorigenesis. Blood 107(6):2223-2233.

Liao S, Xia J, Chen Z, Zhang S, Ahmad A, Miele L, Sarkar FH, Wang Z. 2011. Inhibitory effect of curcumin on oral carcinoma CAL‐27 cells via suppression of Notch‐1 and NF‐κB signaling pathways. Journal of Cellular Biochemistry 112(4):1055-1065.

Liu MC, Gelmann EP. 2002. P53 gene mutations: Case study of a clinical marker for solid tumors. Seminars in Oncology 29(3):246-257.

Liu Z-J, Xiao M, Balint K, Smalley KSM, Brafford P, Qiu R, Pinnix CC, Li X, Herlyn M. 2006. Notch1 signaling promotes primary melanoma progression by activating mitogen-activated protein kinase/phosphatidylinositol 3-kinase-Akt pathways and up-regulating N-cadherin expression. Cancer research 66(8):4182-4190.

Livak KJ, Schmittgen TD. 2001. Analysis of Relative Gene Expression Data Using Real-Time Quantitative PCR and the 2−ΔΔCT Method. Methods 25(4):402-408.

Lowell S, Jones P, Le Roux I, Dunne J, Watt FM. 2000. Stimulation of human epidermal differentiation by Delta–Notch signalling at the boundaries of stem-cell clusters. Current Biology 10(9):491-500.

Lucenteforte E, Garavello W, Bosetti C, La Vecchia C. 2009. Dietary factors and oral and pharyngeal cancer risk. Oral Oncology 45(6):461-467.

Mahale P, Sturgis EM, Tweardy DJ, Ariza-Heredia EJ, Torres HA. 2016. Association between hepatitis C virus and head and neck cancers. Journal of the National Cancer Institute 108(8):djw035.

McCullough MJ, Prasad G, Farah CS. 2010. Oral mucosal malignancy and potentially malignant lesions: an update on the epidemiology, risk factors, diagnosis and management. Australian dental journal 55 Suppl 1:61-65.

McGurk M, Chan C, Jones J, O'regan E, Sherriff M. 2005. Delay in diagnosis and its effect on outcome in head and neck cancer. British Journal of Oral and Maxillofacial Surgery 43(4):281-284.

McMahon HT, Boucrot E. 2011. Molecular mechanism and physiological functions of clathrin-mediated endocytosis. Nature reviews Molecular cell biology 12(8):517-533.

Mehanna HM, Rattay T, Smith J, McConkey CC. 2009. Treatment and follow‐up of oral dysplasia—a systematic review and meta‐analysis. Head & neck 31(12):1600-1609.

Mehrotra R, Gupta A, Singh M, Ibrahim R. 2006. Application of cytology and molecular biology in diagnosing premalignant or malignant oral lesions. Molecular cancer 5(1):11.

Mehrotra R, Gupta D. 2011. Exciting new advances in oral cancer diagnosis: avenues to early detection. Head & Neck Oncology 3(1):1-9.

Meier-Stiegen F, Schwanbeck R, Bernoth K, Martini S, Hieronymus T, Ruau D, Zenke M, Just U. 2010. Activated Notch1 target genes during embryonic cell differentiation depend on the cellular context and include lineage determinants and inhibitors. Public Library of Science One 5(7):e11481.

Mellman I. 1996. Endocytosis and molecular sorting. Annual review of cell and developmental biology 12(1):575-625.

Mellman I, Yarden Y. 2013. Endocytosis and cancer. Cold Spring Harbor perspectives in biology 5(12):a016949.

Mendes SF, Ramos GdO, Rivero ERC, Modolo F, Grando LJ, Meurer MI. 2011. Techniques for precancerous lesion diagnosis. Journal of oncology 2011.

Meyerson M, Counter CM, Eaton EN, Ellisen LW, Steiner P, Caddle SD, Ziaugra L, Beijersbergen RL, Davidoff MJ, Liu Q. 1997. hEST2, the putative human telomerase catalytic subunit gene, is up-regulated in tumor cells and during immortalization. cell 90(4):785-795.

Miller CS, Johnstone BM. 2001. Human papillomavirus as a risk factor for oral squamous cell carcinoma: a meta-analysis, 1982-1997. Oral Surgery, Oral Medicine, Oral Pathology, Oral Radiology, and Endodontology 91(6):622-635.

Miyamoto Y, Maitra A, Ghosh B, Zechner U, Argani P, Iacobuzio-Donahue CA, Sriuranpong V, Iso T, Meszoely IM, Wolfe MS. 2003. Notch mediates TGFα-induced changes in epithelial differentiation during pancreatic tumorigenesis. Cancer cell 3(6):565-576.

Moore AE, Sabachewsky L, Toolan HW. 1955. Culture characteristics of four permanent lines of human cancer cells. Cancer Research 15(9):598-602.

Moretti J, Brou C. 2013. Ubiquitinations in the notch signaling pathway. International journal of molecular sciences 14(3):6359-6381.

Mori J, Tanikawa C, Ohnishi N, Funauchi Y, Toyoshima O, Ueda K, Matsuda K. 2017. EPSIN 3, a novel p53 target, regulates the apoptotic pathway and gastric carcinogenesis. Neoplasia 19(3):185-195.

Morinaka K, Koyama S, Nakashima S, Hinoi T, Okawa K, Iwamatsu A, Kikuchi A. 1999. Epsin binds to the EH domain of POB1 and regulates receptor-mediated endocytosis. Oncogene 18(43):5915–5922

Mukherjee D, Coon BG, Edwards DF, Hanna CB, Longhi SA, McCaffery JM, Wendland B, Retegui LA, Bi E, Aguilar RC. 2009. The yeast endocytic protein Epsin 2 functions in a cell-division signaling pathway. Journal of cell science 122(14):2453-2463.

Mukherjee S, Ghosh RN, Maxfield FR. 1997. Endocytosis. Physiological reviews 77(3):759-803.

Müller S. 2017. Update from the 4th Edition of the World Health Organization of Head and Neck Tumours: Tumours of the Oral Cavity and Mobile Tongue. Head and Neck Pathology 11(1):33-40.

Mumm JS, Kopan R. 2000. Notch signaling: from the outside in. Developmental biology 228(2):151-165.

Munro S. 2002. Organelle identity and the targeting of peripheral membrane proteins. Current opinion in cell biology 14(4):506-514.

Mutvei AP, Fredlund E, Lendahl U. 2015. Frequency and distribution of Notch mutations in tumor cell lines. BioMed Central Cancer 15(1):311.

Naik VG, Adhyaru P, Gudigenavar A. 2015. Tumor suppressor genes in oral cancer. Clinical Cancer Investigation Journal 4(6):697-702.

Navone R, Burlo P, Pich A, Pentenero M, Broccoletti R, Marsico A, Gandolfo S. 2007. The impact of liquid‐based oral cytology on the diagnosis of oral squamous dysplasia and carcinoma. Cytopathology 18(6):356-360.

Navone R. 2009. Cytology of the oral cavity: a re-evaluation. Pathologica 101(1):6-8.

Nguyen B-C, Lefort K, Mandinova A, Antonini D, Devgan V, Della Gatta G, Koster MI, Zhang Z, Wang J, di Vignano AT. 2006. Cross-regulation between Notch and p63 in keratinocyte commitment to differentiation. Genes & development 20(8):1028-1042.

Nichols JT, Miyamoto A, Weinmaster G. 2007. Notch signaling–constantly on the move. Traffic 8(8):959-969.

Nickoloff BJ, Hendrix MJC, Pollock PM, Trent JM, Miele L, Qin J-Z. 2005. Notch and NOXA-Related Pathways in Melanoma Cells. Journal of Investigative Dermatology Symposium Proceedings 10(2):95-104.

Nicolas M, Wolfer A, Raj K, Kummer JA, Mill P, van Noort M, Hui C-c, Clevers H, Dotto GP, Radtke F. 2003. Notch1 functions as a tumor suppressor in mouse skin. Nature genetics 33(3):416-421.

Nowell CS, Radtke F. 2017. Notch as a tumour suppressor. Nature Reviews Cancer 17(3):145-159.

Nylander K, Dabelsteen E, Hall PA. 2000. The p53 molecule and its prognostic role in squamous cell carcinomas of the head and neck. Journal of oral pathology & medicine 29(9):413-425.

Oswald F, Winkler M, Cao Y, Astrahantseff K, Bourteele S, Knöchel W, Borggrefe T. 2005. RBP-Jκ/SHARP recruits CtIP/CtBP corepressors to silence Notch target genes. Molecular and cellular biology 25(23):10379-10390.

Overstreet E, Fitch E, Fischer JA. 2004. Fat facets and Liquid facets promote Delta endocytosis and Delta signaling in the signaling cells. Development 131(21):5355-5366.

Owen DJ, Collins BM, Evans PR. 2004. Adaptors for clathrin coats: structure and function. Annual Review of Cell and Developmental Biology. 20:153-191.

Parks AL, Huppert SS, Muskavitch MAT. 1997. The dynamics of neurogenic signalling underlying bristle development in Drosophila melanogaster. Mechanisms of development 63(1):61-74.

Parks AL, Klueg KM, Stout JR, Muskavitch MA. 2000. Ligand endocytosis drives receptor dissociation and activation in the Notch pathway. Development 127(7):1373-1385.

Pasula S, Cai X, Dong Y, Messa M, McManus J, Chang B, Liu X, Zhu H, Mansat RS, Yoon SJ, et al. 2012. Endothelial epsin deficiency decreases tumor growth by enhancing VEGF signaling. Journal of Clinical Investigation 122(12):4424-4438.

Patton LL, Epstein JB, Kerr AR. 2008. Adjunctive techniques for oral cancer examination and lesion diagnosis a systematic review of the literature. The Journal of the American Dental Association 139(7):896-905.

Pawlowski KM, Król M, Majewska A, Badowska-Kozakiewicz A, Mol JA, Malicka E, Motyl T. 2009. Comparison of cellular and tissue transcriptional profiles in canine mammary tumor. Journal of physiology and pharmacology 60(Suppl. 1):85-94.

Pearse BMF, Robinson MS. 1990. Clathrin, adaptors, and sorting. Annual review of cell biology 6(1):151-171.

Pece S, Serresi M, Santolini E, Capra M, Hulleman E, Galimberti V, Zurrida S, Maisonneuve P, Viale G, Di Fiore PP. 2004. Loss of negative regulation by Numb over Notch is relevant to human breast carcinogenesis. The Journal of cell biology 167(2):215-221.

Perez-Sayans M, Somoza-Martin JM, Barros-Angueira F, Reboiras-Lopez MD, Gándara Rey JM, García-García A. 2009. Genetic and molecular alterations associated with oral squamous cell cancer (Review). Oncology reports 22(6):1277.

Pickering CR, Zhang J, Yoo SY, Bengtsson L, Moorthy S, Neskey DM, Zhao M, Alves MVO, Chang K, Drummond J. 2013. Integrative genomic characterization of oral squamous cell carcinoma identifies frequent somatic drivers. Cancer discovery 3(7):770-781.

Pickering CR, Zhou JH, Lee JJ, Drummond JA, Peng SA, Saade RE, Tsai KY, Curry J, Tetzlaff MT, Lai SY. 2014. Mutational landscape of aggressive cutaneous squamous cell carcinoma. Clinical cancer research 20(24):6582-6592.

Politi K, Feirt N, Kitajewski J. 2004. Notch in mammary gland development and breast cancer. Seminars in Cancer Biology 14(5):341-347.

Polo S, Sigismund S, Faretta M, Guidi M, Capua MR, Bossi G, Chen H, De Camilli P, Di Fiore PP. 2002. A single motif responsible for ubiquitin recognition and monoubiquitination in endocytic proteins. Nature 416(6879):451-455.

Prime SS, Nixon SVR, Crane IJ, Stone A, Matthews JB, Maitland NJ, Remnant L, Powell SK, Game SM, Scully C. 1990. The behaviour of human oral squamous cell carcinoma in cell culture. The Journal of Pathology 160(3):259-269.

Prime SS, Eveson JW, Stone AM, Huntley SP, Davies M, Paterson IC, Robinson CM. 2004. Metastatic dissemination of human malignant oral keratinocyte cell lines following orthotopic transplantation reflects response to TGF - β 1. The Journal of pathology 203(4):927-932.

Proweller A, Tu L, Lepore JJ, Cheng L, Lu MM, Seykora J, Millar SE, Pear WS, Parmacek MS. 2006. Impaired notch signaling promotes de novo squamous cell carcinoma formation. Cancer research 66(15):7438-7444.

Rahman HNA, Wu H, Dong Y, Pasula S, Wen A, Sun Y, Brophy ML, Tessneer KL, Cai X, McManus J. 2016. Selective Targeting of a Novel Epsin–VEGFR2 Interaction Promotes VEGF-Mediated Angiogenesis. Circulation research 118(6):957-969.

Rangarajan A, Talora C, Okuyama R, Nicolas M, Mammucari C, Oh H, Aster JC, Krishna S, Metzger D, Chambon P. 2001. Notch signaling is a direct determinant of keratinocyte growth arrest and entry into differentiation. The EMBO journal 20(13):3427-3436.

Reed AL, Califano J, Cairns P, Westra WH, Jones RM, Koch W, Ahrendt S, Eby Y, Sewell D, Nawroz H. 1996. High frequency of p16 (CDKN2/MTS-1/INK4A) inactivation in head and neck squamous cell carcinoma. Cancer research 56(16):3630-3633.

Reedijk M, Odorcic S, Chang L, Zhang H, Miller N, McCready DR, Lockwood G, Egan SE. 2005. High-level coexpression of JAG1 and NOTCH1 is observed in human breast cancer and is associated with poor overall survival. Cancer research 65(18):8530-8537.

Robinson MS, Bonifacino JS. 2001. Adaptor-related proteins. Current opinion in cell biology 13(4):444-453.

Robinson MS. 2004. Adaptable adaptors for coated vesicles. Trends in Cell Biology 14(4):167-174.

Rosenthal JA, Chen H, Slepnev VI, Pellegrini L, Salcini AE, Di Fiore PP, De Camilli P. 1999. The epsins define a family of proteins that interact with components of the clathrin coat and contain a new protein module. Journal of Biological Chemistry 274(48):33959-33965.

Roy M, Pear WS, Aster JC. 2007. The multifaceted role of Notch in cancer. Current opinion in genetics & development 17(1):52-59.

Sakamoto K, Fujii T, Kawachi H, Miki Y, Omura K, Morita K-i, Kayamori K, Katsube K-i, Yamaguchi A. 2012. Reduction of NOTCH1 expression pertains to maturation abnormalities of keratinocytes in squamous neoplasms. Laboratory Investigation 92(5):688-702.

Santagata S, Demichelis F, Riva A, Varambally S, Hofer MD, Kutok JL, Kim R, Tang J, Montie JE, Chinnaiyan AM, et al. 2004. JAGGED1 Expression Is Associated with Prostate Cancer Metastasis and Recurrence. Cancer Research 64(19):6854-6857.

Scheifele C, Schmidt-Westhausen A-M, Dietrich T, Reichart PA. 2004. The sensitivity and specificity of the OralCDx technique: evaluation of 103 cases. Oral oncology 40(8):824-828.

Scita G, Di Fiore PP. 2010. The endocytic matrix. Nature 463(7280):464-473.

Scully C, Bagan JV. 2009. Oral squamous cell carcinoma: overview of current understanding of aetiopathogenesis and clinical implications. Oral Diseases 15(6):388-399.

Sen A, Madhivanan K, Mukherjee D, Aguilar RC. 2012. The epsin protein family: coordinators of endocytosis and signaling. Biomolecular concepts 3(2):117-126.

Shelly LL, Fuchs C, Miele L. 1999. Notch‐1 inhibits apoptosis in murine erythroleukemia cells and is necessary for differentiation induced by hybrid polar compounds. Journal of cellular biochemistry 73(2):164-175.

Shih SC, Katzmann DJ, Schnell JD, Sutanto M, Emr SD, Hicke L. 2002. Epsins and Vps27p/Hrs contain ubiquitin-binding domains that function in receptor endocytosis. Nature cell biology 4(5):389-393.

Sigismund S, Woelk T, Puri C, Maspero E, Tacchetti C, Transidico P, Di Fiore PP, Polo S. 2005. Clathrin-independent endocytosis of ubiquitinated cargos. Proceedings of the National Academy of Sciences of the United States of America 102(8):2760-2765.

Sigismund S, Confalonieri S, Ciliberto A, Polo S, Scita G, Di Fiore PP. 2012. Endocytosis and signaling: cell logistics shape the eukaryotic cell plan. Physiological reviews 92(1):273-366.

Simonsen A, Wurmser AE, Emr SD, Stenmark H. 2001. The role of phosphoinositides in membrane transport. Current opinion in cell biology 13(4):485-492.

Smith JR, Pereira-Smith OM. 1996. Replicative Senescence: Implications for in Vivo Aging and Tumor Suppression. Science 273(5271):63-67.

Smith SC, Oxford G, Baras AS, Owens C, Havaleshko D, Brautigan DL, Safo MK, Theodorescu D. 2007. Expression of Ral GTPases, Their Effectors, and Activators in Human Bladder Cancer. Clinical Cancer Research 13(13):3803-3813.

Song X, Xia R, Li J, Long Z, Ren H, Chen W, Mao L. 2014a. Common and complex Notch1 mutations in Chinese oral squamous cell carcinoma. Clinical cancer research 20(3):701-710.

Song Y, Li L, Ou Y, Gao Z, Li E, Li X, Zhang W, Wang J, Xu L, Zhou Y. 2014b. Identification of genomic alterations in oesophageal squamous cell cancer. Nature 509(7498):91-95.

Sorkin A, Von Zastrow M. 2009. Endocytosis and signalling: intertwining molecular networks. Nature reviews Molecular cell biology 10(9):609-622.

South AP, Purdie KJ, Watt SA, Haldenby S, Den Breems NY, Dimon M, Arron ST, Kluk MJ, Aster JC, McHugh A. 2014. NOTCH1 mutations occur early during cutaneous squamous cell carcinogenesis. Journal of Investigative Dermatology 134(10):2630-2638.

Spradling KD, McDaniel AE, Lohi J, Pilcher BK. 2001. Epsin 3 is a novel extracellular matrix-induced transcript specific to wounded epithelia. Journal of Biological Chemistry 276(31):29257-29267.

Stransky N, Egloff AM, Tward AD, Kostic AD, Cibulskis K, Sivachenko A, Kryukov GV, Lawrence MS, Sougnez C, McKenna A. 2011. The mutational landscape of head and neck squamous cell carcinoma. Science 333(6046):1157-1160.

Stylianou S, Clarke RB, Brennan K. 2006. Aberrant activation of notch signaling in human breast cancer. Cancer research 66(3):1517-1525.

Sun W, Gaykalova DA, Ochs MF, Mambo E, Arnaoutakis D, Liu Y, Loyo M, Agrawal N, Howard J, Li R, et al. 2014. Activation of the NOTCH pathway in head and neck cancer. Cancer Research 74(4):1091-1104.

Swanson JA. 2008. Shaping cups into phagosomes and macropinosomes. Nature reviews Molecular cell biology 9(8):639-649.

Tessneer KL, Pasula S, Cai X, Dong Y, Liu X, Yu L, Hahn S, McManus J, Chen Y, Chang B. 2013. Endocytic adaptor protein epsin is elevated in prostate cancer and required for cancer progression. ISRN oncology 2013.

Tessneer KL, Pasula S, Cai X, Dong Y, McManus J, Liu X, Yu L, Hahn S, Chang B, Chen Y. 2014. Genetic reduction of vascular endothelial growth factor receptor 2 rescues aberrant angiogenesis caused by epsin deficiency. Arteriosclerosis, thrombosis, and vascular biology 34(2):331-337.

Traub LM. 2003. Sorting it out AP-2 and alternate clathrin adaptors in endocytic cargo selection. The Journal of cell biology 163(2):203-208.

Tsou Y-A, Hua C-H, Tseng H-C, Lin M-H, Tsai M-H. 2007. Survival study and treatment strategy for second primary malignancies in patients with head and neck squamous cell carcinoma and nasopharyngeal carcinoma. Acta oto-laryngologica 127(6):651-657.

van der Waal I, Axéll T. 2002. Oral leukoplakia: a proposal for uniform reporting. Oral Oncology 38(6):521-526.

van der Waal I. 2009. Potentially malignant disorders of the oral and oropharyngeal mucosa; terminology, classification and present concepts of management. Oral Oncology 45(4–5):317-323.

Varun BR, Ranganathan K, Rao UK, Joshua E. 2014. Immunohistochemical detection of p53 and p63 in oral squamous cell carcinoma, oral leukoplakia, and oral submucous fibrosis. Journal of investigative and clinical dentistry 5(3):214-219.

Wallberg AE, Pedersen K, Lendahl U, Roeder RG. 2002. p300 and PCAF act cooperatively to mediate transcriptional activation from chromatin templates by notch intracellular domains in vitro. Molecular and cellular biology 22(22):7812-7819.

Wang NJ, Sanborn Z, Arnett KL, Bayston LJ, Liao W, Proby CM, Leigh IM, Collisson EA, Gordon PB, Jakkula L, et al. 2011. Loss-of-function mutations in Notch receptors in cutaneous and lung squamous cell carcinoma. Proceeding of the National Academy of Science U S A 108(43):17761-17766.

Wang W, Struhl G. 2004. Drosophila Epsin mediates a select endocytic pathway that DSL ligands must enter to activate Notch. Development 131(21):5367-5380.

Wang W, Struhl G. 2005. Distinct roles for Mind bomb, Neuralized and Epsin in mediating DSL endocytosis and signaling in Drosophila. Development 132(12):2883-2894.

Wang Y, Dai Z, Sadee W, Hancock WS. 2006. A Pharmacoproteomics Study of the Cancer Cell Line EKVX Using Capillary-LC/MS/MS. Molecular Pharmaceutics 3(5):566-578.

Wang YJ, Wang J, Sun HQ, Martinez M, Sun YX, Macia E, Kirchhausen T, Albanesi JP, Roth MG, Yin HL. 2003. Phosphatidylinositol 4 phosphate regulates targeting of clathrin adaptor AP-1 complexes to the Golgi. Cell 114(3):299-310.

Warnakulasuriya KAAS, Johnson NW. 1996. Sensitivity and specificity of OraScan® toluidine blue mouthrinse in the detection of oral cancer and precancer. Journal of Oral Pathology & Medicine 25(3):97-103.

Warnakulasuriya S, Reibel J, Bouquot J, Dabelsteen E. 2008. Oral epithelial dysplasia classification systems: Predictive value, utility, weaknesses and scope for improvement. Journal of Oral Pathology and Medicine 37(3):127-133.

Warnakulasuriya S. 2009. Global epidemiology of oral and oropharyngeal cancer. Oral oncology 45(4):309-316.

Warnakulasuriya S, Kovacevic T, Madden P, Coupland VH, Sperandio M, Odell E, Møller H. 2011. Factors predicting malignant transformation in oral potentially malignant disorders among patients accrued over a 10 - year period in South East England. Journal of oral pathology & medicine 40(9):677-683.

Weinmaster G. 1997. The ins and outs of notch signaling. Molecular and Cellular Neuroscience 9(2):91-102.

Weinmaster G, Fischer JA. 2011. Notch ligand ubiquitylation: what is it good for? Developmental cell 21(1):134-144.

Wendland B. 2002. Epsins: adaptors in endocytosis? Nature Reviews Molecular Cell Biology 3(12):971-977.

Weng AP, Ferrando AA, Lee W, Morris JP, Silverman LB, Sanchez-Irizarry C, Blacklow SC, Look AT, Aster JC. 2004. Activating mutations of NOTCH1 in human T cell acute lymphoblastic leukemia. Science 306(5694):269-271.

West MA, Bright NA, Robinson MS. 1997. The role of ADP-ribosylation factor and phospholipase D in adaptor recruitment. Journal of Cell Biology 138(6):1239-1254.

Wilson A, Radtke F. 2006. Multiple functions of Notch signaling in self - renewing organs and cancer. Federation of European Biochemical Societies letters 580(12):2860-2868.

Wong DTW. 1987. Amplification of the c-erb B1 oncogene in chemically-induced oral carcinomas. Carcinogenesis 8(12):1963-1965.

Wong PC, Zheng H, Chen H, Becher MW, Sirinathsinghji DJS, Trumbauer ME, Chen HY, Price DL, Van der Ploeg LHT, Sisodia SS. 1997. Presenilin 1 is required for Notch 1 and Dll1 expression in the paraxial mesoderm. Nature 387(6630):288-292.

Wu J-Y, Yi C, Chung H-R, Wang D-J, Chang W-C, Lee S-Y, Lin C-T, Yang Y-C, Yang W-CV. 2010. Potential biomarkers in saliva for oral squamous cell carcinoma. Oral oncology 46(4):226-231.

Yap LF, Lee D, Khairuddin ANM, Pairan MF, Puspita B, Siar CH, Paterson IC. 2015. The opposing roles of NOTCH signalling in head and neck cancer: a mini review. Oral diseases 21(7):850-857.

Yoshida R, Nagata M, Nakayama H, Niimori-Kita K, Hassan W, Tanaka T, Shinohara M, Ito T. 2013. The pathological significance of Notch1 in oral squamous cell carcinoma. Laboratory Investigation 93(10):1068-1081.

Yoshida R, Ito T, Hassan WA, Nakayama H. 2017. Notch1 in oral squamous cell carcinoma. Histol Histopathol 32(4):315-323.

Yugawa T, Narisawa-Saito M, Yoshimatsu Y, Haga K, Ohno S-i, Egawa N, Fujita M, Kiyono T. 2010. ΔNp63α repression of the Notch1 gene supports the proliferative capacity of normal human keratinocytes and cervical cancer cells. Cancer research 70(10):4034-4044.

Zeng Q, Li S, Chepeha DB, Giordano TJ, Li J, Zhang H, Polverini PJ, Nor J, Kitajewski J, Wang C-Y. 2005. Crosstalk between tumor and endothelial cells promotes tumor angiogenesis by MAPK activation of Notch signaling. Cancer cell 8(1):13-23.

Zhang L, Rosin MP. 2001. Loss of heterozygosity: a potential tool in management of oral premalignant lesions? Journal of oral pathology & medicine 30(9):513-520.

Zhang TH, Liu HC, Zhu LJ, Chu M, Liang YJ, Liang LZ, Liao GQ. 2011. Activation of Notch signaling in human tongue carcinoma. Journal of oral pathology & medicine 40(1):37-45.